MIXING ISSUES IN CO_2 FLOODING: COMPARISON OF COMPOSITIONAL AND EXTENDED BLACK-OIL SIMULATORS

by

Caner Karacaer

A thesis submitted to the Faculty and the Board of Trustees of the Colorado School of Mines in partial fulfillment of the requirements for the degree of Master of Science (Petroleum Engineering).

Golden, Colorado

Date _____

Signed: _____
Caner Karacaer

Signed: _____
Dr. Yu-Shu Wu
Thesis Advisor

Golden, Colorado

Date _____

Signed: _____
Dr. William Fleckenstein
Professor and Head
Department of Petroleum Engineering

ABSTRACT

Extended black oil simulators provide a convenient model for CO_2-EOR flooding projects and are preferred because of less data requirements compared with compositional simulation models, therefore, underlying principles of extended black-oil simulation models deserve scrutiny. The main objective of this study is to investigate the impact of different numerical solution techniques on modeling of oil recovery by CO_2 flooding and compare extended black-oil and compositional simulators in order to examine the capabilities of these simulators with an emphasis on the mixing mechanism of oil and CO_2. Thus, the 2D and 3D miscible and immiscible CO_2 flooding cases is used to compare the results from the extended black-oil simulators (COZSim, Eclipse Solvent Model, Sensor-First Contact Miscibility Option) and compositional simulators (Eclipse and Sensor).

Extended black oil simulators provide an alternative to compositional simulators for the prediction of CO_2 flooding. An analysis is provided of the capabilities, advantages, disadvantages and limitations of the simulators that were investigated. It is found that compositional simulators predict higher oil recoveries due to assumptions of complete mixing and complete vaporization of oil. Moreover, it is shown that usage of a constant mixing parameter in extended black-oil simulators significantly affects oil and gas recovery predictions. CO_2 solubility in water phase is investigated and results suggest that CO_2 solubility is an important factor for the simulation of residual oil zones.

TABLE OF CONTENTS

LIST OF FIGURES

LIST OF TABLES

ACKNOWLEDGEMENT

First and foremost, I would like to express my sincere gratitude to my advisor Prof. Yu-Shu Wu for his help, support and encouragement. He contributed to a rewarding graduate school experience by giving me the intellectual freedom during my master studies. I am deeply indebted to my committee members Prof. Erdal Ozkan, Prof. Hossein Kazemi and Chet Ozgen for their time and effort in reviewing this work. I cannot but express my sincere gratitude to Chet Ozgen to be my mentor. His advice often served to give me a sense of direction during my research.

Special thanks go to my colleagues in NITEC LLC, Dr. Tuba Firincioglu Apaydin and Dr. Basar Basbug, for their invaluable guidance and friendship.

I would like to express my appreciations to Turkish Petroleum Corporation for providing me a full scholarship during my degree education.

I am also grateful to my friends in Golden. I was lucky enough to have the support of many good friends.

I would like to thank my family for always believing in me, their continuous love and support in my decisions. Without whom I could not have made it here.

I cannot finish without acknowledging how grateful and thankful I am to my lovely wife. I am lucky to have met Elif here in Golden. I thank her for her friendship, love and unyielding support.

CHAPTER 1

INTRODUCTION

US Department of Energy (DOE) reported that a total of 1,858 fields/reservoirs have been identified as candidates for CO_2-miscible flooding in United States. These large oil reservoirs have 366 billion barrels of oil in place and 136.6 billion barrels of remaining immobile oil that can be recoverable by CO_2 enhanced oil recovery (EOR) techniques (NETL, 2011). In addition, low saturation or immobile oil in residual oil zones, where oil production is not feasible through primary or secondary recovery mechanisms, can be mobilized by CO_2-EOR methods. These abandoned residual oil zones account for approximately 16.3 billion barrels of technically recoverable oil in the Permian, Big Horn and Williston basins (NETL, 2011). If a proper reservoir management design is used, this huge amount of oil resource can be efficiently recovered. Thus it is important to understand the underlying physics of CO_2 displacement mechanisms in order to design a successful CO_2-EOR project. Therefore, simulation and feasibility studies are very critical for CO_2-EOR projects to optimize oil recovery from these reservoirs.

Fully compositional and extended black oil simulators are two types of modeling tools to predict CO_2 flooding performance. Fully compositional models are considered as the primary tool for CO_2 injection studies but complex engineering analysis requirements push the practitioners to use extended black-oil simulators. Extended black oil simulation is an alternative approach to compositional simulation, and provides an engineering tool to account for oil displacement by a miscible or immiscible fluid. There are different extended black-oil

formulations to handle miscible flooding. However, there is a lack of understating of capability of these models.

1.1 Background

Most of the small and midsize fields have been exploited through primary and secondary recovery techniques, and most of them are presently owned by small and mid-sized operators. Given their operational budgets, these operators generally cannot afford technically sophisticated integrated reservoir simulation studies to assess the feasibility of CO_2 injection projects. Therefore an extended black oil model is preferred due to the detailed data requirements of compositional models. Extended black oil simulators can accelerate technical CO_2 injection studies because it makes the simulation process fast enough, so that an integrated feasibility study can be completed in a short time at a small cost. Such a model is needed because the existing public domain and commercial solutions are either too simplistic to be used for development planning, or too complex (compositional), time consuming and unaffordable.

One of the most sophisticated tools for CO_2-injection studies are the compositional simulators, mostly commercial simulation packages such as Eclipse-300® (Schlumberger), VIP-Comp® (Halliburton), GEM® (CMG), Sensor® (Coats Engineering) and MORE® (Roxar). These simulators can address variety of the technical issues related to CO_2-EOR processes, and their results can be used for development planning and economic analysis. Such sophisticated solutions usually encompass detailed engineering analyses and numerical simulations. The difficulty in development of such models has pushed many practitioners to more convenient solutions such as CO_2 Prophet (DOE) or extended black oil simulators.

CO_2 Prophet, a DOE funded software tool, can be used for modeling of CO_2-EOR processes. This tool is designed to identify the influence of the key parameters on CO_2 injection projects, and predicts especially the performance of the single pattern applications involving Water-Alternating-Gas (WAG) injection cases. It is a three component (solvent, water, and oil) streamline-type finite difference simulator and uses a mixing parameter for miscible displacement. While this tool is able to simulate models up to 10 layers, it cannot account for the impact of gravity forces, cross-flow across reservoir layers and CO_2 solubility in water, which play a significant role in CO_2 displacement processes. It also cannot account for the spatial changes in properties or different shape of reservoirs.

In some of the commercial simulators (such as Eclipse®, CMG®), an intermediate solution exists between compositional and more simplistic models. Those simulators use an extended black oil formulation which utilizes three phases and four components: water, dead oil, hydrocarbon gas, and any solvent (i.e. CO_2). These simulators use Todd-Longstaff mixing parameter treatment for miscible displacement.

A reservoir simulator, COZSim, developed for the DOE, offers an extended black oil formulation for miscible displacement studies. It is a three dimensional, three-phase, four-component, fully implicit, finite difference reservoir simulator. It accounts for CO_2 and hydrocarbon gas solubility in the aqueous phase. The simulator uses black oil type input data and converts it to compositional form internally. Miscibility calculations are based on interfacial tension using black-oil data. Interfacial tension reduction is utilized to model transition from immiscible to partially miscible, and finally to fully miscible conditions.

1.2 Motivation and Objective

Before the 1990s, almost all CO_2-EOR projects were implemented by major oil companies. During the 1990s, CO_2-EOR development technologies were transferred to independent producers, which led to the current situation where independent producers dominate the roster of CO_2-EOR operators (NETL, 2010). However, as stated earlier, these operators generally cannot afford technically sophisticated reservoir simulation studies to assess the feasibility of a CO_2 injection project. Large computation times and detailed data requirements of compositional models pushed practitioners to use extended black oil simulators.

Unlike miscible floods in main pay zones, there is a limited publication and understanding of CO_2 flood modeling in residual oil zones. Extended black oil formulations that are capable of modeling this kind of problem provide an alternative approach to compositional modeling. However, to the best of our knowledge, there is no publication associated with the CO_2-EOR modeling of residual oil zones with an extended black oil approach.

In this regard, extended black oil simulators provide a convenient solution for CO_2-EOR flooding projects and they are preferred because of the ease of use and less data requirements compared with compositional models. Therefore, extended black oil simulators and underlying modeling approaches are needed to be well examined to understand the capabilities of these simulators.

The main objective of this study is to investigate the impact of different solution techniques on modeling of oil recovery by CO_2 flooding and compare extended black oil and compositional simulators in order to examine the capabilities of these simulators. The specific objectives of this study are as following:

i. Review existing extended black-oil and compositional simulators and compare them conceptually in terms of formulation and miscibility treatment.

ii. Compare the simulator results for a depletion/water flooding problem to create benchmark baseline for CO_2 injection studies.

iii. Compare the simulator results for miscible and immiscible displacement of CO_2 in main zone.

iv. Compare the simulator results for miscible displacement in the residual oil zone.

v. Investigate the impact of CO_2 solubility in aqueous phase to oil recovery for exploitation of residual oil zone.

1.3 Methodology

A brief explanation about methodology used throughout this study:

- Extended black oil and compositional formulations will be examined and compared conceptually in terms of CO_2 miscible flood modeling. A conceptual analysis will be given.
- Ninth SPE Comparative solution project (Killough, 1995) will be implemented to create a benchmark baseline for COZSim, Eclipse 100 and Sensor-Black Oil Model.
- Two dimensional (2D) and three dimensional (3D) models will be used for miscible and immiscible CO_2 flooding cases to compare the results from COZSim, Eclipse 100 Solvent Model, Sensor-First Contact Miscibility option, Eclipse Compositional and Sensor-Compositional simulators. 2D planar models (quarter five spot with two wells) are used to examine viscous fingering effects in detail. Also, 2D cross-sectional models

are used to examine the gravity effects. 3D models are used to investigate the combined effects of viscous fingering and gravity overriding.

- 2D planar model will be used to simulate CO_2 flooding in residual oil zone with COZSim, Eclipse Solvent Model, Eclipse Compositional and Sensor-Compositional Simulators. Also, in this part impact of CO_2 solubility in aqueous phase will be investigated.

1.4 Thesis Outline

Chapter 2 provides a literature review on simulation techniques of CO_2-EOR flooding including compositional simulation and extended black-oil simulation. Also, physical displacement mechanisms of CO_2 flooding are presented in this chapter.

Chapter 3 introduces the numerical reservoir simulators used throughout this study. Compositional and extended black oil simulators, Eclipse and Sensor, and an extended black oil simulator, COZSim is introduced with an emphasis on modeling of miscible displacement.

Chapter 4 presents Ninth SPE Comparative Solution project which is implemented to create a benchmark baseline for COZSim, Eclipse 100 and Sensor black-oil simulator with a challenging depletion/water flooding problem.

Chapter 5 introduces the conceptual simulation models used throughout this study. Model configurations, fluid system, petrophysical data, operation parameters and case designs are explained.

Chapter 6 presents the comparison of simulators for immiscible (near miscible) CO_2 flooding in main oil zone. Two dimensional planar, two dimensional cross-sectional and three dimensional models are used in this chapter.

Chapter 7 presents the comparison of simulators for multi-contact miscible CO_2 flooding in main oil zone. Two dimensional planar, two dimensional cross-sectional and three dimensional models are used in this chapter.

Chapter 8 presents the comparison of simulators for first-contact miscible CO_2 flood flooding in main oil zone. Two dimensional planar, two dimensional cross-sectional and three dimensional models are used in this chapter.

Chapter 9 presents the comparison of simulators for multi-contact miscible CO_2 flooding in residual oil zone. Two dimensional planar models are used in this chapter. Also, the impact of CO_2 solubility in water on oil recovery is investigated.

Chapter 10 provides a discussion and conclusion of the study.

CHAPTER 2

LITERATURE REVIEW

In the 1970s, a dramatic rise in oil prices led to widespread implementation of enhanced oil recovery methods. Miscible flooding, chemical flooding, CO_2 injection and thermal EOR methods brought more complex problems beyond the conventional depletion and pressure maintenance. Also, drilling technologies that allowed reaching deeper resources resulted in discovery of reservoirs with complex fluid characteristics. Therefore, more sophisticated models needed to be developed to understand the dynamics of these complex fluid systems. Compositional models are designed to address all the issues associated with these complicated fluid property problems (Coats, 1982).

Compositional models can be used for any type of reservoir fluids. Any combination of those reservoir fluids can be divided into pure compounds called components such as methane, butane, and propane. Flow of each component is tracked and simulated individually. Oil and gas phases consist of the same components with different amounts. Compositional simulators are able to account for mass transfer between vapor and liquid phases. Mass transfer depends on phase compositions and pressure. Thus, vapor-liquid equilibrium (flash) calculations are needed to simulate composition dependent systems such as gas condensates and volatile oils. Calculation of composition dependent equilibrium ratios (K-values) is essential for these types of systems and requires a rigorous equation of state based flash procedure.

Compositional modeling efforts began in the late 1950s to understand how compositional changes effect oil recovery. Primary studies mostly used zero dimensional tank and 1D models.

These studies were insufficient to capture the required physics. Early compositional models used table lookup K-values or fitted values of GPSA K-values. The disadvantage of this approach is that reservoir simulator may experience convergence problems in the near critical region (Thele, 1983). The first generally applicable compositional simulators were presented by Kazemi et al. (1978) and Fussel and Fussel (1979). Fussel and Fussel (1979) were the first to incorporate a cubic equation of state to a multidimensional compositional simulator. Coats (1980) proposed a fully implicit compositional formulation. Ngheim, Fong and Aziz (1981) modified the model presented by Kazemi et al. (1978) and added an equation of state. Young and Stephenson (1983) proposed a model with different set of primary variables to construct a better-conditioned matrix. Several authors have presented compositional simulators and today compositional simulators coupled with an EOS package has become an industry standard application for modeling of compositional problems.

Compositional simulators are generally employed for cases that include composition dependency such as miscible flooding by a non-equilibrium gas, cycling of gas-condensate reservoir with dry gas, gas injection into volatile oil reservoirs, and natural depletion of volatile oil or gas condensate reservoir (Nolen, 1973). Many reservoir fluids, on the other hand, consist of composition independent systems which have much simpler fluid behavior such as black-oil systems (Wattenbarger, 1970).

Reservoir simulation research during the 1960s focused on black-oil model because of computing requirements and complexity of compositional model. Black-oil simulation offers much shorter run time and an easy-to-implement procedure compared with compositional simulation. In addition, many reservoir problems at that time were associated with natural

depletion and pressure maintenance which can be solved with black oil simulators. Black-oil simulation approach is actually a special two-component compositional case and uses a hypothetical binary fluid system. Conventional black-oil model assumes two pseudo-components as stock tank oil (non-volatile surface oil) and separator gas (surface dry gas). Two pseudo-component representation of hydrocarbon content assumes constant compositions for oil and gas phases. Surface gas may exist both in gas phase and oil phase. Gas phase is assumed to contain no liquids at surface conditions. Stock tank oil component can exist only in oil phase. The dissolved gas and free gas needs to be identical (i.e. has same physical properties). Also, any injecting gas should be the same as the produced gas. The amount of dissolved gas is pre-determined by the value of a solution gas oil ratio. Moreover, solubility of oil and gas components in water is negligible.

Conventional black-oil (beta-type) models assume that the binary fluid system is only a function of pressure and temperature. For isothermal systems, black oil models are based on the pressure-dependent parameters such as solution gas oil ratio, formation volume factors, oil and gas gravities, and viscosities. Therefore, black-oil model can account for recovery mechanisms involving pressure depletion and maintenance such as primary depletion, waterflooding and gas recycling.

PVT treatment is the most fundamental difference between compositional and black-oil approach. The black oil approach treats fluid properties as pressure dependent, whereas the compositional approach uses pressure and composition dependent fluid properties. Therefore the compositional approach is more representative of the fluid system than the conventional black-oil approach as it captures flow dynamics triggered by compositional changes. One of the

drawbacks of compositional simulators is input data requirements. Generally, compositions of produced and injected fluids are missing or incorrect. Thus, conventional black-oil model is more appealing because of the fewer data requirements. Numerical dispersion is a problem for both simulation techniques yet much larger in compositional simulation. However, fully compositional models may need a coarse grid due to CPU time limitations especially for full-field studies. These restrictions cause poor representation of heterogeneities and scaling effects (Montel et al., 2004). Also, compositional approach uses instantaneous local equilibrium concept to be able to use equation of state. For large grid blocks as used in compositional simulations, this assumption may not be valid because of the assumption of complete and instantaneous mixing of fluids within a grid block. It especially leads to poor modeling of viscous fingering and overestimate miscibility effects. Furthermore, scaling issues may cause excessive vaporization of oil for gas injection process or gas condensation near wellbore even though injected gas is not contacted with oil phase (Montel et al., 2004).

When two fluids become completely miscible, they form a single phase and no interfaces can be observed between two miscible fluids, indicating no interfacial tension. Miscibility can be achieved through two mechanisms: first-contact miscibility and multi-contact miscibility. First contact miscibility occurs when two fluids immediately form one phase regardless of fluid proportions such as ethanol and water or butane and oil. If two fluids are not miscible on first contact, miscibility requires many contacts until these two fluids cannot be distinguished from each other. This process is called as multi-contact miscibility. CO_2 and oil are the example for multiple-contact miscibility. In this process, miscibility is achieved because of the mass transfer between oil and CO_2 components. When CO_2 and oil are mixed together, first, CO_2 condenses into oil, make it lighter and drives light components out. Lighter components of oil vaporize into

CO_2 rich phase and make it denser and more soluble in oil. This mass transfer continues until two fluids form one single phase (Jarrell et al., 2002).

Dissolution and vaporization between oil and CO_2 increase as pressure increases, which lead the situation where oil can dissolve more CO_2, and more oil components can be vaporized by CO_2. Above a specific pressure, oil and CO_2 form a single phase. This pressure is called minimum miscibility pressure (MMP). CO_2 flooding below MMP is referred as immiscible flooding. Below MMP, pressure is not high enough to allow sufficient CO_2 dissolution into oil or vaporization of oil into CO_2 to form a single phase. When the pressure is below the MMP, CO_2 swells the oil and reduces its viscosity. Addition to viscosity reduction, oil saturation may increase due to swelling. Therefore, some of the residual oil can be mobilized and recovered. If pressure is below but near MMP, vaporization increases and more oil becomes recoverable.

As described above, classical black oil models cannot be used for problems involving miscible displacement due to the mass transfer between phases. Thus, the compositional model is considered as the primary tool to simulate miscibility-type problems. However, an alternative approach was needed to model miscible flooding processes because of the disadvantages of compositional simulation stated above. First approach was using simulators based on the solution of diffusion/convection equation. Peaceman and Rachford (1962) used diffusion/convection equation to model miscible displacement produced by diffusion and convective dispersion. They proposed a finite difference simulator to calculate two-dimensional miscible displacement, where solvent (CO_2) is first contact miscible with oil. They showed that the model accurately characterized the viscous fingering for one and two-dimensional displacement experiments. However, numerical dispersion is much greater than physical dispersion, and a large number of

grid blocks are needed to overcome numerical dispersion. Garder et al. (1964) proposed using the method of characteristics to simulate multidimensional miscible displacement using diffusion/convection equation. Unlike the usual stationary grid structure, their method uses moving points to accurately model physical dispersion in miscible displacement problems and does not introduce any numerical dispersion. However, the method has not been received widespread application because of the difficulty to employ reservoir type complex geometries and solvent slug calculations (Stalkup, 1983). A common drawback of diffusion/equation type solutions is that numerical dispersion may mask the physical dispersion and resolving this issue requires a fine grid, which is unfavorable for full-scale reservoir simulations. (Aziz and Settari, 1979)

Unlike the diffusion/convection type simulators, black oil models have been used for many years by industry. Therefore, researchers have exerted effort to create black oil type models to handle problems involving miscibility. Hybrid models, i.e. extended/modified black oil simulators and limited compositional simulators, are aimed to take the best features of black oil and compositional models. Lantz (1970) showed that an analogy exist between two phase flow equation in black oil model and diffusion/convection equation if permeability and capillary pressure functions are adjusted. Lantz (1970) was the first to modify a classical black oil reservoir simulator to model two-component miscible displacement. Lantz (1970) showed that miscible displacement can be modeled by classical black oil formulation for a constant dispersion field. Capillary pressures and relative permeabilities were modified to create first contact miscible displacement and mixing by diffusion. However, this analogy is valid only for incompressible components, and also the model is not able to model viscous fingering or gravity tongue.

2.1 Unstable Displacement in Miscible Flooding

The reasons for unstable displacement in miscible flooding can be summarized as:

- Longitudinal dispersion (spreading of solvent due to microscopic heterogeneities)
- Channeling (due to macroscopic heterogeneities e.g. permeability variation)
- Viscosity differences (fingering of less viscous solvent – viscous fingering)
- Gravity differences (overriding of less viscous solvent – gravity tonguing)
- Diffusion and Flooding Rate

Miscible flooding may create an unstable frontal advance due to viscous fingering (dispersion) or gravity tonguing because of unfavorable viscosity ratio and density difference between solvent (CO_2) and oil as seen from Figure 2.1. Accurate characterization of sweepout requires describing unstable frontal advance in connection with physical dispersion. However, both diffusion/convection and classical black oil simulators with stationary grid structure referred above lack the ability to produce unstable front for large grid blocks. Both models assume that solvent and oil are completely mixed within a grid block, which causes optimistic sweepout for coarsely gridded models. Using fine gridded models, on the other hand, are impractical for full-scale miscible flooding projects.

If the dispersed zone is large with respect to grid size block, oil and solvent can be treated as completely mixed in the grid block. On the other hand, if the dispersed zone is so small with respect to size of grid block, oil and solvent can be considered completely segregated as pure components and no mixing occurs. Most of the time, actual fluid behavior is expected to produce a case between those mixing limits, which correspond to partial mixing (Stalkup, 1983).

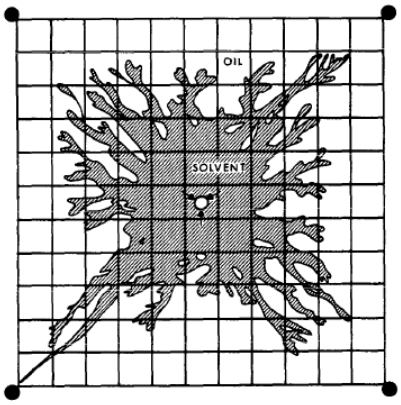

Figure 2.1 Swept zone for a five spot pattern flood (Todd and Longstaff, 1972).

2.2 Modeling of Unstable Displacement

Koval (1963) presented a K-factor method analogous to Buckley-Leverett Model to calculate oil recovery and solvent cut as a function of solvent/oil viscosity ratio. Koval (1963) suggested a K value to represent viscous fingering based on the unfavorable viscosity ratio of oil and solvent as following:

$$K = \left[0.78 + 0.22 \left(\frac{\mu_o}{\mu_s} \right)^{1/4} \right]^4 \tag{2.1}$$

Todd and Longstaff (1972) proposed a three-component empirical model to include dispersion effects for coarse gridded models assuming partial mixing of solvent and oil. They used a fluid system involving oil and solvent with no solution gas and no mobile water. The model is based on the modification of classical black oil type properties such as relative permeabilities, densities and viscosities. Effective viscosities of oil and solvent system were calculated from their immiscible values as following:

$$\mu_{oe} = \mu_o^{1-\omega} \mu_m^{\omega} \tag{2.2}$$

$$\mu_{se} = \mu_s^{1-\omega} \mu_m^{\omega} \tag{2.3}$$

where

$$\mu_m = \mu_o \mu_s \Big/ \left(\frac{S_g}{S_n} \mu_o^{1/4} + \frac{S_o}{S_n} \mu_s^{1/4} \right)^4 \tag{2.4}$$

where μ_m is viscosity of mixture and ω is mixing parameter. ω represents a fingering parameter to correct mixing within a grid. A value of $\omega = 1$ corresponds to complete mixing of solvent and oil within a grid block; it results in piston like displacement. Whereas $\omega = 0$ corresponds negligible mixing or negligible dispersion similar to immiscible displacement except in relative permeability treatment. Partial mixing is represented by values of $0 < \omega < 1$. In this case, effective viscosity of the solvent will be less than the effective viscosity of oil. Solvent will travel faster than oil and create viscous fingers as seen in Figure 2.2. The Todd and Longstaff model, on the other hand, does not characterize the structure of viscous fingers in a detailed manner; instead it approximates the effect of viscous fingers on sweepout.

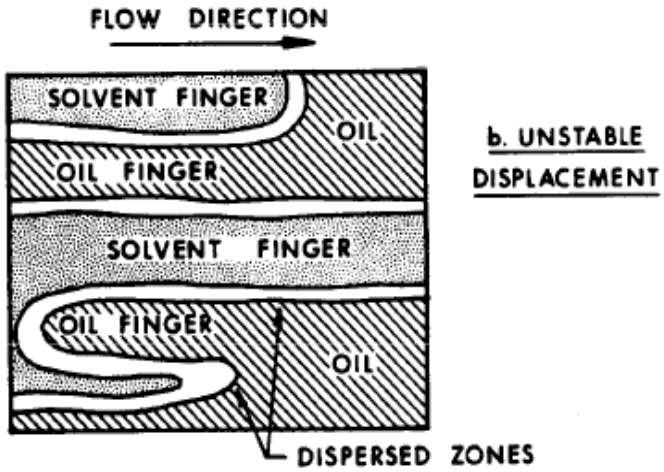

Figure 2.2 Representation of solvent displacing oil in a grid block (Todd and Longstaff, 1972).

Todd and Longstaff (1972) proposed a density model consistent with viscosity model. If the oil and solvent are completely mixed, density of the mixture defined as follows:

$$\rho_m = \rho_o \frac{S_o}{S_n} + \rho_s \frac{S_s}{S_n} \tag{2.5}$$

For partial mixing, effective densities are

$$\rho_{oe} = (1-\omega)\rho_o + \omega\rho_m \tag{2.6}$$

and

$$\rho_{se} = (1-\omega)\rho_s + \omega\rho_m \tag{2.7}$$

Todd and Longstaff (1972) also recommend modifying solvent and oil relative permeabilities as following:

$$k_{ro} = \frac{S_o}{S_n} k_{rn} \tag{2.8}$$

and

$$k_{rg} = \frac{S_g}{S_n} k_{rn} \tag{2.9}$$

The original Todd and Longstaff model assumes that oil and solvent are miscible on first contact, and multi-contact mechanism is neglected, which means that regardless of the proportions of two fluids, they instantaneously form one phase. Therefore, recovery mechanisms at below multi-contact miscibility pressure, such as oil swelling, oil viscosity reduction and decreasing oil solvent interfacial tension, cannot be accounted for. Another limitation of the

original Todd-Longstaff model is the estimation of ω. Todd and Longstaff (1972) recommend $\omega = 2/3$ for laboratory experiments, and $\omega = 1/3$ for fields projects. As a first guess, a value in the range of 0.5 and 0.7 is suggested by Stalkup (1983). However, this range gives a large variation for sweepout and oil recovery. Bilhartz et al. (1978) suggest ω as a history matching parameter obtained from pilot tests.

Todd and Longstaff (1972) extended their three component mixing model to a four component model by adding an immiscible chase gas component. Again, solvent and oil are miscible whereas chase gas is not miscible with oil. Figure 2.3 shows a representation of three component miscible displacement model in a grid block excluding water.

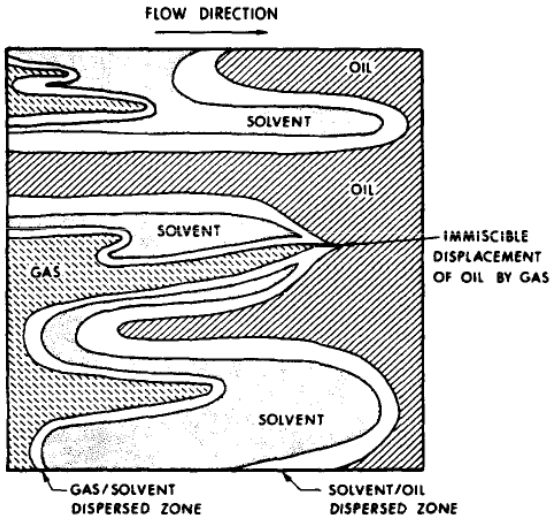

Figure 2.3 Representation of a three component miscible displacement in a grid block (Todd and Longstaff, 1972).

At pressures above miscibility pressure, the mixing parameter formulation is used as follows for extended model:

$$\mu_{oe} = \mu_o^{1-\omega} \mu_{mos}^{\omega} \tag{2.10}$$

$$\mu_{ge} = \mu_g^{1-\omega} \mu_{mgs}^{\omega} \tag{2.11}$$

and

$$\mu_{se} = \mu_s^{1-\omega} \mu_m^{\omega} \tag{2.12}$$

Despite the shortcomings and assumptions of Todd-Longstaff model, it has become an industry standard application for extended black oil simulators for modeling of miscible displacement.

2.3 Extended Black Oil Simulators

Kazemi et al. (1978) presented the first generally applicable compositional simulator in which compositions dependence of K-values is modeled by using convergence pressure. They presented a pseudo-two component system approach, which can be considered as a limited compositional model. The term of limited compositional models are used here to mean that the model employs an equilibrium concept with pressure dependent K-values to calculate fluid phase properties. Also, their model is capable to obtain pressure dependent K-values from engineering charts. A pressure equation is used to solve pressure of each cell using Newton-Raphson iteration. After pressures are calculated, water saturation and overall compositions are calculated explicitly. Watkins (1982) proposed a four-component (water, oil, hydrocarbon gas and solvent) miscible flood IMPES simulator extending Todd-Longstaff type viscous fingering model. Below miscibility pressure, oil and solvent are assumed to be immiscible. Saturations are calculated explicitly after oil pressure has been calculated. The model uses the Todd-Longstaff viscosity model and fluid densities are calculated as following:

$$\rho_{oe} = (1-\omega)\rho_o + \omega\rho_m \tag{2.13}$$

$$\rho_{ge} = (1-\omega)\rho_g + \omega\rho_m \tag{2.14}$$

and

$$\rho_{se} = (1-\omega)\rho_s + \omega\rho_m \tag{2.15}$$

where density of the mixture:

$$\rho_m = \frac{S_s}{S_n}\rho_s + \frac{S_o}{S_n}\rho_o + \frac{S_g}{S_n}\rho_g \tag{2.16}$$

Above miscibility pressure, relative permeabilities are calculated as:

$$k_{ro} = \frac{S_o - S_{orm}}{1 - S_w - S_{orm}} k_{rn}(S_w) \tag{2.17}$$

$$k_{ro} = \frac{S_g}{1 - S_w} k_{rn}(S_w) \tag{2.18}$$

and

$$k_{rs} = \frac{S_s}{1 - S_w} k_{rn}(S_w) \tag{2.19}$$

where k_{rn} is the non-wetting phase relative permeability in a water oil two phase system. In this model, below miscibility pressure solvent and hydrocarbon gas remain miscible.

Chase and Todd (1984) proposed a seven-component limited IMPES compositional simulator using user-specified K-values with an emphasis on CO_2 modeling flow. They

presented several features associated with miscible flooding such as water blocking of oil from an invading solvent, miscibility transition as a function of pressure and composition and CO_2 loss to the aqueous phase. A modified version of water blocking relationship derived by Raimondi and Torcaso (1964) is used to describe oil that is not accessible to the solvent as a function of water saturation:

$$S_{twb} = \frac{S_{orw}}{1+\beta\left(k_{ro}/k_{rw}\right)} \tag{2.20}$$

S_{twb} represents the oil saturation that is blocked from contact with encroaching solvent by the intervening water saturation. Here, parameter β weakens the water blocking function if a value greater than 1 is used. They used parameter α to provide transition from immiscible conditions to miscible conditions. α varies linearly between zero and one for a specified pressure and miscibility pressure. Solubility of solvent (CO_2) in aqueous phase needs to be entered by user as a function of pressure. A modified version of Todd-Longstaff model adding parameter α is used, an example for viscosity treatment:

$$\mu_{oe} = \mu_o^{1-\alpha\omega}\mu_m^{\alpha\omega} \tag{2.21}$$

Huan (1985) proposed a fully implicit limited compositional simulator using a phase equilibrium concept and Newton-Raphson iteration. Primary variables to be solved are pressure and three component masses per unit formation volume instead of pressure and saturations. Components are oil, water and two gas components. Phase equilibrium calculations use black oil type PVT data. Miscibility type problems are not included to simulator. Bolling (1987) introduced a multicomponent limited compositional simulator similar to Huan's (1985) using pressure dependent *K-values* for miscible and immiscible displacement problems. Primary

variables, pressure and component masses, are solved implicitly with Newton-Raphson procedure or IMPES. For miscibility problems they used Todd-Longstaff viscosity model with a different calculation strategy. Overall compositions are used for modification of hydrocarbon mobilities, capillary pressure and density caused by miscibility. Viscosity of the mixture is calculated from:

$$\mu_m = \left[\left(\frac{z_o}{\mu_o} \right)^{\frac{1}{2}} + \left(\frac{z_s}{\mu_s} \right)^{\frac{1}{2}} \right]^4 \tag{2.22}$$

Effective densities are calculated from Todd-Longstaff model, density of the mixture in the model calculated as:

$$\rho_m = \left[\frac{z_o}{\rho_o} + \frac{z_s}{\rho_s} \right]^{-1} \tag{2.23}$$

Bolling (1987) indicated that model shows higher retention of CO_2 compared with classical four component black oil models. Also, the results indicate that input parameters are needed to be properly tuned. Moreover, the selection of primary variables allows including any PVT package to model phase behavior.

Ammer et al. (1988) proposed an IMPES extended black oil simulator similar to Chase and Todd's model (1984), containing mass balance equations of oil, water, hydrocarbon gas and up to four solvents. Hydrocarbon gas and solvent 1 are allowed to partition between the gas, oil, and aqueous phases while solvents 2, 3, and 4 partition among the gas and oil phases only. Solvent loss to aqueous phase and water blocking oil from contacting injected solvent are incorporated into their model for miscible gas injection problems. Both hydrocarbon gas and

solvent is soluble in aqueous phase. Fluid properties are based on both pressure and the amounts of soluble components in solution using an adaptation of Chase and Todd's method (1984). They used the mixing-rule approach introduced by Todd and Longstaff (1972) and later extended by Watkins (1982) to calculate effective fluid densities and viscosities. To model transition from immiscible to miscible condition, a weight factor is defined as:

$$\alpha = \frac{P - P_1}{P_2 - P_1} \quad , \qquad \text{and} \quad P_1 \le P \le P_2 \tag{2.24}$$

P_2 is minimum miscibility pressure, above that pressure injected solvent are fully miscible with reservoir oil and hydrocarbon gas. P_1 is the pressure where the oil recovery versus pressure curve for slim tube displacement experiments begins to bend over. The pressure range between P_1 and P_2 is defined as zone of transition from immiscible to fully miscible conditions. Here α is 0 for $P < P_1$ and 1 for $P > P_2$. Viscosity and density model are defined as:

$$\mu_{ie} = (1-\alpha)\,\mu_i^1 + \alpha\mu_i^2 \tag{2.25}$$

and

$$\rho_{ie} = (1-\alpha)\,\rho_i^1 + \alpha\rho_i^2 \tag{2.26}$$

Here, i represents components, superscript 1 denotes effective properties for $P < P_1$ and superscript 2 denotes effective properties for $P > P_2$. Permeabilities and capillary pressures are also modified using α parameter. Due to the large saturation changes usually associated with well-bore coning, it is not recommended for coning problems by Ammer et al. (1988).

Tang and Zick (1993) proposed a simplified compositional model, and the main difference from a fully compositional simulator is that equilibrium calculations are based on non-iterative procedure with the pseudoternary, equilibrium phase diagrams. Todd-Longstaff model is also used. They stated that PVT model can handle miscibility above or below minimum miscibility pressure, but it is not adequate for near-miscible conditions.

CHAPTER 3

GENERAL DESCRIPTION OF SIMULATORS

This chapter introduces the numerical reservoir simulators used throughout this study. Compositional and black oil simulators, Eclipse and Sensor, and an extended black oil simulator, COZSim is introduced with an emphasis on modeling of miscible displacement.

Throughout this study, compositional simulators are defined as the numerical reservoir simulators which use multi-component vapor-liquid equilibrium (flash) calculations. On the other hand, extended black-oil simulators do not use flash calculations and requires classical black-oil data which fluid properties, such as formation volume factor and viscosity, are function of pressure solely.

3.1 Eclipse

Eclipse is a widely used industry standard commercial simulator and provides a broad range of modeling facilities. The Eclipse simulator suite consists of two separate simulators: Eclipse 100 for black-oil modeling and Eclipse 300 for compositional modeling. Eclipse 100 is a fully-implicit, three-phase, three-dimensional, general purpose black oil simulator with pseudo-miscible option. Eclipse 300 is a compositional simulator and can be run in fully implicit, IMPES and adaptive implicit (AIM) modes with cubic equation of state. Primary solution variables are pressure and two phase saturations for black oil cases in Eclipse 100; pressure, water saturation, molar densities of each component in Eclipse 300. Newton's method is used to solve non-linear conservation equations (Eclipse Technical Description, 2012).

Eclipse 100 provides three and four-component Miscible Flood Model. The three component miscible flood option assumes that the reservoir fluids consist of three components: reservoir oil (stock tank oil and solution gas), injection gas (solvent) and water. The reservoir oil and solvent gas components are assumed to be miscible in all proportions. Physical dispersion (viscous fingering) of the miscible components is treated using the Todd- Longstaff model (CMG extended black-oil simulator also use Todd-Longstaff method).

Todd-Longstaff mixing parameter (w) is an input parameter to account effects of viscous fingering. As discussed in previous chapter, formulation in Todd-Longstaff method uses either fully miscible or fully immiscible cases. In reality, there should be a transition between the two displacement characters. Transition between miscibility and immiscibility can be modeled by miscible model with a pressure dependent miscibility function which can be tabulated between 0 and 1. 0 indicates immiscible displacement, and 1 represents miscible displacement. This function interpolates immiscible and miscible PVT properties, relative permeabilities and capillary pressure data.

Solvent model is an extension to miscible flood option, and it consists of four components as water, reservoir oil, reservoir gas and solvent gas. In this model, solvent displacement can be modeled in the presence of free hydrocarbon gas. The solvent gas gravity can differ from the free solution gas.

Another advantage of miscible flood or solvent model is that it is able to model residual oil saturation to miscible flood. Compositional simulators cannot handle residual oil saturation to miscible flood directly. Eclipse 300 has an option to set a residual oil saturation to avoid vaporization of oil due to the continuous CO_2 injection. A specified fraction of oil is to exclude

from the flash calculations. Composition of specified residual oil is set as a fraction of initial oil composition and does not change with time. An analysis regarding this option is provided in Chapter 10. Besides, Eclipse compositional model is capable to simulate CO_2 solubility in water phase. CO_2 component is then allowed to exist in all three phases.

Eclipse compositional simulator predicts miscibility using surface tensions based on Macleod-Sugden correlation between the two hydrocarbon phases. The surface tension between the oil and gas phases is used to measure how miscible two fluids are. Miscibility occurs when surface tension between the two hydrocarbon phases drops to zero. Relative permeabilities and capillary pressures are interpolated as functions of surface tension between immiscible and miscible values. Critical saturations are scaled so that both miscible and miscible relative permeabilities have the same end-points. For instance, oil and gas relative permeability calculated as following:

$$k_{ro} = F_k \cdot k_{ro}^{imm} + \left(1 - F_k\right) \cdot k_{ro}^{mis} \tag{3.1}$$

$$k_{rg} = F_k \cdot k_{rg}^{imm} + \left(1 - F_k\right) \cdot k_{rg}^{mis} \tag{3.2}$$

k_{ro}^{imm} and k_{rg}^{imm} are the immiscible oil and gas relative permeabilities defined by user. k_{ro}^{mis} and k_{rg}^{mis} are the miscible oil and gas relative permeabilities, which are taken as straight lines. Interpolation parameter F_k defined by Coats (1980) is a function of surface tension as following:

$$F_k = \min\left[1, \left(\frac{\sigma}{\sigma_0}\right)^{0.25}\right] \tag{3.3}$$

σ is surface tension and σ_0 is reference surface tension. The capillary pressure interpolation parameter F_p is linear function of surface tension and it is calculated as:

$$F_p = \min\left[1, \left(\frac{\sigma}{\sigma_{p_0}}\right)\right] \tag{3.4}$$

where σ_{p_0} is a reference surface tension. Macleod-Sugden correlation uses parachors to calculate surface tension as following:

$$\sigma = \left[\sum_{i=1}^{N_c} P_i \left(b_L^m x_i - b_V^m y_i\right)\right]^4 \tag{3.5}$$

where x_i and y_i are the liquid and vapor mole fractions, b_L^m and b_V^m liquid and vapor phase molar densities and P_i is the parachors of the component. The value of surface tension will decline to zero when the phase compositions and phase molar densities become equal. Here, zero surface tension represents one phase, fully miscible case.

3.2 Sensor

Sensor is a generalized three-dimensional and three-phase simulator offering both black-oil and compositional simulation models (Sensor Manual, 2011). It includes IMPES and implicit formulations. Sensor uses Peng-Robinson and Soave-Redlich-Kwong equations of state for compositional model. Primary variables are mole fractions of liquid and gas phases (x_i and y_i), oil and gas saturation (S_o and S_g) and pressure. Sensor compositional model also use Macleod-Sugden correlation for surface tensions in miscible flooding discussed previously.

Sensor First-Contact Miscibility Option is available for solvent flooding. This option provides pseudoization of components and control of bypassed oil (residual oil saturation to

miscible flood) and dispersion for miscible flooding problems. In this option, compositional input data (EOS description) is internally used to generate black oil fluid properties (viscosity and density) as two pseudo-components: original reservoir oil and solvent as explained in Chapter 5. First contact miscibility option assumes that all cells are always undersaturated. No flash or saturation pressure calculations are performed. The composition of hydrocarbon phase can differ from original oil composition to solvent composition (Coats et al., 2007).

Unlike the compositional simulation, first-contact miscibility option is able consider bypassed oil or residual oil saturation to miscible flooding. Residual oil saturation and physical dispersion control calculations are performed as following:

$$X_2 = f \times x_2 = 1 - X_1 \tag{3.6}$$

where X_1 and X_2 are flowing mole fractions of oil and solvent respectively, x mole fraction in liquid phase, f is dispersion factor defined as:

$$f = \frac{K}{\left[1 - x^* + x_2 \left(K - 1\right)\right]} \tag{3.7}$$

Dispersion factor is a function of mole fraction of bypassed oil, x^*, and dispersion control coefficient, K. Dispersion control coefficient is defined by Koval (1963) to model viscous fingering in miscible floods based on the oil and solvent viscosity ratio. Table 3.1 explains the relationship between dispersion and dispersion control coefficient (Coats et al., 2007).

Table 3.1 Relationship between dispersion control coefficient and dispersion

Dispersion-Control Coefficient	Dispersion
K=1	Dispersion will be normal numerical dispersion
K >1	Increases dispersion to represent viscous fingering
K <1	Controls or reduces numerical dispersion

3.3 COZSim

COZSim is a three dimensional, three-phase, four-component, fully implicit, finite difference extended black oil simulator. The simulator uses black oil type input data and convert it to compositional form internally. Miscibility calculations are based on interfacial tension using black-oil data. Interfacial tension reduction is utilized to model transition from immiscible to partially miscible, and finally to fully miscible conditions. Physical dispersion is handled through Todd-Longstaff type viscosity model using a function based on the interfacial tension. Model considers three phases (oleic, gaseous and aqueous) and consists of mass balances for four components (water, oil, hydrocarbon gas and CO_2). Components may partition among three phases as presented in Table 3.2. Four independent variables (bulk pressure and overall mole fractions of water, hydrocarbon gas and CO_2) are solved in fully implicit manner.

Even though the data that is required to run the simulator is in black-oil format, all the information is converted to compositional form internally. Built-in correlations estimate component molecular weights, parachors, fluid properties and mole fractions based on the specific gravity of oil and hydrocarbon gas.

Table 3.2 Phase and component diagram of COZSim

Component Number	Component	Phase		
		Oleic	**Gaseous**	**Aqueous**
1	Water	-	-	w_1
2	Oil	x_2	-	-
3	HC Gas	x_3	y_3	w_3
4	CO_2	x_4	y_4	w_4

Miscibility calculations are based on interfacial tension using black-oil data. Interfacial tension reduction due to partitioning of CO_2 in the oleic and gaseous phases is calculated using parachors; it is also used to simulate transition from immiscible to partially miscible, and finally to fully miscible conditions. Viscous fingering is handled through a Todd-Longstaff type viscosity model using interfacial tension rather than using a constant mixing parameter. Residual oil saturation can be modeled under fully or partial miscibility conditions. The impact of both full and partial miscibility on gas-oil capillary pressure and relative permeability is accounted with fully implicit formulation.

The model consists of four coupled component mass balance equations for each cell. Conservation equation for component *c* is:

$$\nabla\left(\rho \vec{v} w_c\right)_a + \nabla\left(\rho \vec{v} x_c\right)_o + \nabla\left(\rho \vec{v} y_c\right)_g - q_c = \frac{\partial\left(\phi z_c \rho_t\right)}{\partial t} \tag{3.8}$$

where subscript a, o and g denotes the phase – aqueous, oleic and gaseous phase, respectively and ρ is molar density of a phase. z is overall mole fraction of component c. w, x and y are mole fractions of component in aqueous, oleic and gaseous phases respectively. q is the molar rate and is the directional darcy velocity, and it is defined as:

$$v = kk_r\lambda\left(\nabla P - \gamma\nabla D\right) \tag{3.9}$$

Non-linear partial continuum equation is discretized in time and space by using standard finite differences. Times dating of variables are all fully implicit. Four independent variables, bulk pressure (gas phase pressure for this study) and overall mole fractions of water, hydrocarbon gas and CO_2, are solved in fully implicit manner.

The fluid data required by COZSim is in black-oil format, and it is converted to compositional form internally. This procedure consists of the calculation of overall mole fractions and mole fractions for each component. As an example, calculation of overall mole fraction of oil component from black oil data for initialization:

$$z_2 = \left(\frac{S_o}{B_o\rho_o^{sc}}\right) \Bigg/ \left(\frac{S_a}{B_a\rho_w^{sc}} + \frac{S_o}{B_o\rho_o^{sc}} + \frac{S_g}{B_g\rho_g^{sc}}\right) \tag{3.10}$$

Mole fraction of oil component in oleic phase:

$$x_2 = 1 \Bigg/ \left(1 + R_{sa}\frac{\rho_o^{sc}}{\rho_g^{sc}}\right) \tag{3.11}$$

COZSim does not use fugacity constraints, and equation of state based flash procedure or table lookup *K-values*. Equilibrium *K-values* used in COZSim are defined as:

$$K_{o,3} = \frac{y_3}{x_3} \qquad K_{w,3} = \frac{y_3}{w_3}$$
$$K_{o,4} = \frac{y_4}{x_4} \qquad K_{w,4} = \frac{y_4}{w_4} \tag{3.12}$$

K-values are calculated internally using solution gas-oil ratio, solution gas-water ratio and molar density of the phases. The following is an example calculation of equilibrium *K-values* for the oleic phase with hydrocarbon gas.

$$K_{o,3} = \frac{1 + R^m_{so,3}}{R^m_{so,3}} \tag{3.13}$$

where

$$R^m_{so,3} = R_{so,3} \frac{\rho^{sc}_o}{\rho^{sc}_g} \tag{3.14}$$

$R_{so,3}$ is solution hydrocarbon gas – oil ratio; ρ^{sc}_o and ρ^{sc}_g densities of oleic and gaseous phase pressures at standard pressure and temperature conditions, respectively. $R^m_{so,3}$ is molar solution gas – oil ratio.

COZSim uses a viscous fingering model based on the interfacial tension function rather than using a constant mixing parameter proposed by Todd-Longstaff (1972). Effective viscosities of the oil and solvent system are calculated from their immiscible viscosity values as following:

$$\mu_{oe} = \mu_o^{1-f(\sigma)} \mu_m^{f(\sigma)} \tag{3.15}$$

and

$$\mu_{se} = \mu_s^{1-f(\sigma)} \mu_m^{f(\sigma)} \tag{3.16}$$

where

$$\mu_m = \mu_o \mu_s \Big/ \left(\frac{S_g \mu_o^{1/4} + S_o \mu_s^{1/4}}{S_o + S_g} \right)^4 \tag{3.17}$$

where μ_m is viscosity of the mixture and $f(\sigma)$ is the mixing parameter function. $f(\sigma)$ represents a channeling function to impose partial or full mixing within a grid. It is calculated internally. $f(\sigma)$ is a function of pressure, molar densities, parachors and mole fraction of components. A value of $f(\sigma)$ =1 corresponds to full mixing of solvent and oil within a grid block, and it results a piston like displacement. $f(\sigma)$ =0 corresponds to negligible mixing or negligible dispersion similar to immiscible displacement. Partial mixing is represented by values of 0< $f(\sigma)$ <1. In this case, effective viscosity of the solvent will be less than the effective viscosity of oil. Hence, solvent will travel faster than oil and create viscous fingers. It is calculated as following:

$$f(\sigma) = 1 - \left[\frac{\sigma - \sigma_{FCM}}{\sigma_{MM} - \sigma_{FCM}} \right] \tag{3.18}$$

where σ_{FCM} and σ_{MM} is the pseudo interfacial tension for first contact miscibility and minimum miscibility, respectively. These pseudo interfacial tensions can be defined by the user or default values can be used ($\sigma_{FCM} = 1.0$ and $\sigma_{MM} = 5\ dynes/cm$). To avoid the excess numbers for the mixing parameter function, following algorithm is used:

$$f(\sigma) = \max\left\{ \min\left[f(\sigma), 1.0 \right], 0.0 \right\} \tag{3.19}$$

COZSim predicts miscibility using interfacial tension based on Macleod-Sugden[3] correlation between the two phases. The interfacial tension between the oil and gas phases is used to measure how miscible two fluids are. Relative permeabilities and capillary pressures are

interpolated as functions of interfacial tension between immiscible and miscible values. The Macleod-Sugden correlation is used to calculate pseudo interfacial tension as following:

$$\sigma = \left[\sum_{i=1}^{4} P_i \left(\rho_o x_i - \rho_g y_i \right) \right]^4 \tag{3.20}$$

where x_i and y_i are the liquid and gas mole fractions, ρ_o and ρ_g oleic and gaseous phase molar densities and P_i is the parachors of the i^{th} component. Parachor value for oil component is calculated from:

$$P_2 = 18.824 + 3.0453 MW_{C_{5+}} \tag{3.21}$$

where $MW_{C_{5+}}$ is C_{5+} oil molecular weight and it can be defined by the user or can be estimated internally from the API value of oil by using Lasater correlation (Lasater, 1958):

$$MW_{C_{5+}} = \left(\frac{7864.9}{API} \right)^{1/1.0386} \tag{3.22}$$

Gas parachor value:

$$P_g = 18.824 + 3.0453 \times MW_g \tag{3.23}$$

CHAPTER 4

BLACK OIL BENCHMARK PROBLEM

This chapter presents Ninth SPE Comparative Solution project (Killough, 1995) which will be implemented to create a benchmark baseline for COZSim, Eclipse 100 and Sensor black-oil simulator with a depletion/water flooding problem.

4.1 Description of Ninth SPE Comparative Solution Project

Ninth SPE Comparative Solution project is a challenging black oil simulation problem consisting of a dipping reservoir which has 25 producers and 1 water injector. Total simulation time is 900 days. Reservoir is dipping with an angle of 10 degrees in *X* direction, where the top point is at a depth of 9000 feet. Static model is divided into 9000 cells based on 24x25x15 grid. The dimensions of grid blocks are 300 feet in both *X* and *Y* direction. A simulation pre-processor software (LYNX) is used to generate grid data for all three simulators using grid tops and layer thicknesses. Figure 4.1 shows the static reservoir model.

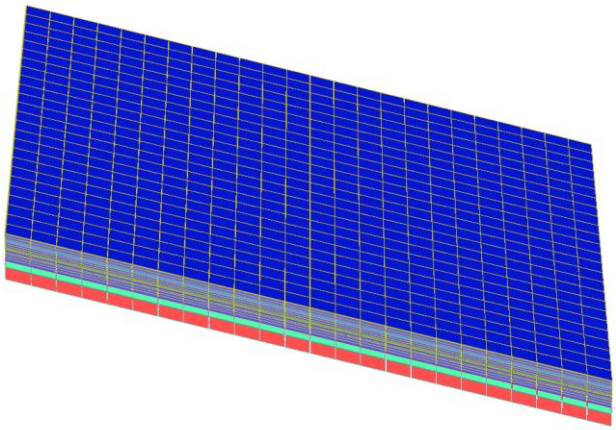

Figure 4.1 Grid structure of the static model.

Porosity and layer thickness are given in Table 4.1

Table 4.1 Porosity and layer thickness by layer

Layer	Porosity, [-]	Thickness, [ft]
1	0.087	20
2	0.097	15
3	0.111	26
4	0.16	15
5	0.13	16
6	0.17	14
7	0.17	8
8	0.08	8
9	0.14	18
10	0.13	12
11	0.12	19
12	0.105	18
13	0.12	20
14	0.116	50
15	0.157	100

Relative permeabilities are shown in Figure 4.2. Connate water saturation is 0.178 and residual oil saturation is 0.11851 throughout the model. All simulators use STONE 2 as three phase relative permeability correlation. Capillary pressure curve is presented in Figure 4.2, which is used as both imbibition and drainage capillary pressure curve. Capillary pressure curve has a discontinuity at about 35% water saturation, which may cause convergence problems for cases in which water saturations are changing significantly (Killough, 1995).

Initial reservoir temperature is 100 °F, and initial pressure is 3600 psi at the depth of 9035 feet. The bubble point pressure is 3600 psi. Oil-water contact is 9950 feet subsea. No free-gas available at initial conditions. Gas-oil solution ratio (R_s) and oil formation volume factor (B_o) versus saturation pressures are shown in Figure 4.3.

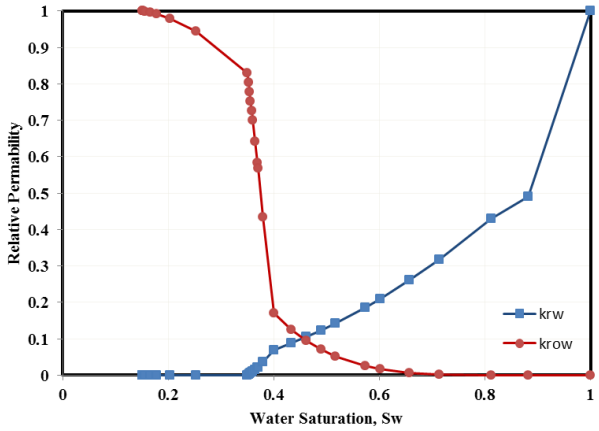

(a)

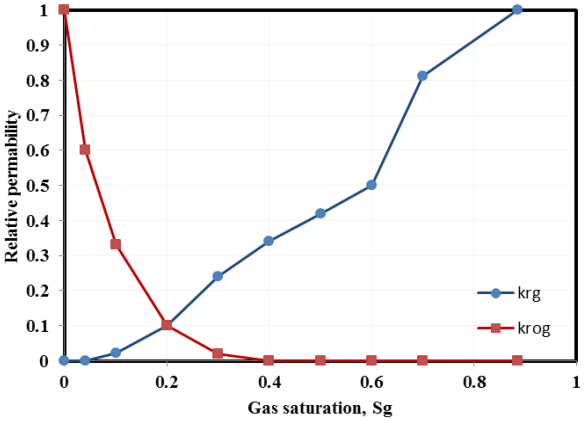

(b)

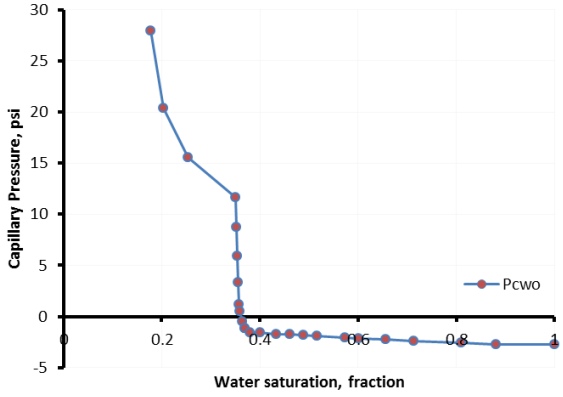

(c)

Figure 4.2 (a) Oil-water relative permeability data (b) oil-gas relative permeability data,(c) oil-water capillary pressure.

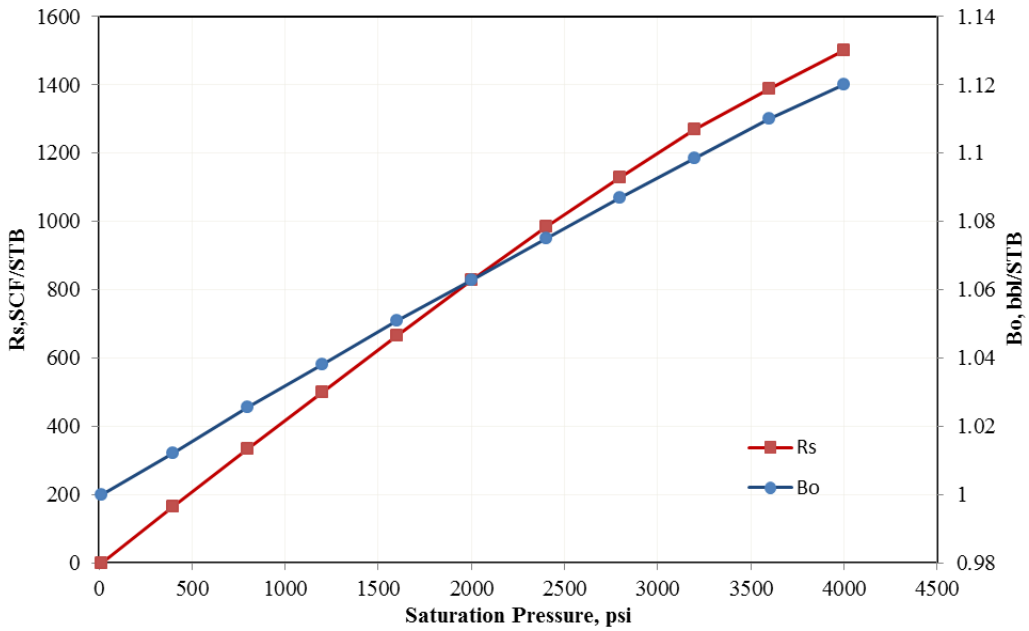

Figure 4.3 Oil formation volume factor and solution gas oil ratio.

Maximum oil rates for producers are 1500 STB/D, and minimum following bottom hole pressure is 1000 psi. Between 300 days and 360 days, rate is lowered to 100 STB/D for all production wells. Maximum water injection rate for the injector is 5000 STB/D and the maximum bottomhole pressure is 4000 psi. All producers are completed in layers 2, 3, 4 and injector completed in layers 11,12,13,14, and 15. Water injection well is located in the corner of the grid at grid block (24, 25).

A geostatistically generated permeability field with high degree heterogeneity is supplied for the problem. Figure 4.4 presents permeability values of layer 2 and layer 3. Permeability distribution has a correlation length in the *X* direction about 1800 feet or 6 grid blocks. Permeability values show a large variation between 0.0031 mD to 10,053 mD.

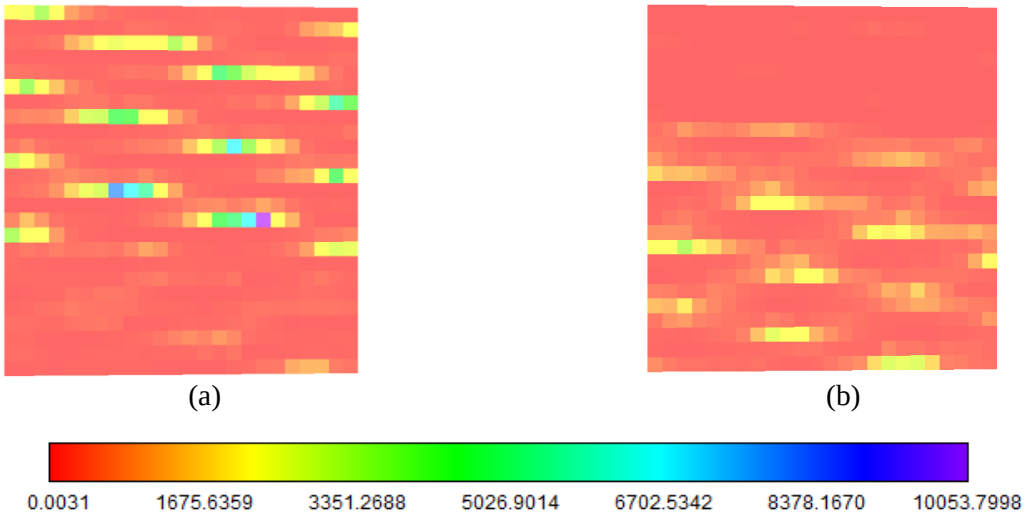

Figure 4.4 Permeability distribution for (a) layer 2 and (b) layer 3.

4.3 Results and Discussion

Table 4.2 gives the fluid in-place values for each simulator. All simulators gives the same initial fluid in place results.

Table 4.2 Initial in place results for each simulator

Simulator	Oil in-Place MMSTB	Water in-Place MMSTB	Gas in-Place, MMSCF
Eclipse	216	212	301
Sensor	216	212	301
COZSim	216	212	301

Hydrocarbon gas appears right after the start of the simulation because of the pressure decline in the reservoir and percolates to top of the reservoir and formed a secondary gas cap. Also, water invades from the aquifer and causes high water production in wells that is close to water-oil contact.

Figure 4.5 shows field cumulative oil, gas and water production for COZSim, Eclipse 100 and Sensor. Cumulative oil production results shows very similar trend for each simulator. Cumulative oil production at the end of 900 days simulation is 18.8, 18.6 and 18.0 MMSTB for Sensor, Eclipse and COZSim respectively. Cumulative gas and water production profiles also show a good agreement for each simulator. However, cumulative water production values give a wider range of results compared with the oil production profiles. Eclipse gives the highest cumulative water and gas production whereas Sensor gives the lowest one.

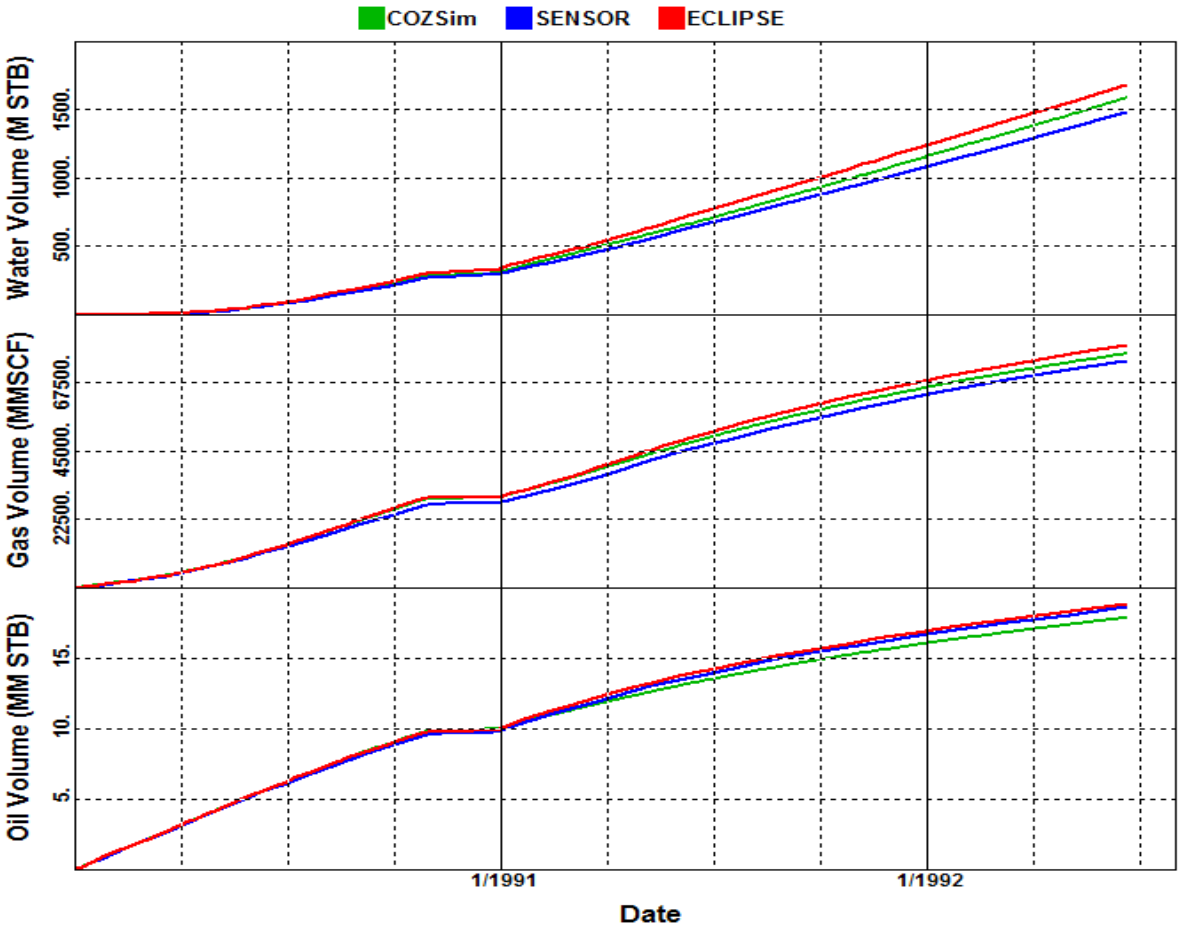

Figure 4.5 Cumulative oil, gas and water production of reservoir.

COZSim takes smaller time steps compared to other simulators. After the date 1/1991 COZSim gives less oil rate compared to other two simulators for about six months. This difference can be referred to productivity index calculations, because bottom hole pressure

profiles agree quite well for all simulators. This difference is also reported by Killough (1995). Gas and water production rate profiles are very similar for each simulator. Eclipse water production rates are slightly higher for about 6 months compared to other simulators.

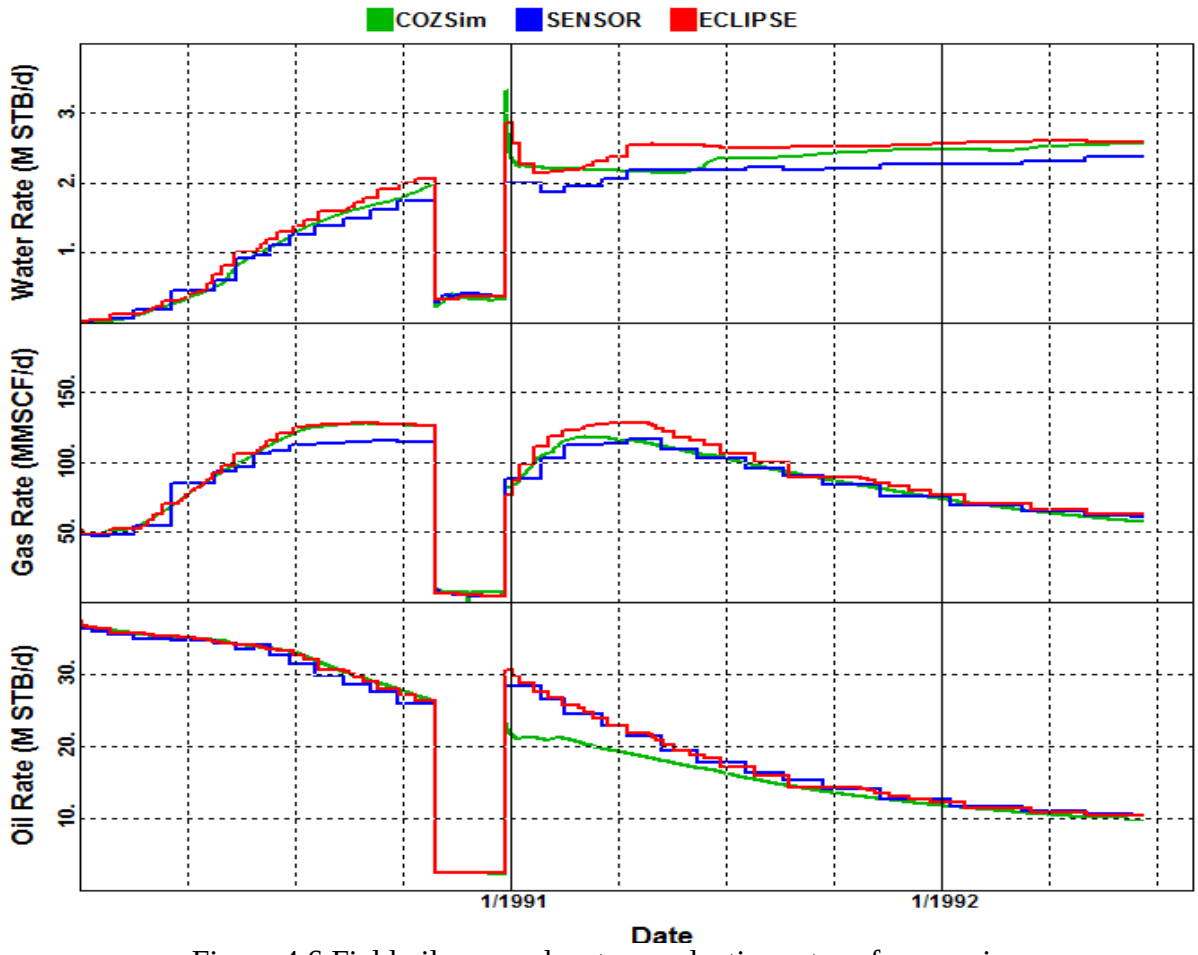

Figure 4.6 Field oil, gas and water production rates of reservoir.

4.4 Conclusions

Ninth SPE Comparative Solution project is implemented to create a benchmark base line between the simulators. The objective was to provide assurance that results of the COZSim, Eclipse and Sensor were compatible with each other for challenging reservoir simulation problems. The results from each simulator provide confirmation that the results are consistent for all simulators.

CHAPTER 5

CONCEPTUAL MODELS FOR SIMULATION STUDIES

This chapter introduces conceptual simulation models used throughout main oil zone studies. Model configurations, fluid system, petrophysical data, operation parameters and case designs are explained.

5.1 Model Configurations

This section describes the static model configuration used throughout this study. These configurations include planar, cross-sectional and 3D static models.

5.1.2 Planar Models

2D planar models are designed to investigate the effect of viscous fingering effects. The quarter five spot pattern indicated as grey in the Figure 5.1 shows the study area. Corresponding area is 60 acre with an injection and production well. Reservoir boundaries are considered as no-flow boundary.

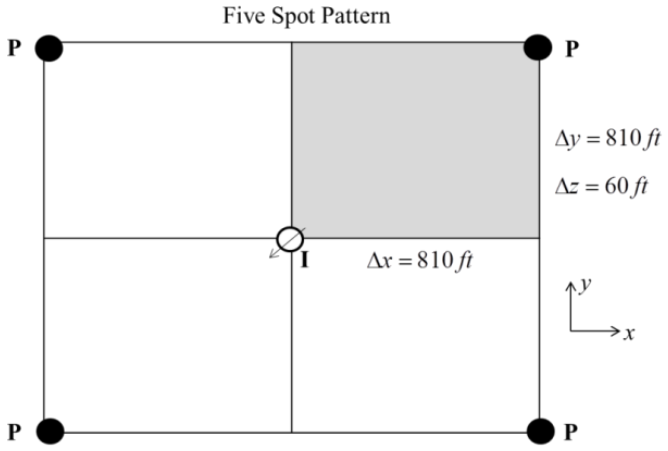

Figure 5.1 2D planar quarter five spot displacement model.

5.1.3 Cross-Sectional Models

2D cross-sectional line-drive displacement models were implemented to examine the viscous and gravity effects. Vertical pattern is presented in Figure 5.2. The distance between injector and producer is 1000 ft. Injector is placed in the middle of the first grid block (far left) and producer is placed in the middle of the last grid block of the model.

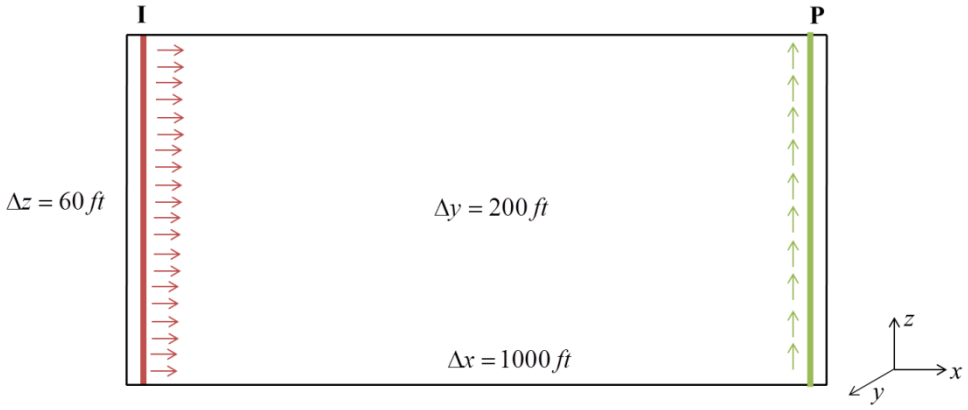

Figure 5.2 Two-dimensional cross-sectional line-drive displacement model.

5.1.4 3D Models

3D models are used to investigate unstable displacement created by both viscosity and gravity differences. Simply, 3D model is a quarter five spot pattern displacement which is same with planar configuration except 3D models have multiple layers.

5.1.5 The Grid Structure

For all cases five point discretization in two dimensions and seven point discretization in three dimensions are used. Cartesian grid is oriented as a diagonal grid at 45 degrees to the injector-producer pair to avoid grid orientation effects as possible.

Grid size is selected using several runs for each case. For example, a series of grid changing from 5x5, 10x10, 15x15, 20x20, 30x30, 40x40, 60x60 and 80x80 is used for planar configurations. Then, the coarsest grid is chosen based on the cumulative oil and gas production and oil and gas rates, where finer grid size does not affect the results. Similar procedure is used for cross-sectional and 3D configurations. A 20x20 grid is selected as the coarsest grid to investigate viscous fingering effects in detail for planar models.

5.2 Reservoir Fluid System

Postle field fluid system is selected to use in this study. PVT data acquired from a published reservoir characterization project (Heris, 2011). In this project, Peng-Robinson equation of state (EOS) model was tuned to produce a reasonable representation of the fluid and also predicted the phase behavior of the Postle oil with undergoing miscible CO_2 injection process. Therefore, 25-component Postle oil was reduced to 4-pseudo component as shown in Table 5.1. Postle fluid system contains a large fraction of light and intermediate components which creates a relatively light oil system.

Table 5.1 Pseudo-components of Postle Oil

Component	**Molar fraction, %**
CO_2	0.24
C_1	30.14
C_2-C_6	31.64
C_{7+}	37.98

CO_2 was added to the fluid system as a separate compound to mimic CO_2 injection process. Peng-Robinson EOS was used to match simulation results with laboratory experiments which are constant composition expansion (CCE), differential liberation (DL), separator test, swelling test and slim tube minimum miscibility pressure (MMP) test (Heris, 2011). Table 5.2 summarizes the simulated temperature and saturation pressure, estimated MMP, viscosity ratio and oil and gas properties for Postle fluid system.

Table 5.2 PVT properties of Postle fluid system

Property	Value
Reservoir temperature	147 °F
Bubble point pressure	1625 psia
Oil gravity	38.8 API
Minimum miscibility pressure	2100 psia
Viscosity ratio (μ_o/μ_{CO2}) at 1625 psi	35

CO_2 solubility in water values is acquired from Eclipse "CO2SOL" option which is based on the correlation of Chang, Coats and Nolen (1996). Figure 5.3 shows CO_2 solubility in water as a function of pressure. Solubility values of CO_2 in water will used in residual oil zone studies.

5.3 Black-Oil Fluid Generation

Sensor "BLACKOIL" option is used to generate black-oil PVT tables from the multi-component compositional data to use in Eclipse solvent model and COZSim. Sensor "BLACKOIL" option uses constant volume depletion method of compositional reservoir fluid description proposed by Whitson and Torp (1983) to obtain both saturated and undersaturated

black-oil data. Black-oil pseudoization process preserves the densities and viscosities of the pseudo-components (surface gas and oil) and produces PVT tables of B_o, R_s, μ_o, B_g, μ_g versus pressure. Generated black-oil fluid property tables agree quite well with experimental data. CO_2 properties for black-oil simulators are shown in Figure 5.4.

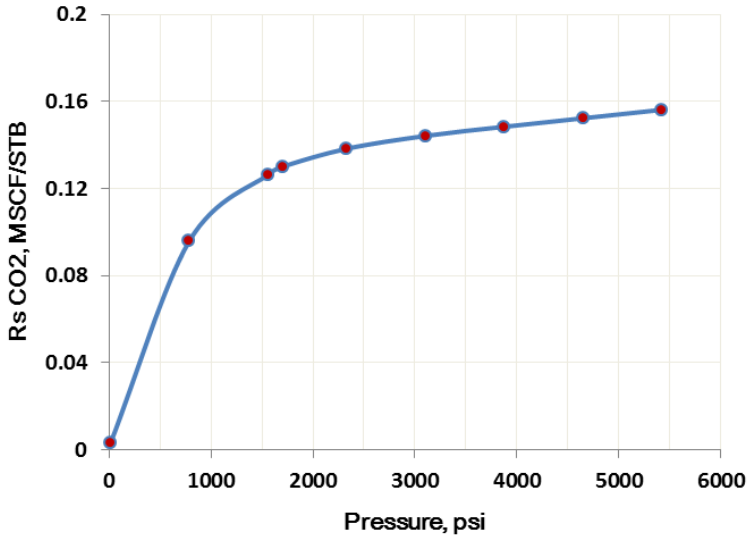

Figure 5.3 Solubility of CO_2 in water as a function of pressure

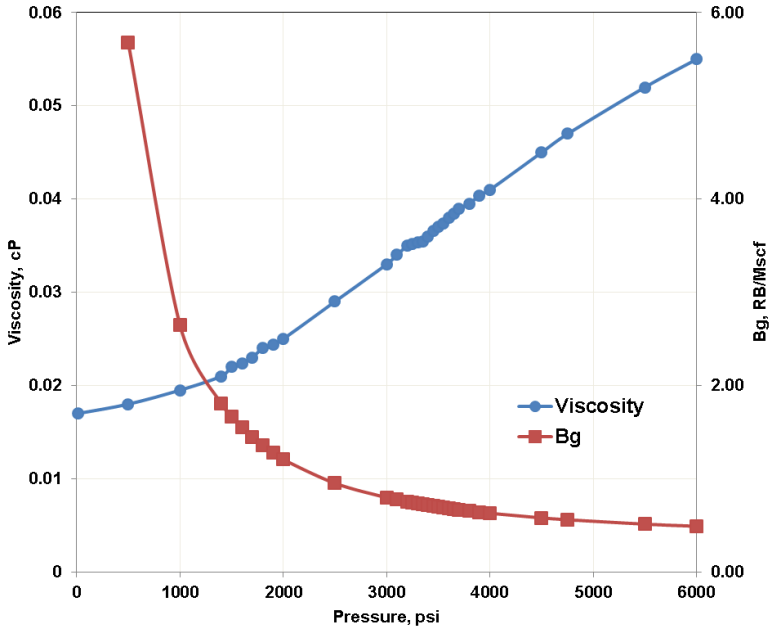

Figure 5.4 CO_2 properties for black-oil simulators

5.4 Petrophysical Data

Relative permeability data is generated with analytical expressions using end-point values of Postle field intermediate quality reservoir. Relative permeability data is given in Table 5.3, and relative permeability curves are illustrated in Figure 5.5 and Figure5.6.

Haajizadeh et al. (1999) state that oil and gas capillary pressures have very small effect on production profile except for oscillations created by CO_2 displacements in main oil zone. They indicate that capillary pressure effects are mainly seen in the transition zones because the saturation gradients are more variable. Therefore, capillary pressures are ignored in main oil zone study and assumed to be zero to simplify the problem.

Porosity and permeability values of medium quality zone of Postle field are used for homogenous cases presented in Table 5.4. All configurations are treated as homogenous and isotropic.

Table 5.3 Relative permeability data

Property	**Value**
Connate water saturation S_{wc}	0.2
Residual oil saturation to water, S_{orw}	0.3
Residual oil saturation to gas, S_{org}	0.18
Critical gas saturation, S_{gc}	0.02

Table 5.4 Porosity and permeability values for all cases

Property	Value
Porosity	0.18
Permeability X-direction, k_x	32.7 md
Permeability Y-direction, k_y	32.7 md
Permeability Z-direction, k_z	1.0 md

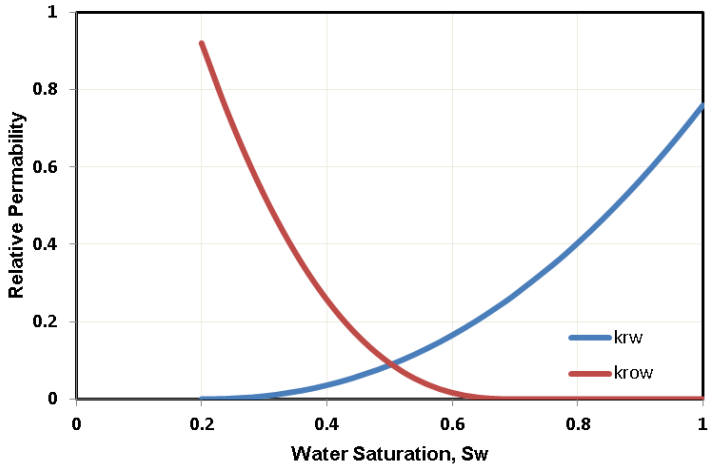

Figure 5.5 Oil and water relative permeability.

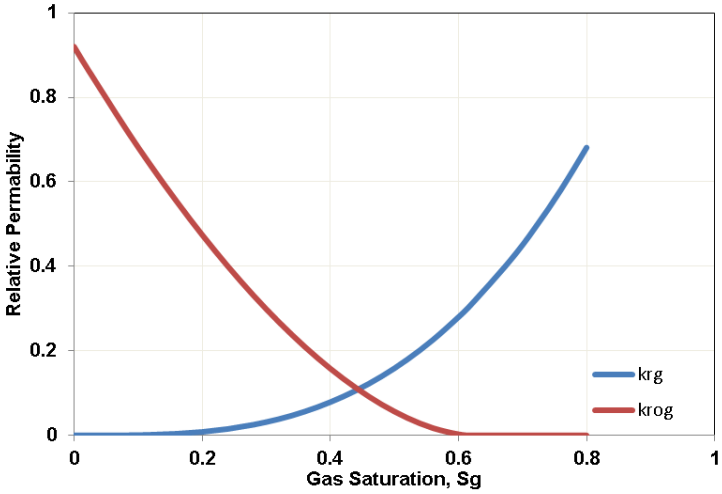

Figure 5.6 Oil and gas relative permeability.

5.6 Operation Parameters and Case Designs

Wells are completed through the all layers, and producer well operates with constant bottom hole pressure control for all cases. Injection well is controlled by constant CO_2 injection rate. Multiple drive mechanisms are used to investigate unstable displacement of CO_2. First contact miscibility (FCM), multi contact miscibility (MCM) and immiscible CO_2 injection cases are designed using the same fluid and petrophysical data. Well operation parameters and initial pressure of reservoir are changed to create different mechanisms of CO_2 displacement.

Saturation pressure and overall composition (Psat - z) diagram is created using Flash calculations of Sensor compositional simulator to identify first contact miscibility pressure limits. Figure 5.7 shows Psat – Mole fraction diagram for Postle field fluid system. As can be seen from Figure 5.7, maximum pressure in P_{sat} vs z diagram is ~5000 psi. If minimum operating pressure is higher than that value, CO_2 displacement mechanism will be considered as first-contact miscibility (Stalkup, 1983; Coats et al., 2007) On the other hand, if maximum operating pressure is less than MMP, CO_2 displacement mechanism will be immiscible displacement. Any case between those limits corresponds to MCM. Table 5.5 presents operating parameters for each case.

Table 5.5 Miscibility operating parameters

Parameter	FCM	MCM	Immiscible
Initial Pressure, psi	5400	3500	1700
Production Well Bottom Hole Pressure, psi	5100	3200	1400
Injection Well Maximum Bottom Hole Pressure, psi	5900	3900	2000

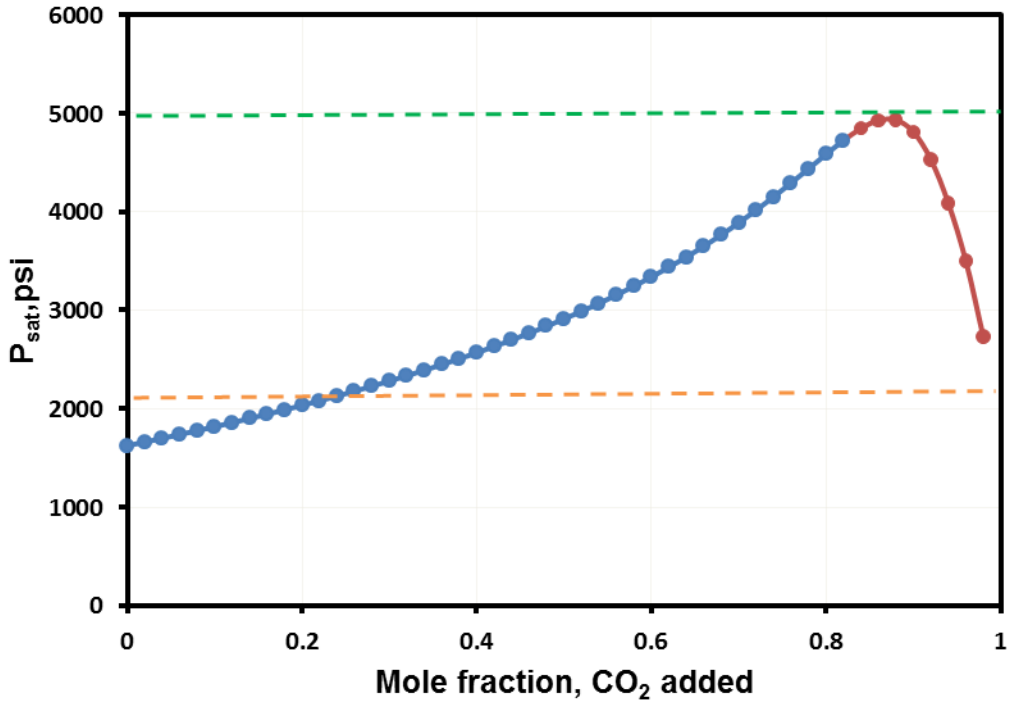

Figure 5.7 Saturation pressure versus mole fraction of CO_2 added.

5.7 Selection of Viscous Fingering Parameters

Koval's viscous fingering parameter (dispersion control coefficient-K) is calculated using viscosity ratio of reservoir oil and CO_2 from the following equation:

$$K = \left[0.78 + 0.22 \left(\frac{\mu_o}{\mu_s} \right)^{1/4} \right]^4 \tag{5.1}$$

Dispersion control coefficient for this fluid system at 1625 psi is approximately 3.00. Two different K parameters (3.00 and 5.00) are used throughout the study for sensitivity analysis. Contrary to Koval's method, there is no method to calculate Todd-Longstaff mixing parameter (w). An equation can be used analogous to Koval's Method (User Guide IMEX, 2012):

$$\omega = \frac{1 - 4\log\left(0.78 + 0.22\left(\mu_o/\mu_s\right)^{1/4}\right)}{\log\left(\mu_o/\mu_s\right)} \tag{5.2}$$

Equation 5.2 yields approximately a mixing parameter equal to 0.4. Two mixing parameters (0.4 and 0.7) are used throughout the study for sensitivity analysis.

CHAPTER 6

IMMISCIBLE FLOODING IN MAIN OIL ZONE

This chapter presents the comparison of simulators for immiscible (near miscible) CO_2 flooding. Two dimensional planar, two dimensional cross-sectional and three dimensional models will be used throughout this chapter.

6.1 Description

Minimum miscibility pressure (MMP) is defined as the lowest pressure at which CO_2 can develop miscibility with the reservoir oil. Figure 6.1 shows that oil recovery is increasing with pressure and become flat after reaching the thermodynamic Minimum Miscibility Pressure (MMP) assuming 1-D CO_2 displacement, constant system pressure and little reservoir mixing (Jarrell et al, 2002). Minimum miscibility pressure is 2100 psi for the fluid system used in this study; thus for pressures less than MMP is treated as immiscible (or near miscible).

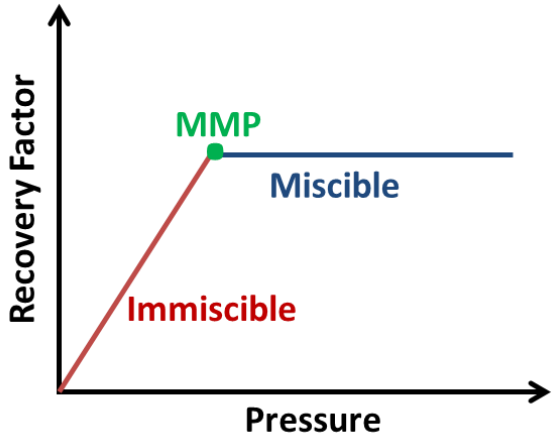

Figure 6.1 Pressure dependency of miscibility.

At pressures lower than the MMP, pressure is not high enough to sufficient CO_2 to dissolve into the oil or vaporize enough oil components to form miscibility. (Jarrell et al, 2002) CO_2 partition to oil and increase recovery with oil swelling and viscosity reduction. Oil swelling and oil viscosity reduction with CO_2 can be beneficial to mobilize some of the residual oil and increase the recovery.

Conceptual models explained in Chapter 5 are used. Table 6.1 summarizes operating parameters for immiscible CO_2 flooding study..

Table 6.1 Operating parameters for immiscible displacement

Parameter	Value
Initial Pressure, psi	1700
Production Well Bottom Hole Pressure, psi	1400
Maximum Injection Well Bottom Hole Pressure, psi	1900
Minimum Miscibility Pressure, psi	2100
Bubble Point Pressure, psi	1625

6.2 Results

This section presents the simulation results for immiscible CO_2 displacement study with planar, cross-sectional and three-dimensional static models for Eclipse and Sensor compositional simulators, Eclipse solvent model and COZSim. Sensor FCM option is not used in this chapter, because it is not capable to simulate immiscible CO_2 flooding.

6.2.1 Planar Model

Table 6.2 gives specific values for planar model. Initialization results for planar model are given in Table 6.3. All simulators give the same initialization results. Model is initialized with uniform 80% oil saturation and 20% water saturation (immobile). No free hydrocarbon gas is present in the system initially. Near the production well region will experience pressures below the bubble point pressure right after production start and thus free hydrocarbon gas will be produced.

Table 6.2 Parameters for immiscible planar model

Parameter	Value
Grid	20x20x1
Grid Block Size, ft	40.5x40.5x60
CO_2 Injection Rate, MSCF/day	250
CO_2-Reservoir Pore Volume at 1500 psi, MMMSCF	0.3

Table 6.3 Fluid in-place results for immiscible planar model

Property	Value
Oil In-Place, MSTB	736
Water In-Place, MSTB	249
Gas In-Place, MMSCF	439

Recovery performance predicted by simulators is shown in Figure 6.2. Figure 6.2 compares oil and gas rates and cumulative production and injection results for Sensor and Eclipse compositional simulators (with and without residual oil imposition-Sorg), Eclipse solvent model and COZSim. Sensor compositional and Eclipse compositional simulators give the

exact results for this problem. Likewise, Eclipse solvent model and COZSim predicts very similar cumulative production results and rates. Eclipse compositional simulator with residual oil imposition (E300-Sorg) predicts lower oil production and early breakthrough.

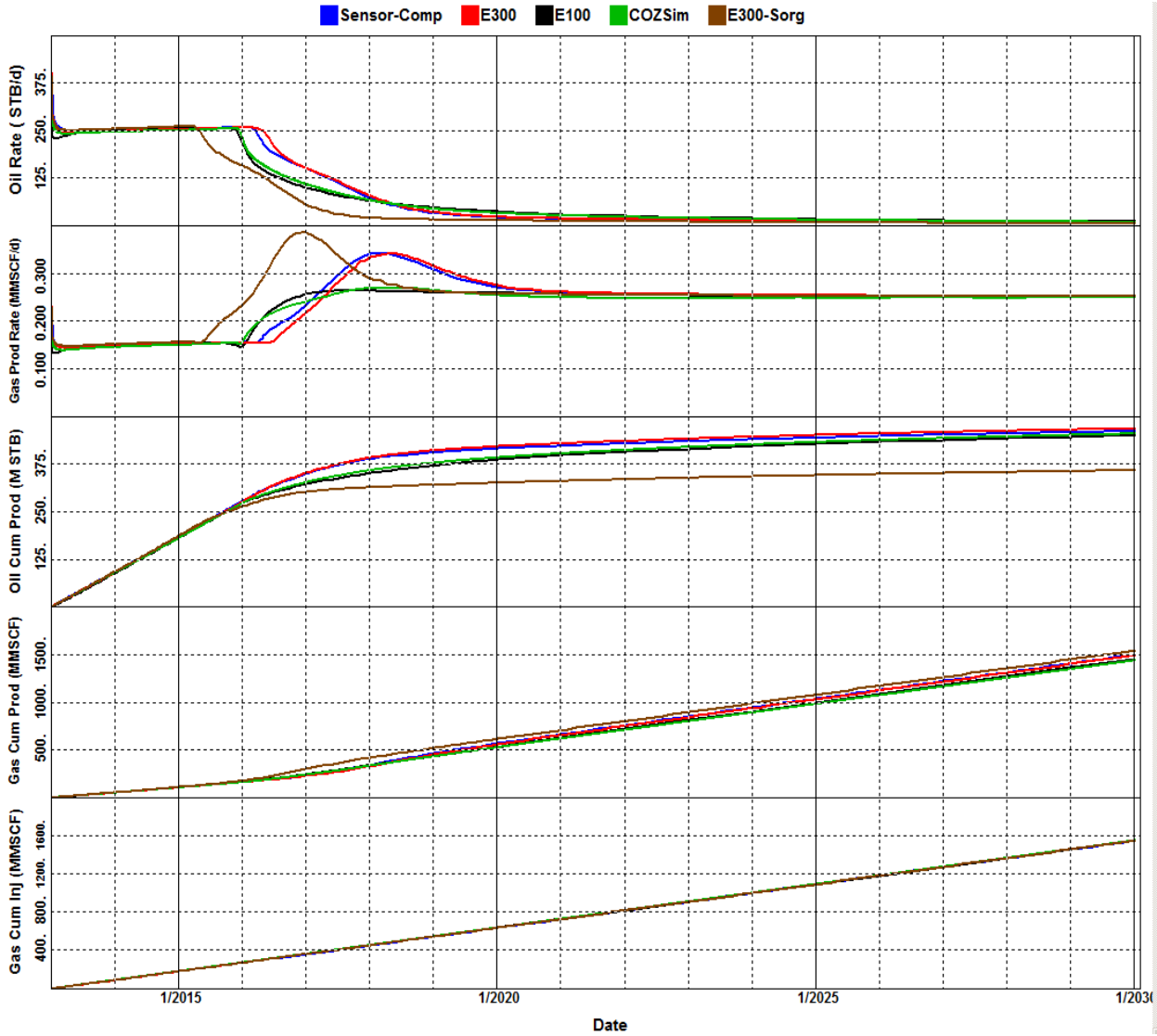

Figure 6.2 Recovery performance results of immiscible planar model for COZSim and Eclipse Solvent Model (E100), Sensor Compositional, Eclipse Compositional (E300) simulator and Eclipse Compositional simulator with residual oil saturation imposition (E300-Sorg).

Figure 6.3 shows gas saturation profiles at date 2015-1-1 after 2 years of continuous CO_2 injection (0.3 PVI). Gas saturation profiles are very similar for each simulator at that date because the difference in recovery values between compositional and extended black oil

simulators begins after compositional runs reach oil saturations below residual oil to gas (0.18) values at near well region. Residual oil (to gas) completely vaporizes with continuous gas injection and leaving zero oil saturation for compositional runs especially in near injection well, see Figure 6.4. COZSim and Eclipse solvent model gives slightly less oil recovery (maximum difference 10%) and early gas breakthrough (3-6 month) compared with compositional simulators because those are capable of the simulate residual oil saturation to gas injection.

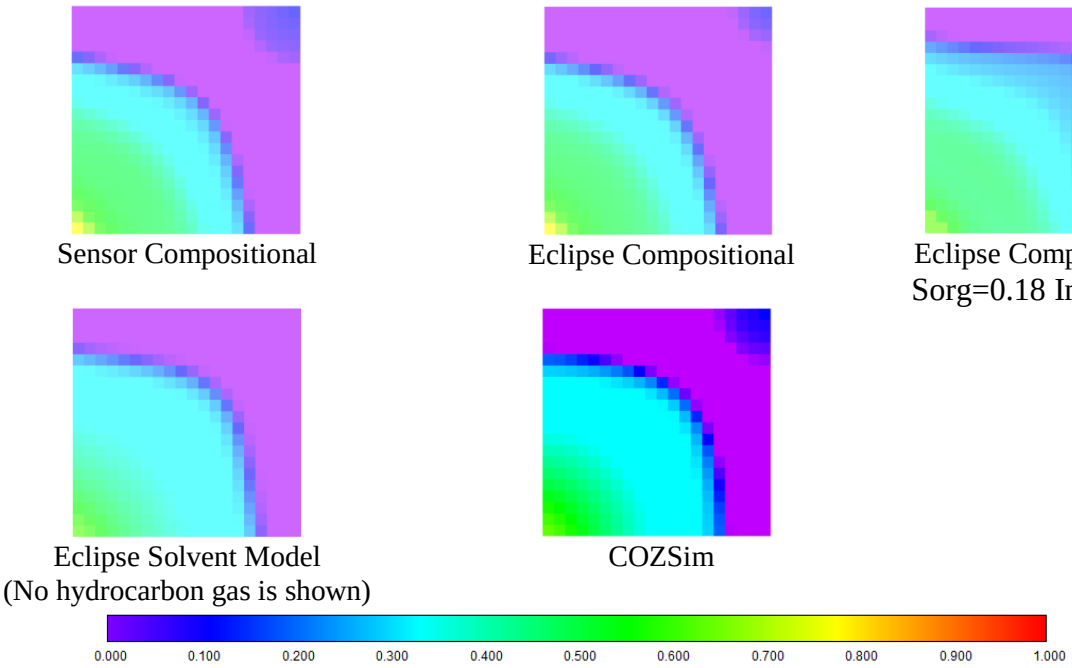

Figure 6.3 Gas saturation profile at 1/1/2015 (0.3 PVI) for immiscible planar case.

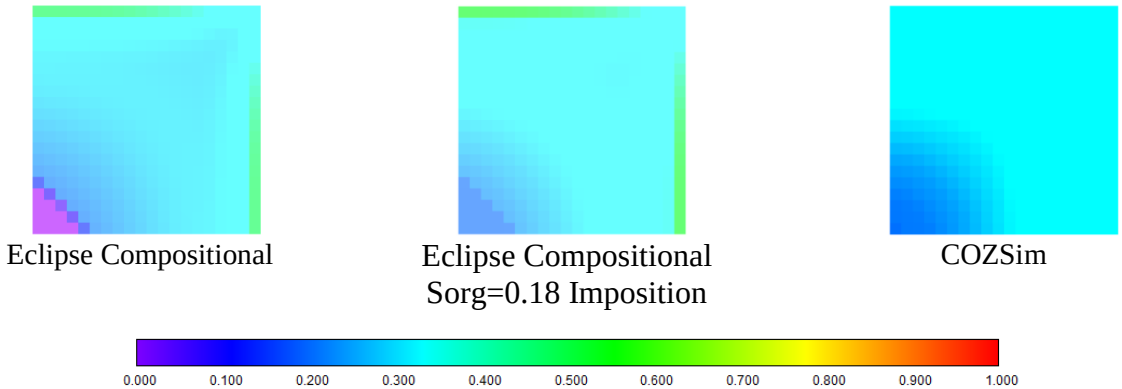

Figure 6.4 Oil saturation profile at 1/1/2030 (2.4 PVI) for immiscible planar case.

6.2.2 Cross-Sectional Model

Table 6.4 gives specific values for cross-sectional model. Initialization results are given in Table 6.5. All simulators give the same initialization results. Model is initialized with 80% oil saturation and 20% water saturation. No free hydrocarbon gas is present in the system.

Table 6.4 Parameters for immiscible cross-sectional model

Parameter	Value
Grid	20x1x20
Grid Block Size, ft	50x200x3
CO_2 Injection Rate, MSCF/day	100
CO_2-Reservoir Pore Volume at 1500 psi, MMMSCF	0.18

Table 6.5 Fluid in-place results for immiscible cross-sectional model

Property	Value
Oil In-Place, MSTB	224
Water In-Place, MSTB	75
Gas In-Place, MMSCF	134

Recovery performance results are shown in Figure 6.5. Figure 6.5 compares oil and gas rates and cumulative production and injection results for Sensor and Eclipse compositional simulator (with and without residual oil imposition-Sorg), Eclipse solvent model and COZSim. All simulators give similar production profiles for this case. Oil production for Eclipse solvent model and COZSim is slightly lower compared with compositional simulators. Also, Eclipse

Solvent Model and COZSim predict breakthrough time 6 months later than the compositional runs.

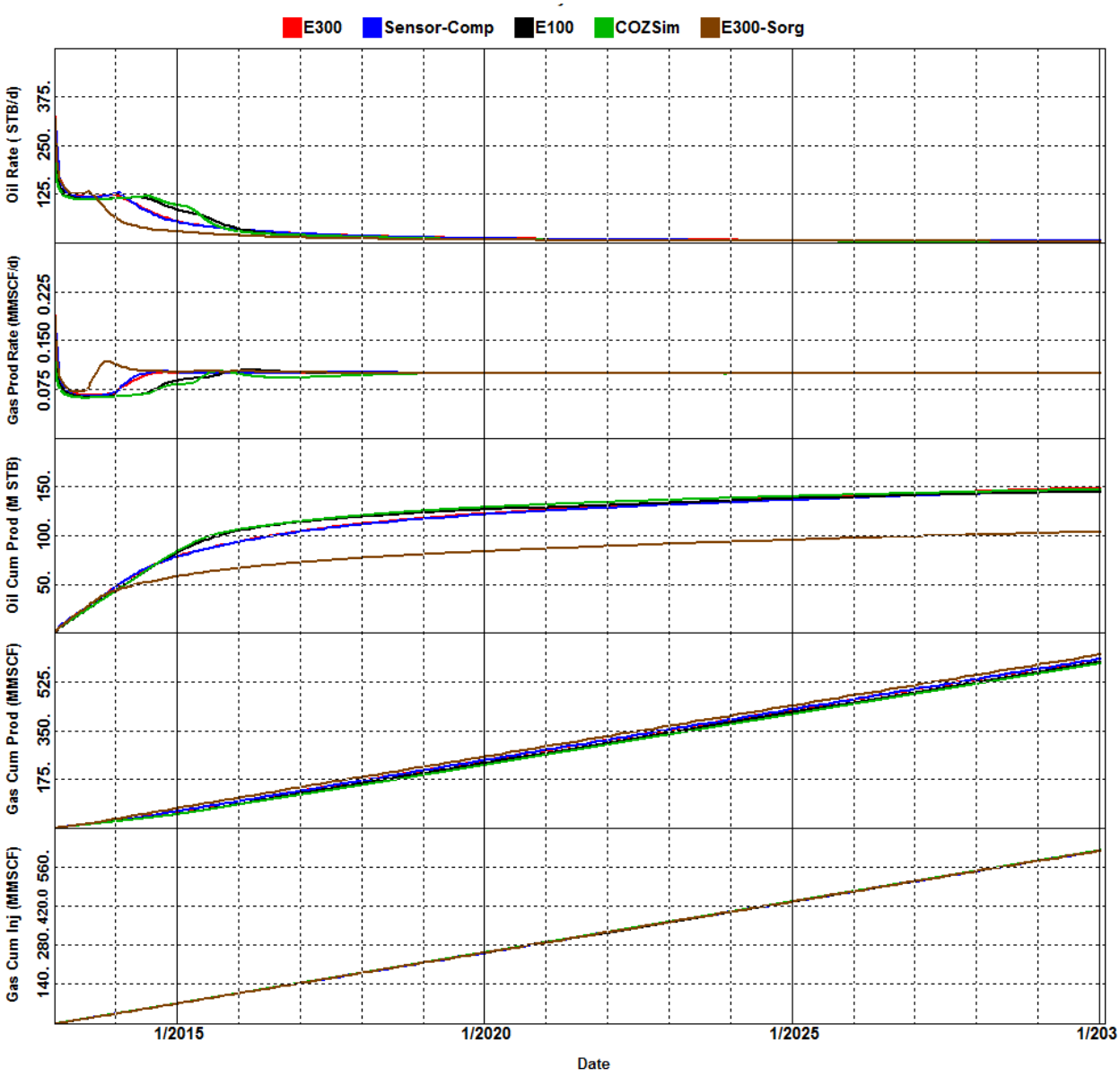

Figure 6.5 Recovery performance results of immiscible cross-sectional model for for COZSim and Eclipse Solvent Model (E100), Sensor Compositional, Eclipse Compositional (E300) simulator and Eclipse Compositional simulator with residual oil saturation imposition (E300-Sorg).

Figure 6.6 shows gas saturation profiles at the date 2014-1-1 after 1 year of continuous CO_2 injection (0.2 PVI). Because of the density difference between the reservoir oil and CO_2,

CO_2 percolates to top layer and reaches the production well. Eclipse solvent model and COZSim shows more piston-like displacement rather than the gravity-override displacement that compositional simulators predict.

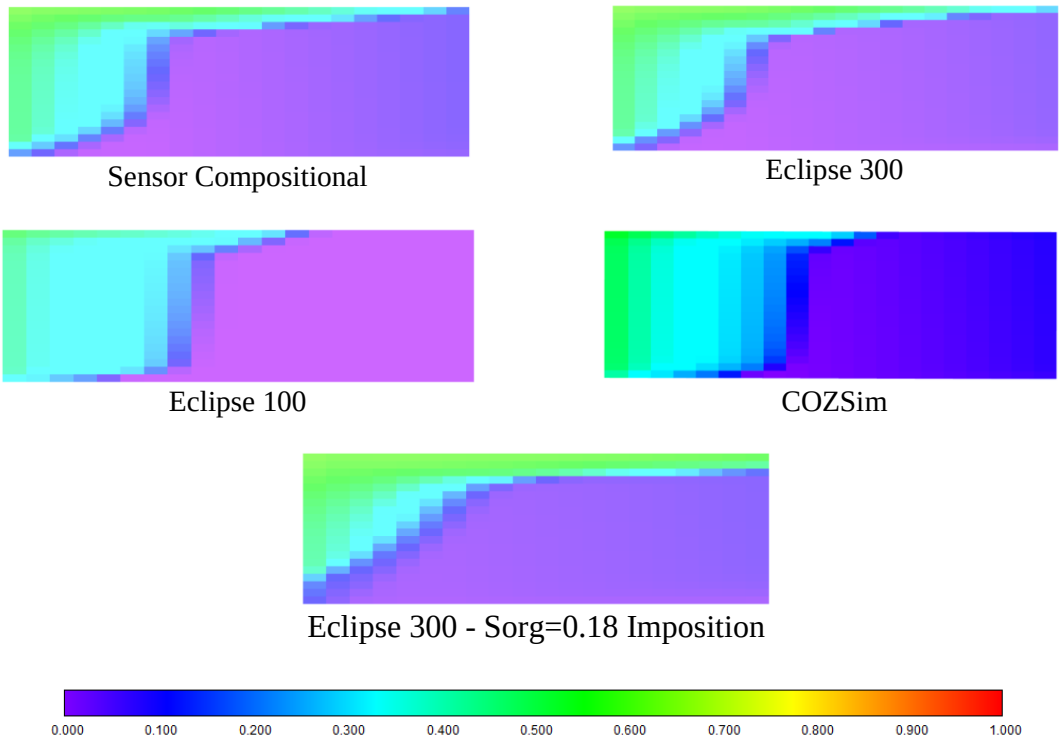

Figure 6.6 Gas saturation profile at 1/1/2014 (0.2 PVI) for immiscible cross-sectional model.

6.2.3 3D Models

Table 6.6 gives specific values for 3D model. 3D model configuration is identical to planar model except the number of layers, therefore initialization results are given in 6.3. All simulators give the same initialization results. Model is initialized with average 80% oil saturation and 20% water saturation. No free hydrocarbon gas is present in the system.

Figure 6.7 compares oil and gas rates and cumulative production and injection results for Sensor and Eclipse compositional simulator (with and without residual oil imposition-Sorg), Eclipse solvent model and COZSim for 3-D models. Results for each simulator agree well for

this problem similar to planar model. Compositional simulator predicts slightly more oil (5%) due to the complete vaporization of oil in near well region similar to planar model.

Table 6.6 Parameters for immiscible 3D model

Parameter	Value
Grid	10x10x10
Grid Block Size, ft	81x81x6
CO_2 Injection Rate, MSCF/day	250
CO_2-Reservoir Pore Volume at 1500 psi, MMMSCF	0.76

Figure 6.8 shows gas saturation profiles at date 2014-1-1 after 1 year of continuous CO_2 injection (0.2 PVI). Gas saturation profiles are very similar for each simulator at that date 1-1-2016 because the difference in recovery values between compositional and extended black oil simulators begins after compositional runs reach oil saturations below residual oil to gas (0.18) values at near well region. Residual oil (to gas) completely vaporizes with continuous gas injection and leaving zero oil saturation for compositional runs especially in near injection well, see Figure 6.9. Eclipse compositional simulator with residual oil imposition predicts early breaktrough time (6 months) and significantly lower oil production (40%)

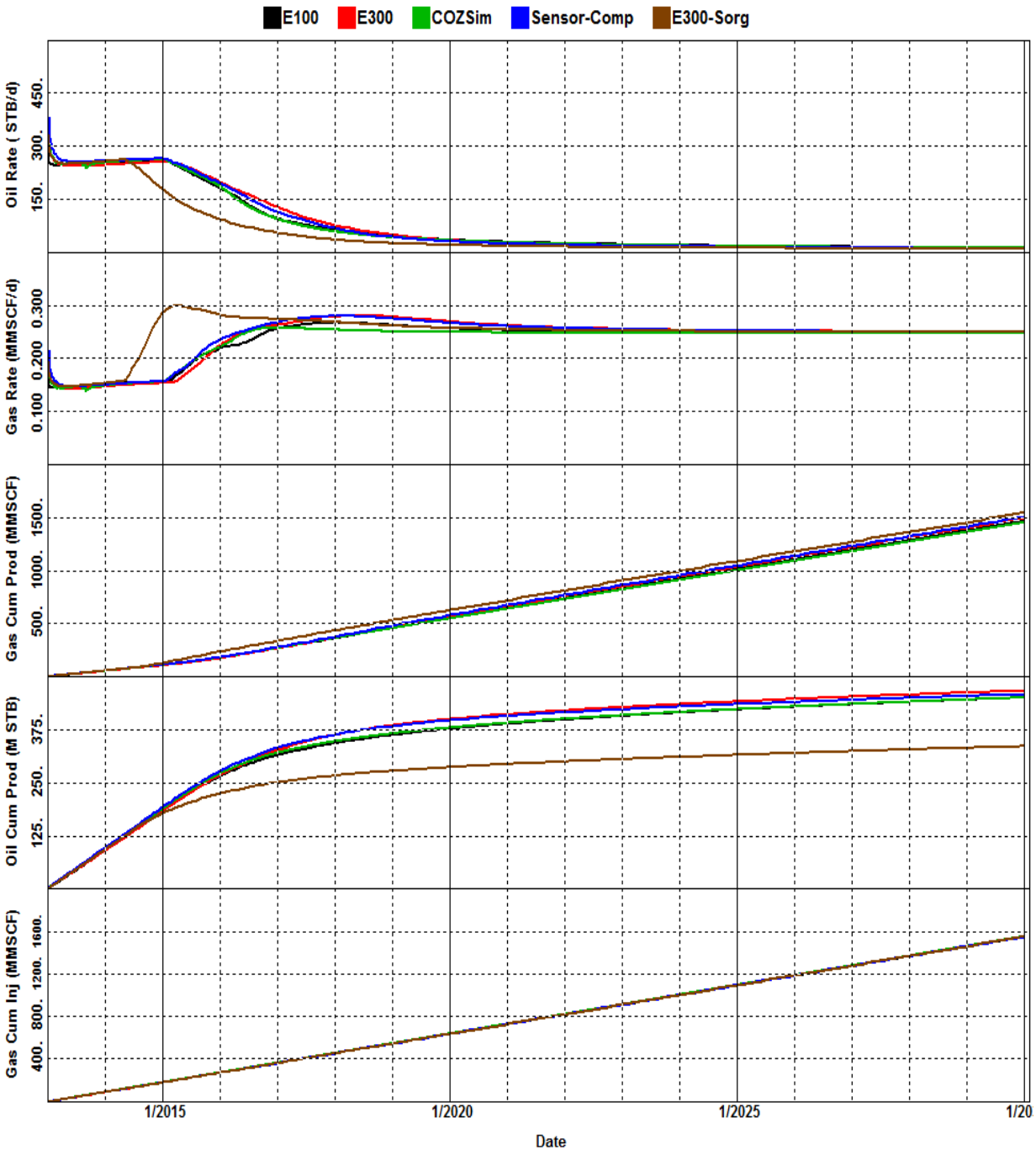

Figure 6.7 Recovery performance results of immiscible 3D model for Sensor compositional, Eclipse compositional (E300), Eclipse Compositional with Sorg imposition (E300-Sorg) and Eclipse 100 (solvent model) and COZSim.

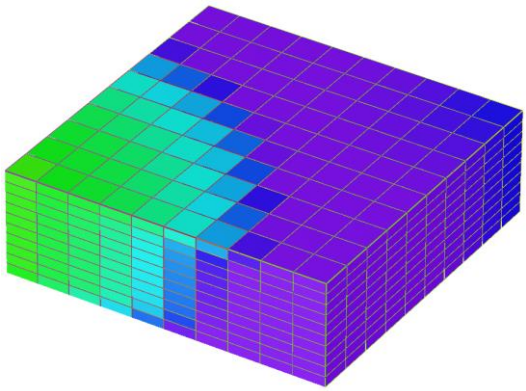

Sensor Compositional

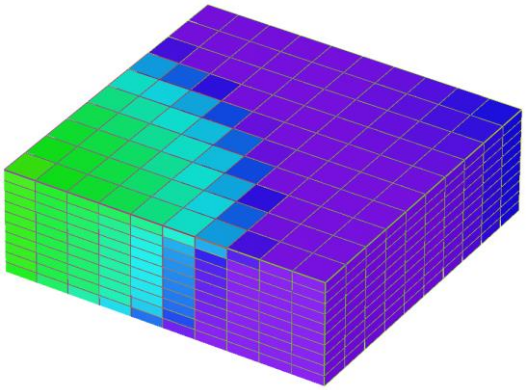

Eclipse Compositional

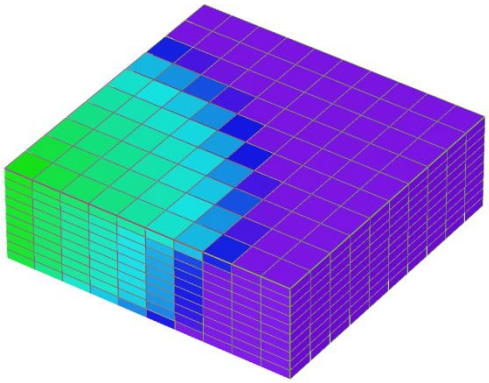

Eclipse Solvent Model

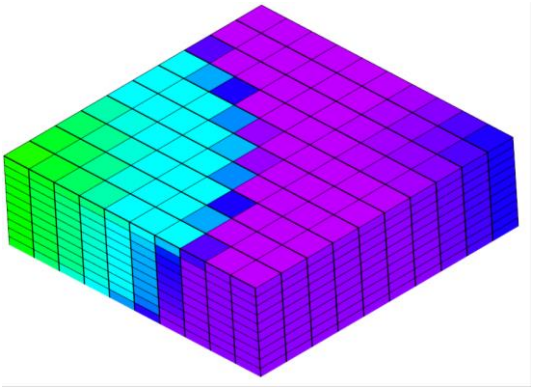

COZSim

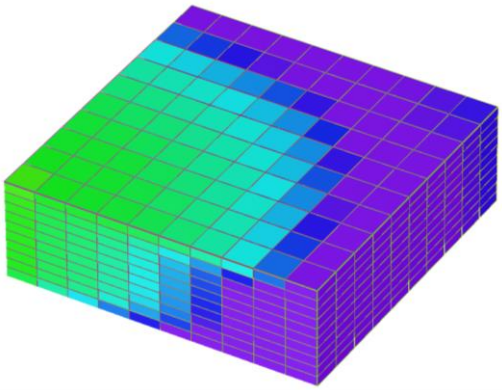

Eclipse Compositiona – Sorg=0.18

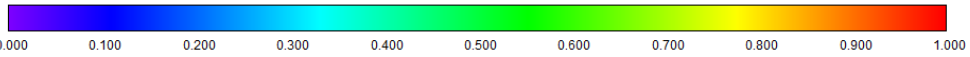

Figure 6.8 Gas saturation profile at 1/1/2014 (0.2 PVI) for immiscible 3D model.

CHAPTER 7

MULTI-CONTACT MISCIBLE FLOODING IN MAIN OIL ZONE

This chapter presents comparisons of simulators for multi-contact miscible CO_2 flood. Two dimensional planar, two dimensional cross-sectional and three dimensional models will be used throughout this chapter.

7.1 Description

The interface between gas and oil phases disappears and miscibility is achieved when interfacial tension (IFT) reduces to zero. Minimum miscibility pressure (MMP) is defined as the lowest pressure at which CO_2 can develop miscibility with the reservoir oil. Any CO_2 displacement case between minimum miscibility pressure and first contact miscibility pressure is considered as multi-contact miscible. The area between the green and orange pressure limit lines in Figure 7.1 corresponds to multi-contact miscibility (see Chapter 5.6 for details).

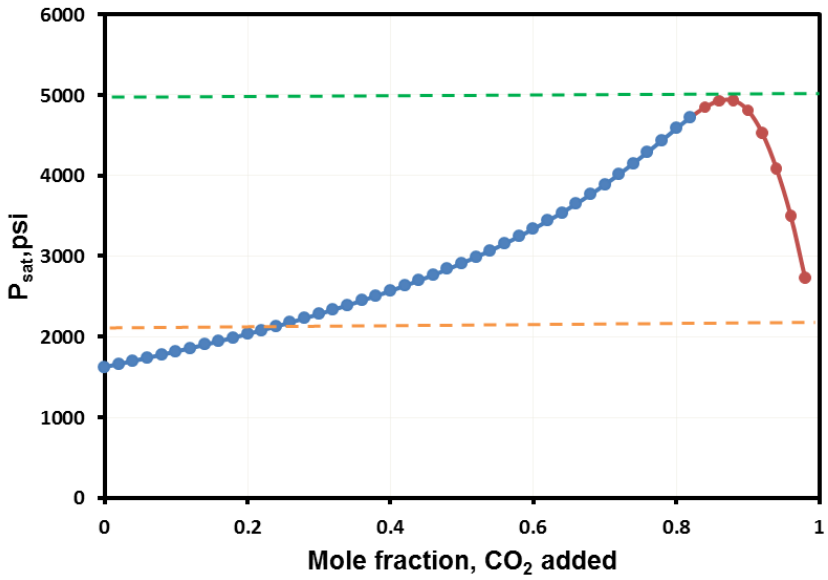

Figure 7.1 Saturation pressure versus mole fraction of CO_2 added.

Multi-contact miscibility mechanism can be described conceptually for the fluid system and operating parameters used in this study as following:

- The reservoir is initially saturated with original reservoir oil and immobile water.
- As CO_2 injection starts, saturation pressure rises (see Figure 7.1).
- When the oil near the injection well has around 60% of injected CO_2, oil and CO_2 forms 2 phase. As CO_2 injection continues, two phase region expands.
- When CO_2 near the injection well reach around 95% of injected CO_2, oil and CO_2 forms single phase again.

Operating parameters are explained in Chapter 5 is used. Table 7.1 summarizes multi-contact miscible fluid displacement parameters.

Table 7.1 Operating parameters for multi-contact miscible displacement

Parameter	Value
Initial Pressure, psi	3500
Production Well Bottom Hole Pressure, psi	3200
Minimum Miscibility Pressure, psi	2100
Bubble Point Pressure, psi	1625

7.2 Results

This section presents the simulation results for multi-contact miscible CO_2 displacement study with planar, cross-sectional and three-dimensional static models for Eclipse and Sensor compositional simulators, Eclipse solvent model and COZSim.

7.2.1 Planar Model

Table 7.2 gives specific parameters for planar model. Initialization results for planar model are given in Table 7.3. All simulators give the same initialization results. Model is initialized with uniform 80% oil saturation and 20% water saturation (immobile). No free hydrocarbon gas is present in the system.

Table 7.2 Parameters for multi-contact miscible planar model

Parameter	Value
Grid	20x20x1
Grid Block Size, ft	40.5x405x60
CO_2 Injection Rate, MSCF/day	500
CO_2-Reservoir Pore Volume at 3200 psi, MMMSCF	1.34

Table 7.3 Fluid in-place results for multi-contact miscible planar model

Property	Value
Oil In-Place, MSTB	774
Water In-Place, MSTB	250
Gas In-Place, MMSCF	463

Recovery performance predicted by simulators is shown in Figure 7.2 and Figure 7.3. Case names indicate the simulation specifications. For example a case name with Sorm represents that the simulation includes residual oil saturation to miscible displacement.

Figure 7.2 shows oil and gas rates and cumulative production and injection results for Sensor and Eclipse compositional simulators, COZSim and Eclipse solvent model. Results for Sensor and Eclipse compositional simulators and Eclipse solvent model with no mixing parameter (w=1) and zero residual oil saturation (Sorm=0.0) matches very well. COZSim predicts lower oil production and early breakthrough because it uses a built-in mixing parameter calculation based on the interfacial tension.

Figure 7.3 compares the Eclipse solvent model with different Todd-Longstaff mixing parameters (w). Also cases with residual oil saturation to miscible flooding are included. Lower mixing parameter (w) causes:

- Early gas breakthrough. The dominant factor is mixing parameter for breakthrough times. Breakthrough time range varies between about 1 year and 3 years.
- Lower oil production. If it is combined with residual oil saturation, cumulative oil recovery at the end of the simulation (~2.4 PVI) varies between 518 MSTB and 667 MSTB corresponding recovery factors of 0.70 and 0.86, respectively. Cumulative oil recovery at 1-1-2020 (~1.0 PVI) varies between 361 MSTB and 548 MSTB corresponding recovery factors of 0.47 and 0.7.
- Higher gas production. The variation of cumulative gas production is within 1-10% of the mean value. The main difference is the start time of the gas production.

Including residual oil saturation decreases the cumulative oil production, increases the cumulative gas production, and causes early gas breakthrough. Because the model initialized at

80% oil saturation, the effect of residual oil saturation is not dominant yet an important factor. Residual oil saturation after miscible flooding will be very important factor if the system is initialized with lower oil saturation, see chapter 9.

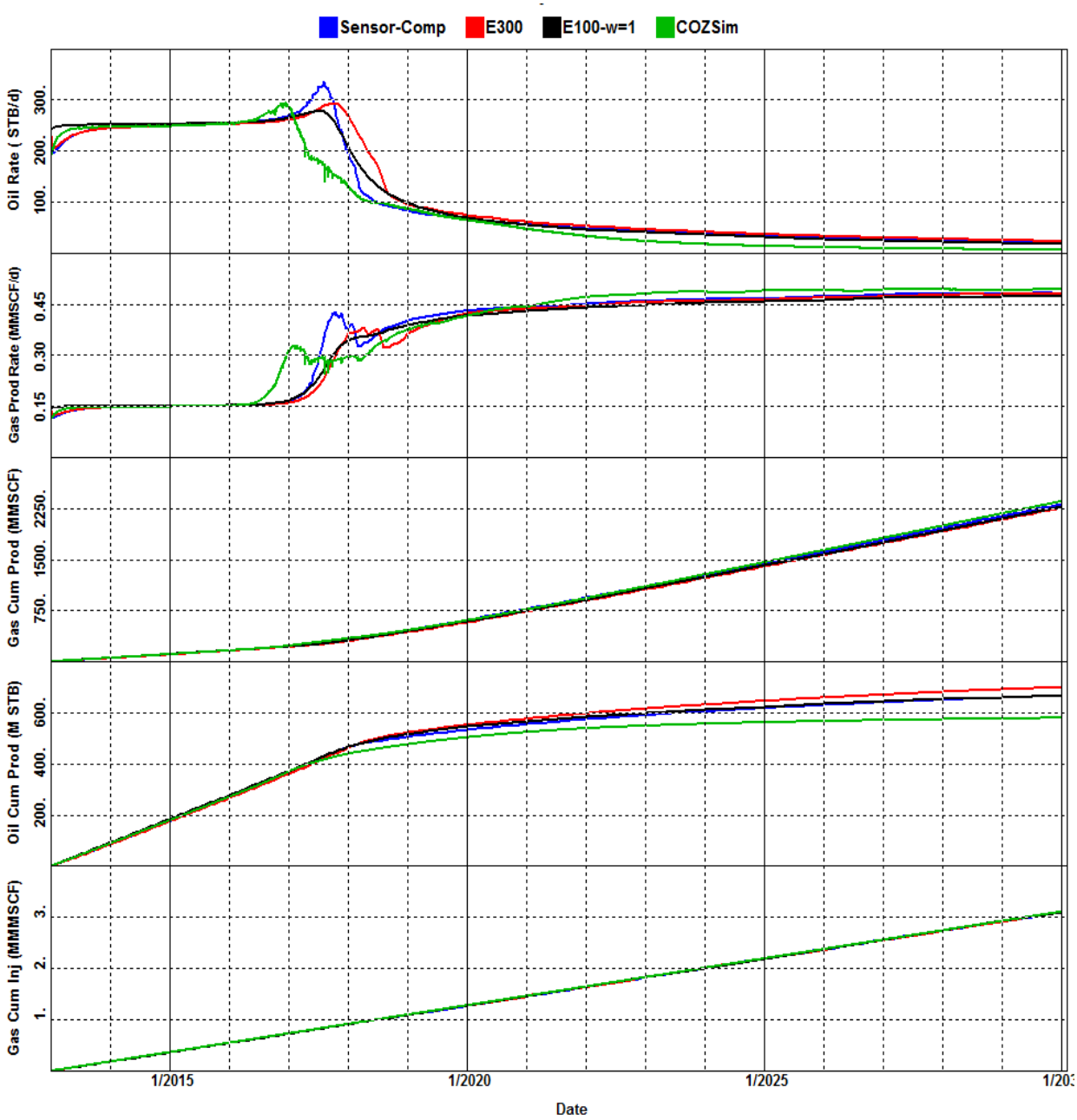

Figure 7.2 Recovery performance results of multi-contact miscibility planar model for COZSim and Eclipse Solvent Model (E100), Sensor Compositional and Eclipse Compositional (E300) simulators.

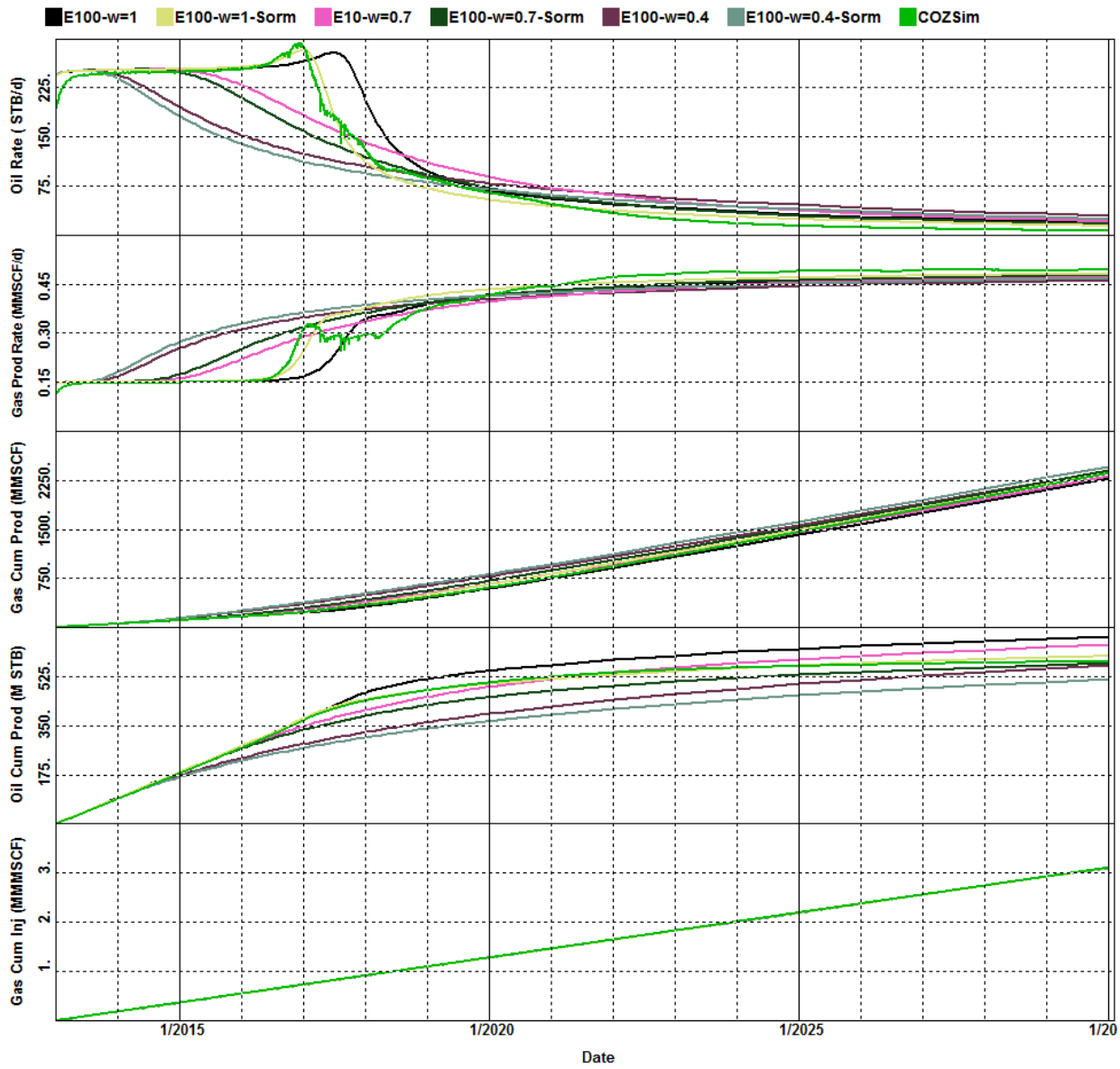

Figure 7.3 Recovery performance results of multi-contact miscibility planar model for Eclipse Solvent Model (E100) with different Todd-Longstaff mixing parameter (w) and residual oil saturation (Sorm=0.1), and COZSim.

COZSim does not use a constant mixing parameter like Eclipse Solvent Model. Mixing parameter values for COZSim varies between 0.5 and 0.9 as shown in Figure 7.5. Breakthrough time predicted by COZSim is between the times predicted by Eclipse Solvent Model with constant mixing parameter of 1.0 and 0.7. Because residual oil saturation to miscible flooding is not reached at COZSim, including Sorm to the system does not affect the production profiles.

Figure 7.4 compares gas saturation profiles at the date 1/1/2016 (0.4 PVI). Saturation profiles for Sensor Compositional, Eclipse Compositional and Eclipse solvent model (w=1, Sorm=0.0) matches very well. COZSim predicts larger gas saturation area because of the mixing parameter shown in Figure 7.6.

Figure 7.6 compares oil saturation at the date of 1/1/2016 (0.4 PVI). Compositional simulators leave zero oil saturation after continues CO_2 injection whereas Eclipse Solvent Model and COZSim is able to prevent complete sweep of oil and model residual oil saturation to miscible flooding.

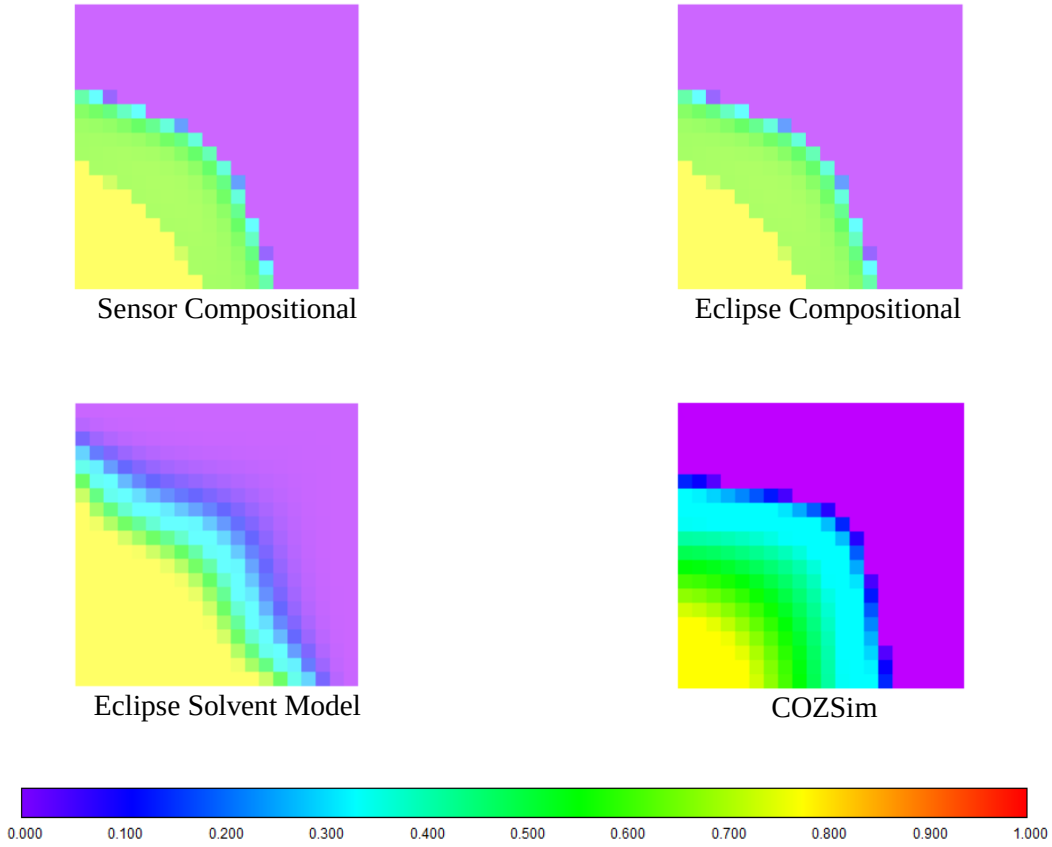

Figure 7.4 Gas Saturation at 1/1/2016 (0.4 PVI) for multi-contact miscibility planar model.

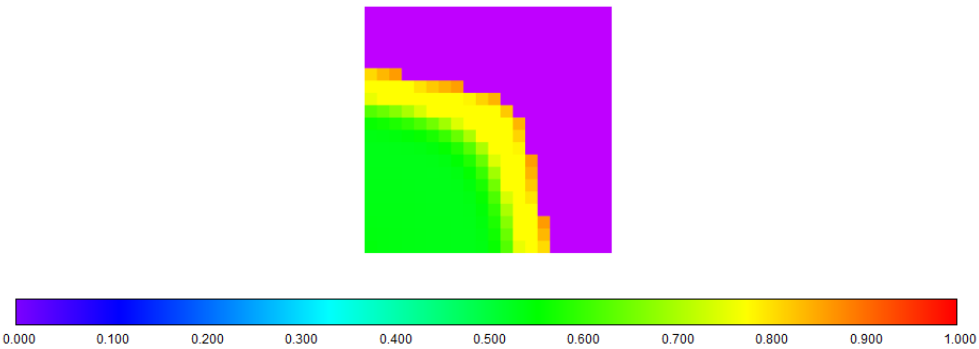

Figure 7.5 COZSim mixing parameter at 1/1/2016 for multi-contact miscibility planar model.

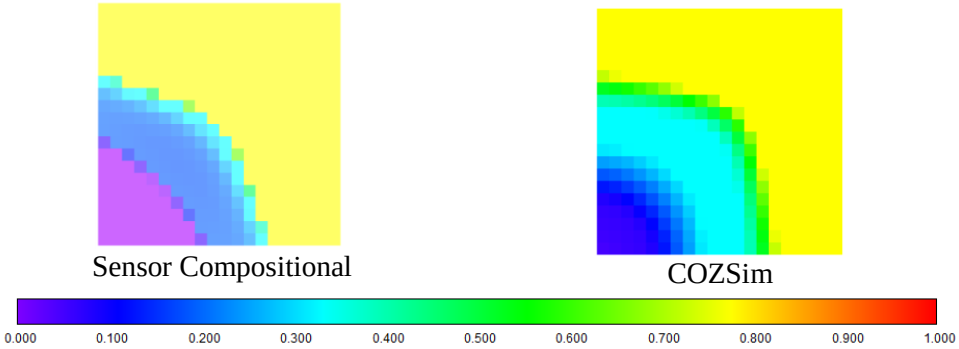

Figure 7.6 Oil saturation profile at 1/1/2016 (0.4 PVI) for multi-contact miscibility planar model.

7.2.2 Cross-sectional Model

Table 7.4 gives specific parameters for cross-sectional model. Initialization results are given in Table 7.5. All simulators give the same initialization results. Model is initialized with 80% oil saturation and 20% water saturation. No free hydrocarbon gas is present in the system.

Table 7.4 Parameters for multi-contact miscibility cross-sectional model

Parameter	Value
Grid	20x1x20
Grid Block Size, ft	40.5x200x40.5
CO_2 Injection Rate, MSCF/day	170
CO_2-Reservoir Pore Volume at 3200 psi, MMMSCF	0.41

Table 7.5. Fluid in-place results for multi-contact miscibility cross-sectional model

Property	Value
Oil In-Place, MSTB	236
Water In-Place, MSTB	76
Gas In-Place, MMSCF	141

Recovery performance predicted by simulators is shown in Figure 7.7 and Figure 7.7. Figure 7.7 shows oil and gas rates and cumulative production and injection results for Sensor and Eclipse compositional simulators, COZSim and Eclipse solvent model. Results for Sensor and Eclipse compositional simulators and Eclipse solvent model with no viscous fingering (w=1) and zero residual oil saturation (Sorm=0.0) matches very well. COZSim predicts lower oil production and early breakthrough because it uses a built-in mixing parameter calculation based on the interfacial tension. Figure 7.8 compares the Eclipse solvent model with different Todd-Longstaff mixing parameters (w) and COZSim. Similar to planar case, Eclipse Solvent model with viscous fingering imposition shows a wide range of oil production data and breakthrough time. Lower mixing parameter causes early gas breakthrough, lower oil production recovery factors and similar cumulative gas production. Mixing parameter values for COZSim varies between 0.44 and 0.8 as shown in Figure 7.10. Breakthrough time predicted by COZSim is between the times predicted by Eclipse Solvent Model with constant mixing parameter of 1.0 and 0.7. Production profile for COZSim is very similar to Eclipse solvent model with mixing parameter 0.7.

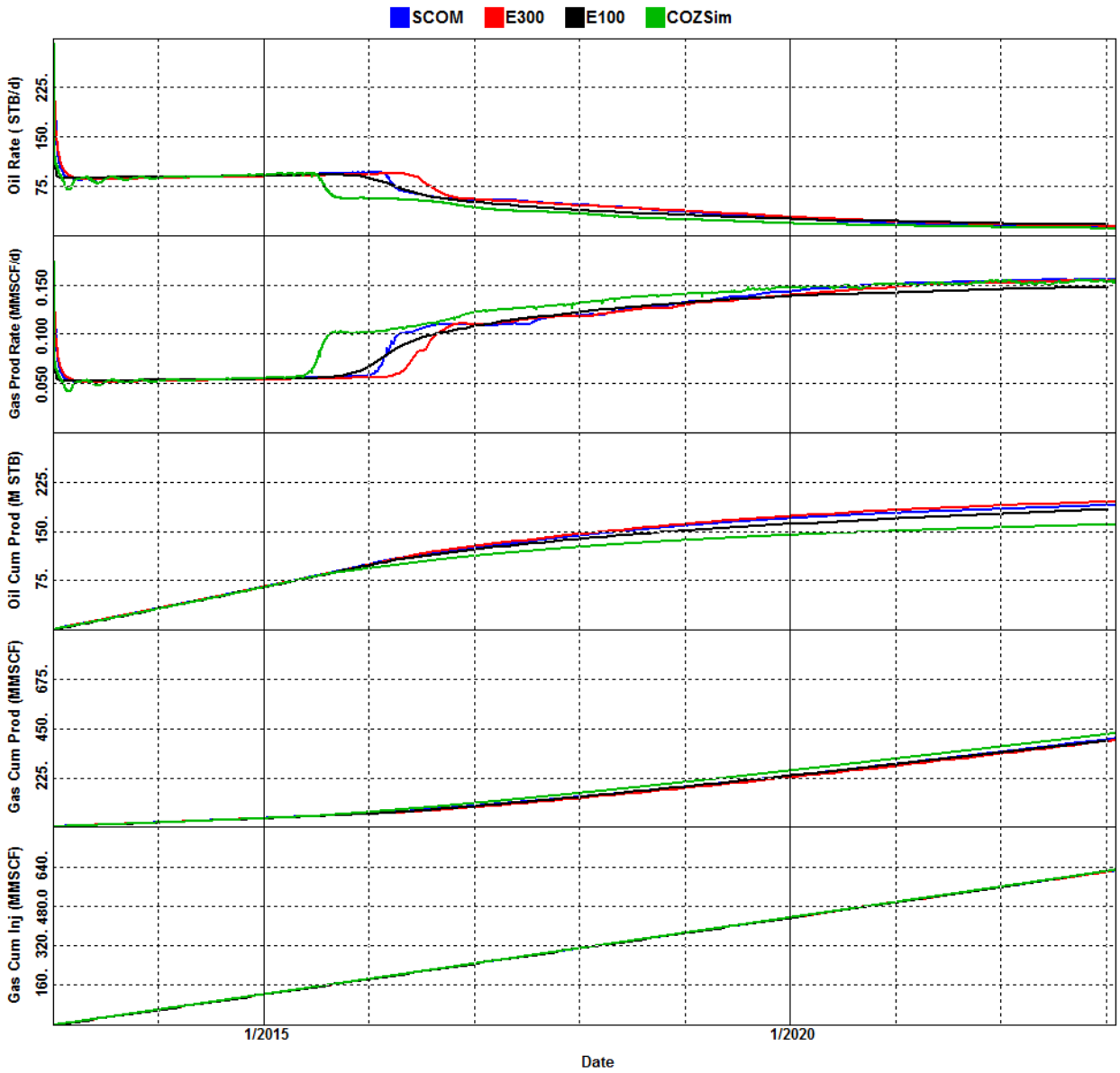

Figure 7.7 Recovery performance results of multi-contact miscibility cross-sectional model for COZSim and Eclipse Solvent Model (E100), Sensor Compositional, and Eclipse Compositional (E300) simulators.

Figure 7.9 compares gas saturation profiles at the date 1/1/2015 (0.3 PVI). Saturation profiles for Sensor Compositional, Eclipse Compositional and Eclipse solvent model (w=1, Sorm=0.0) matches very well. COZSim predicts larger gas saturation area because of the mixing parameter calculation.

Figure 7.11 compares oil saturation at the date of 1/1/2016 (0.4 PVI). Compositional simulators leave zero oil saturation after continues CO_2 injection whereas Eclipse Solvent Model and COZSim is able to prevent complete sweep of oil and model residual oil saturation to miscible flooding.

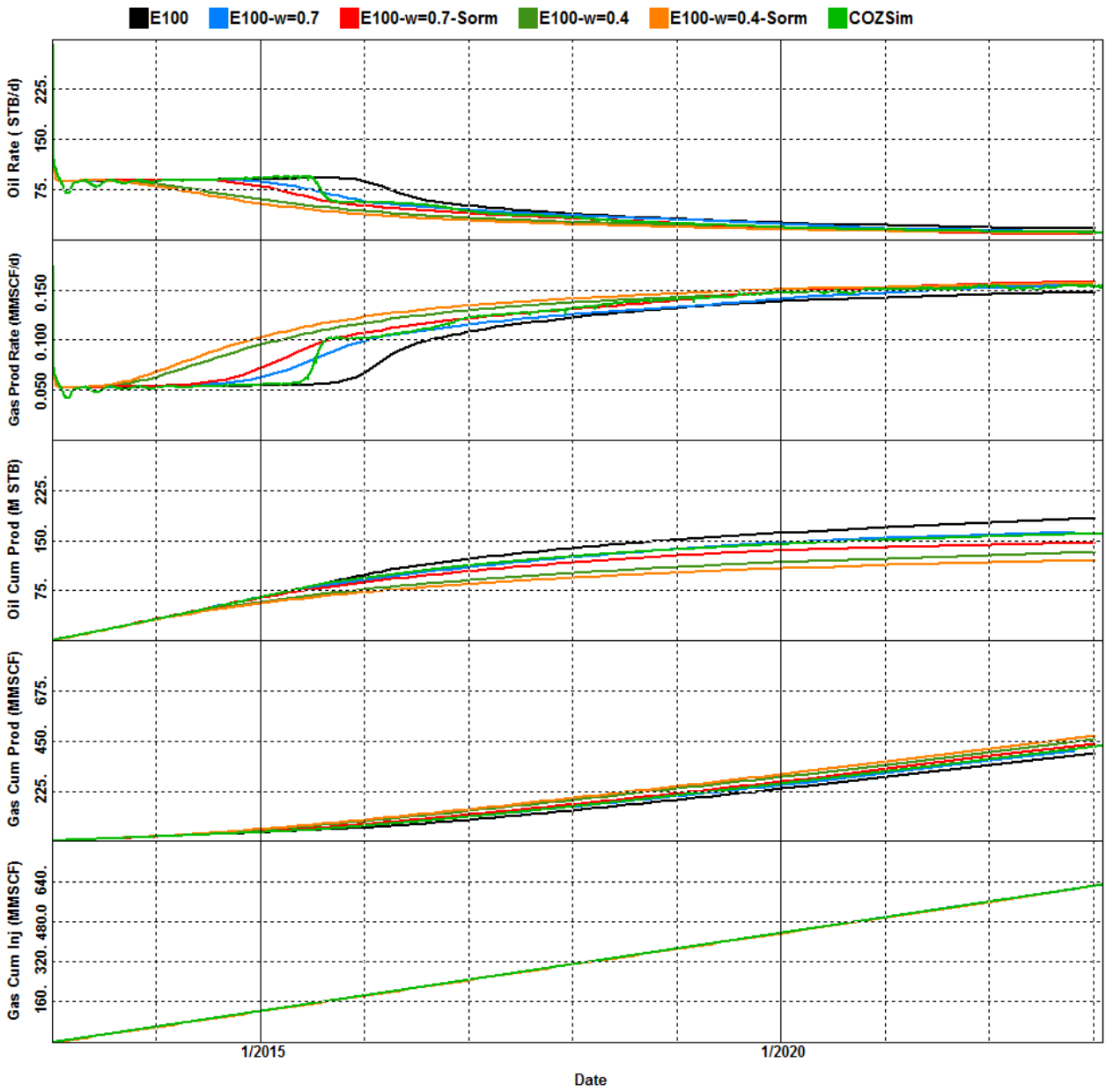

Figure 7.8 Recovery performance results of multi-contact miscibility cross-sectional model for Eclipse Solvent Model (E100) with different Todd-Longstaff mixing parameter (w) and residual oil saturation (Sorm), and COZSim.

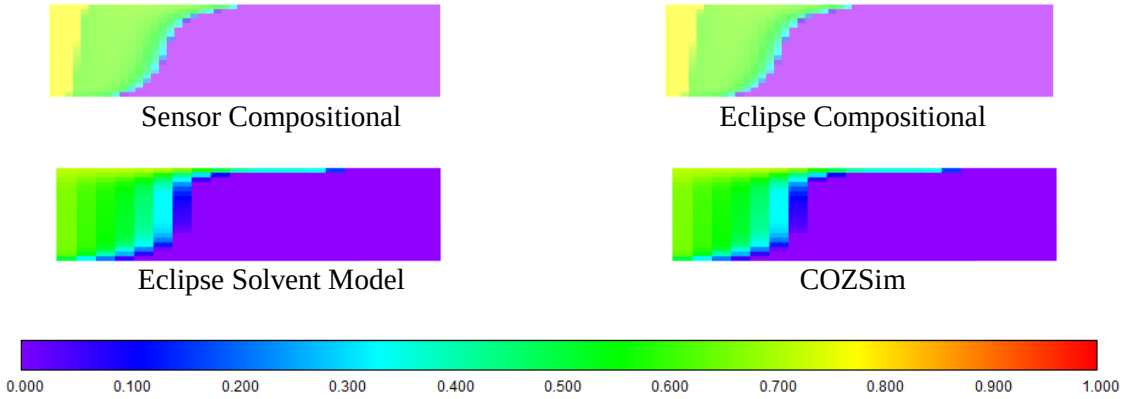

Figure 7.9 Gas saturation at 1/1/2015 (0.30 PVI) for multi-contact miscibility cross-sectional model.

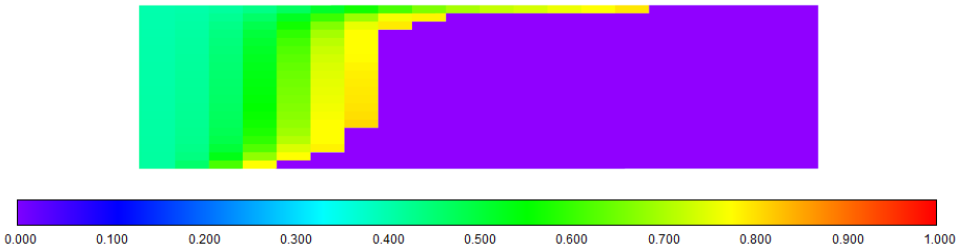

Figure 7.10 COZSim mixing parameter function at 1/1/2015 (0.30 PVI) for multi-contact miscibility cross-sectional model.

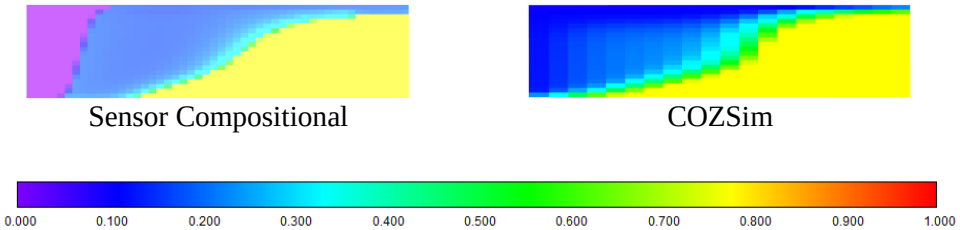

Figure 7.11 Oil saturation profile 1/1/2016 (0.4 PVI) for multi-contact miscibility cross-sectional model.

7.2.3 3D Model

3D model configuration is identical to planar model except the number of layers; therefore initialization results are given in Table 7.3. Table 7.6 gives specific parameters for 3D model. COZSim suffers from convergence problems for 10x10x10 grid. Time step tuning was unsuccessful to overcome convergence problems. Therefore 10x10x3 grid is used instead of

10x10x10 to get rid of convergence issues for COZSim. However, further investigation shows that finer grid has a minimal effect on production results.

Table 7.6 Parameters for 3D model

Parameter	Value
Grid	10x10x10 and 10x10x3 for COZSim
Grid Block Size, ft	81x81x6 and 81x81x20
CO_2 Injection Rate, MSCF/day	500
CO_2-Reservoir Pore Volume at 3200 psi, MMMSCF	1.34

Recovery performance predicted by simulators is shown in Figure 7.12 and Figure 7.13. Figure 7.12 shows oil and gas rates and cumulative production and injection profiles for Sensor and Eclipse compositional simulators, COZSim and Eclipse solvent model. Production profiles agree quite well for Sensor and Eclipse compositional simulators and Eclipse solvent model with no viscous fingering (w=1) and zero residual oil saturation (Sorm=0.0). COZSim predicts lower oil production and early breakthrough because it uses a built-in mixing parameter calculation based on the interfacial tension.

Figure 7.15 compares the Eclipse solvent model with different Todd-Longstaff mixing parameters (w) and COZSim. Similar to planar case, Eclipse Solvent model with viscous fingering imposition shows a wide range of oil production data and breakthrough. Lower mixing parameter causes early gas breakthrough, lower oil recovery factors and similar cumulative gas production. Mixing parameter values for COZSim varies between 0.5 and 0.8 as shown in Figure 7.15. Breakthrough time predicted by COZSim is between the times predicted by Eclipse Solvent Model with constant mixing parameter of 1.0 and 0.7.

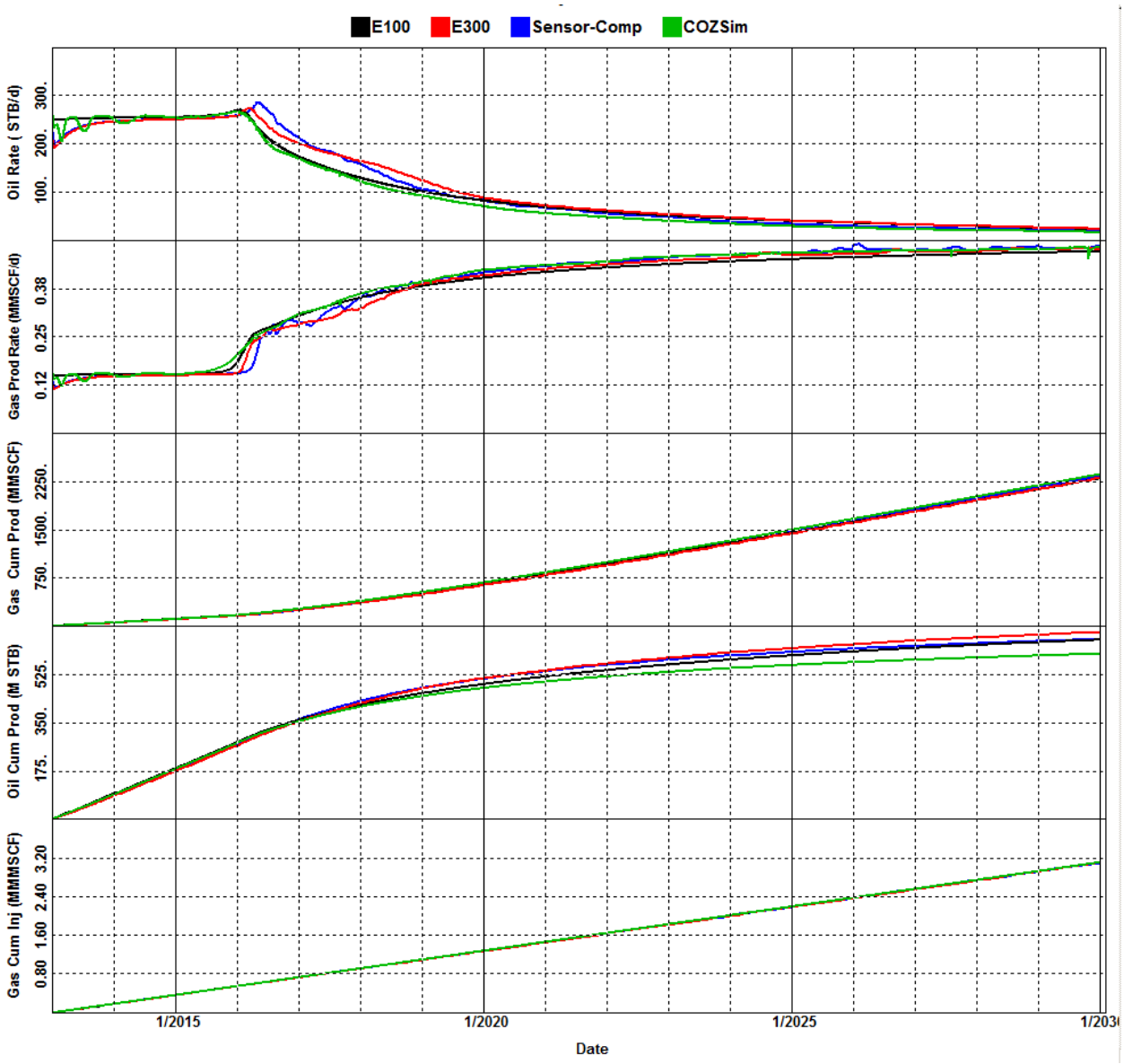

Figure 7.12 Recovery performance results of multi-contact miscibility 3D model for COZSim and Eclipse Solvent Model (E100), Sensor Compositional, Eclipse Compositional (E300) simulators.

Figure 7.14 compares gas saturation profiles at the date 1/1/2015 (0.3 PVI). Saturation profiles for Sensor Compositional, Eclipse Compositional and Eclipse solvent model (w=1, Sorm=0.0) matches very well. COZSim predicts larger gas saturation area because of the mixing parameter calculation shown in Figure 7.15. Figure 7.16 shows Eclipse Solvent model with different mixing parameter (w) and residual oil saturation to miscible flooding (Sorm). Lower

mixing parameter creates more viscous fingering. Figure 7.17 and 7.18 compares oil saturation at the date of 1/1/2016 (0.4 PVI) and 1/1/2030 (2.4 PVI), respectively. Compositional simulators leave zero oil saturation after continues CO_2 injection whereas Eclipse Solvent Model and COZSim is able to prevent complete sweep of oil and model residual oil saturation to miscible flooding.

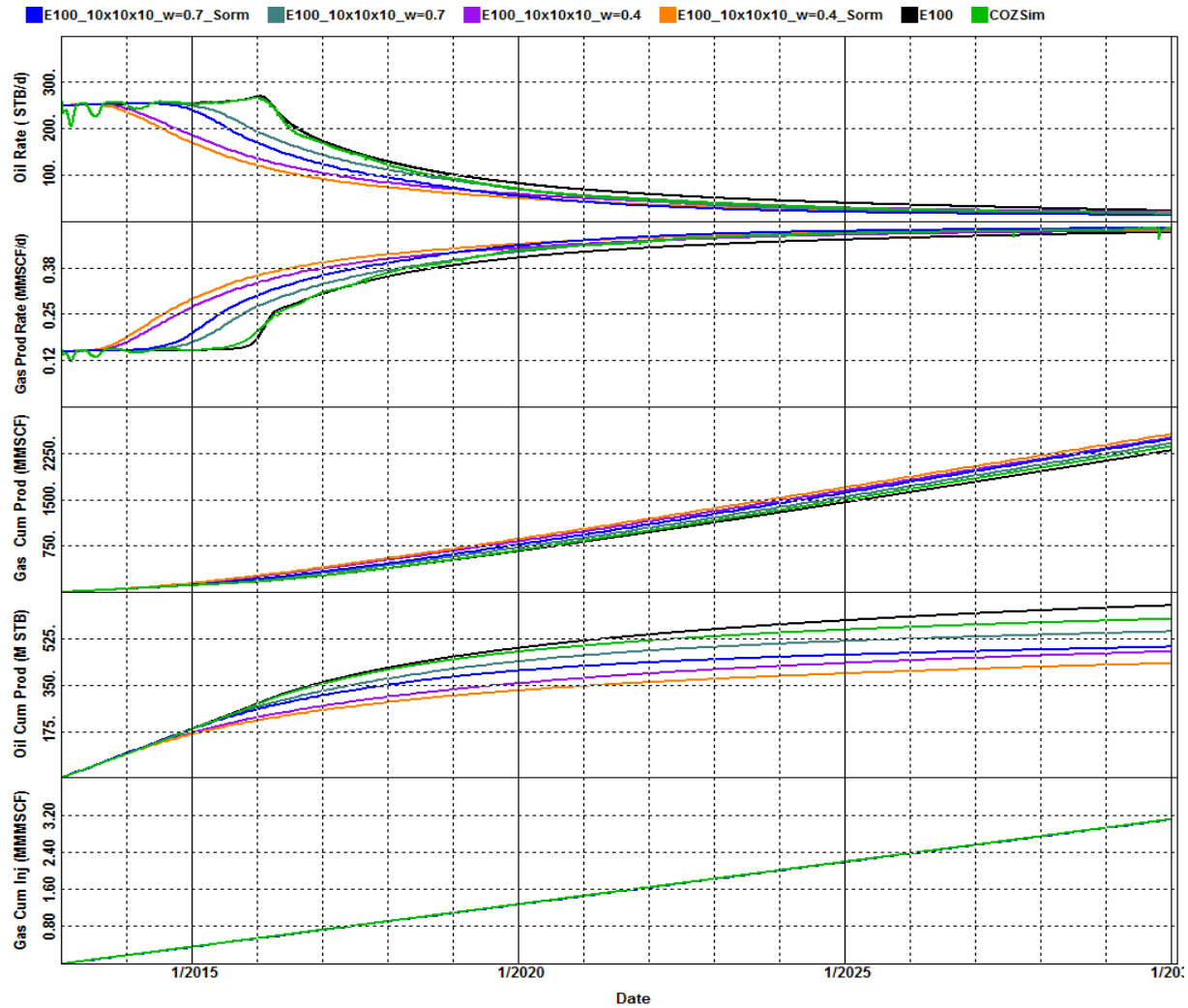

Figure 7.13 Recovery performance results of multi-contact miscibility 3D model for Eclipse Solvent Model (E100) with different Todd-Longstaff mixing parameter (w) and residual oil saturation (Sorm), and COZSim.

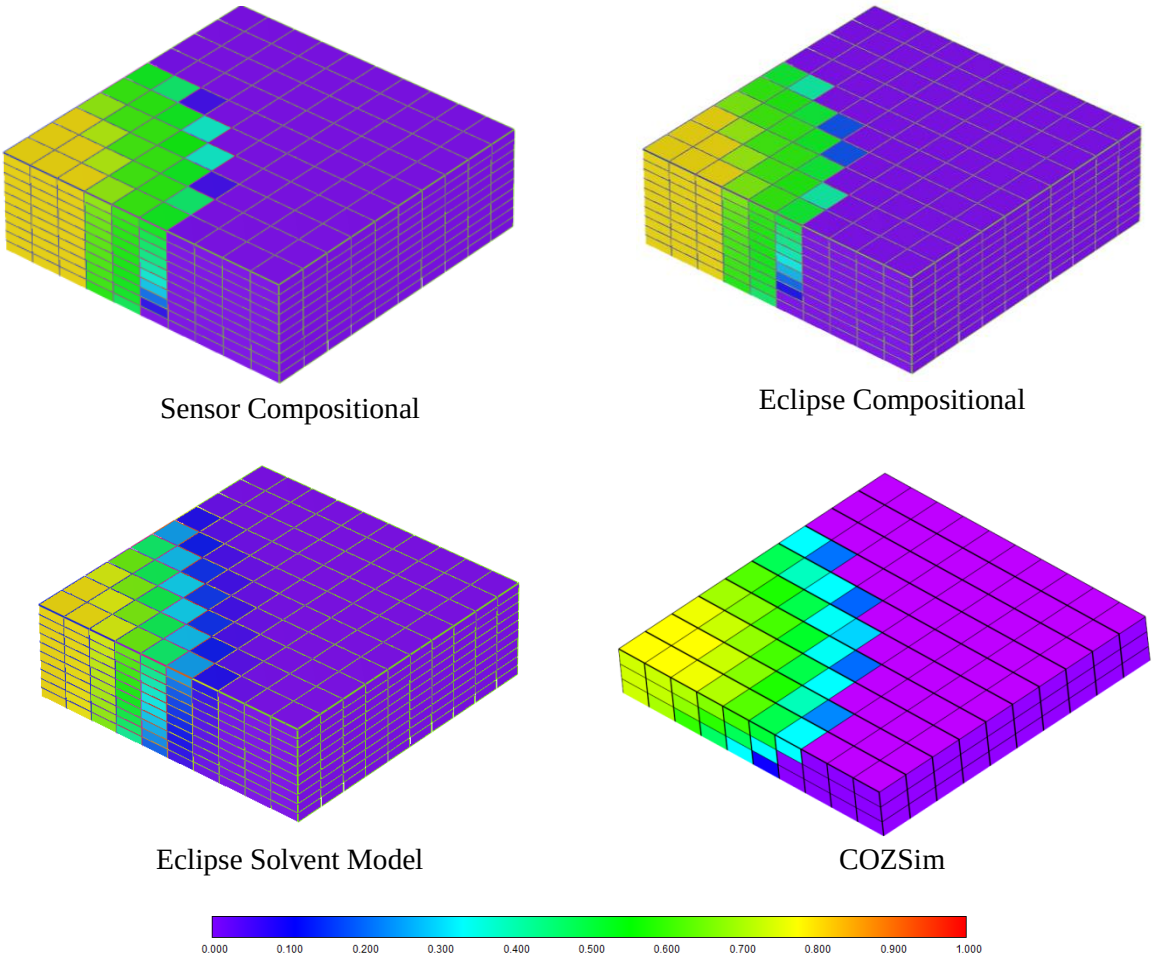

Figure 7.14 Gas Saturation at 1/1/2015 (0.30 PVI) for multi-contact miscibility 3D model.

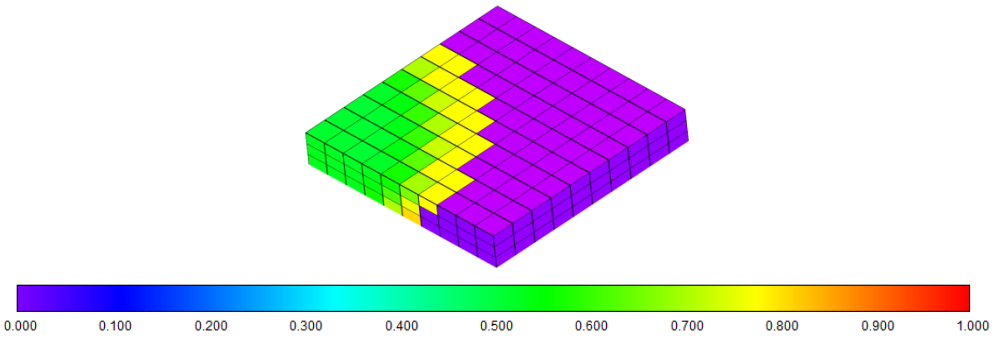

Figure 7.15 COZSim mixing parameter at 1/1/2015 (0.30 PVI) for multi-contact miscibility 3D model.

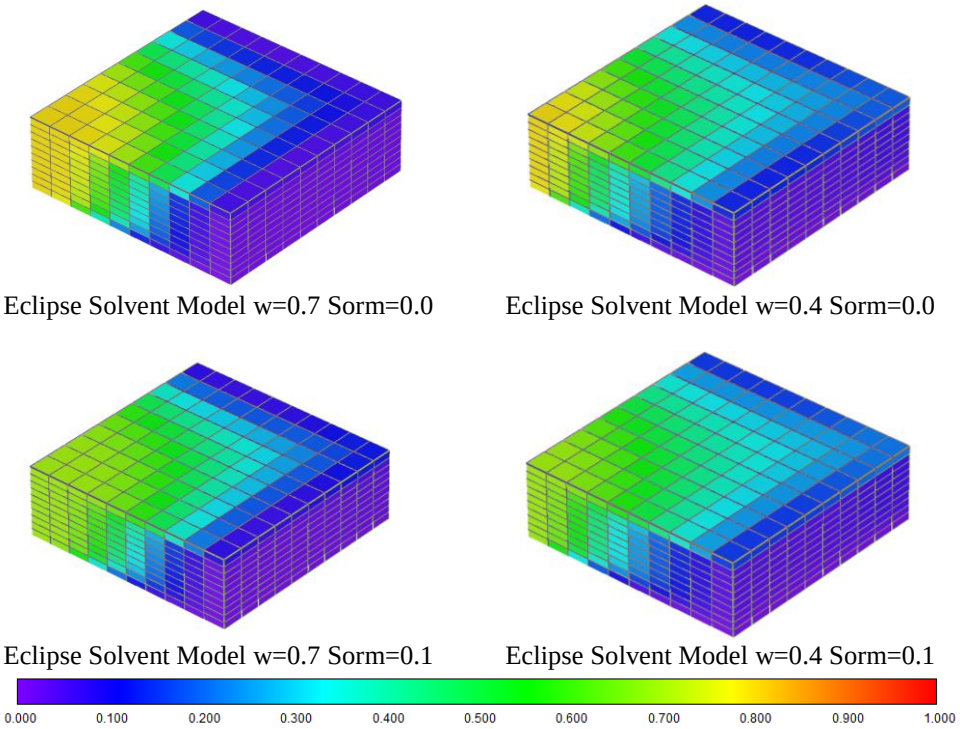

Figure 7.16 Gas saturation at 1/1/2015 (0.3 PVI) for multi-contact miscibility 3D model.

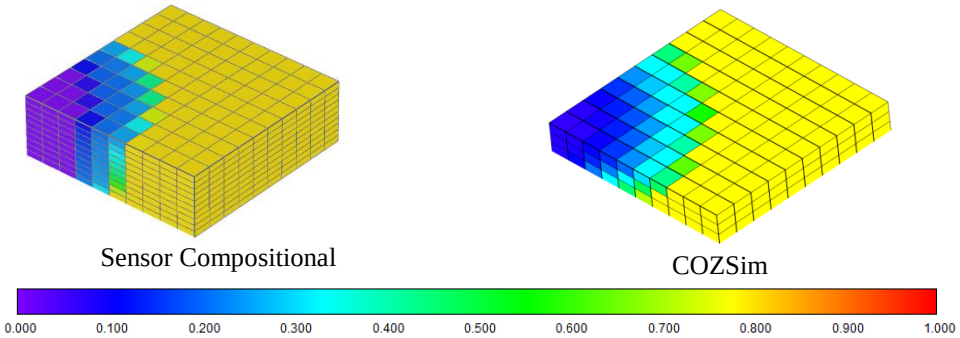

Figure 7.17 Oil saturation profile at 1/1/2015 (0.3 PVI) for multi-contact miscibility 3D model.

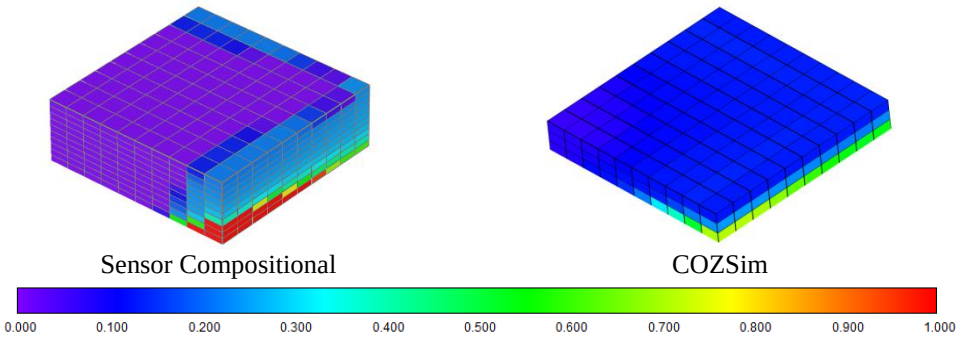

Figure 7.18 Oil saturation profile at 1/1/2030 (2.4 PVI) for multi-contact miscibility 3D model.

HAPTER 8

FIRST-CONTACT MISCIBLE FLOODING IN MAIN OIL ZONE

This chapter presents comparisons of simulators for first-contact miscible CO_2 flooding in main oil zone. Two dimensional planar, two dimensional cross-sectional and three dimensional models will be used throughout this chapter.

8.1 Description

First contact miscibility occurs when two fluids forms one phase regardless of the proportions of two fluid. First contact miscibility pressure is the minimum pressure at which any mixture of the reservoir oil and injected solvent forms a single phase. First contact miscibility can be achieved at sufficiently high pressures for CO_2 and oil systems (Coats et al, 2007). Fluid system used for this study has a first contact miscibility pressure approximately at 5000 psi (see Chapter 5.6). Above the green line shown in Figure 8.1, oil and CO_2 forms single phase regardless of their proportions.

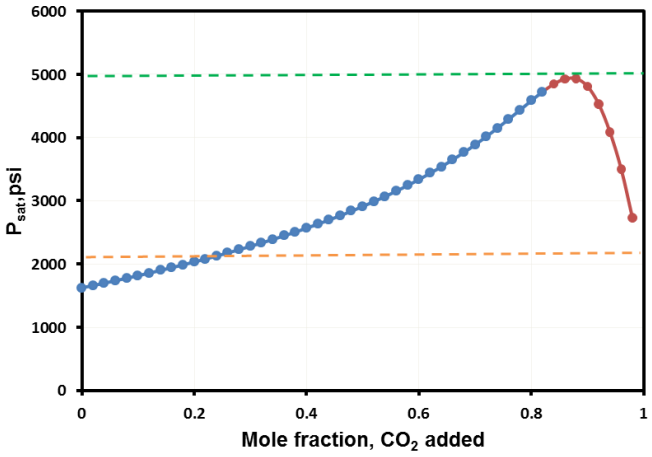

Figure 8.1 Saturation pressure versus mole fraction of CO_2 added.

Operating parameters are explained in Chapter 5 is used. Table 8.1 summarizes first contact miscible displacement parameters.

Table 8.1 Operating parameters for first-contact miscible displacement

Parameter	Value
Initial Pressure, psi	5400
Production Well Bottom Hole Pressure, psi	5100
First Contact Miscibility Pressure, psi	5000
Residual Oil Saturation to Miscible Displacement	0.1

8.2 Results

This section presents the simulation results for first-contact miscible CO_2 displacement study with planar, cross-sectional and three-dimensional static models for Eclipse and Sensor compositional simulators, Eclipse solvent model and Sensor first contact miscibility (FCM) option. COZSim is not used in this chapter, because built-in correlations used in COZSim for CO_2 displacement problems is not valid for high pressure systems (4500 psi and higher).

8.2.1 Planar Model

Table 8.2 gives specific parameters for planar model. Initialization results for planar model are given in Table 8.3. All simulators give the same initialization results. Model is initialized with uniform 80% oil saturation and 20% water saturation. No free hydrocarbon gas is present in the system.

Table 8.2 Parameters for first-contact miscible planar model

Parameter	Value
Grid	30x30x1
Grid Block Size, ft	27x27x60
CO_2 Injection Rate, MSCF/day	500
CO_2-Reservoir Pore Volume at 5100 psi, MMMSCF	1.93

Table 8.3 Fluid in-place results for first-contact miscible planar model

Property	Value
Oil In-Place, MSTB	800
Water In-Place, MSTB	252
Gas In-Place, MMSCF	478

Recovery performance predicted by simulators is shown in Figure 8.2, Figure 8.3 and Figure 8.4. Case names indicate the simulation specifications. For example a case name with Sorm represents that the simulation includes residual oil saturation to miscible displacement.

Figure 8.2 shows oil and gas rates and cumulative production and injection results for Sensor and Eclipse compositional simulators, Sensor first contact miscibility option and Eclipse solvent model. Sensor compositional and Sensor FCM option with no mixing parameter (K) imposition almost give exact results for this problem. Likewise, Eclipse compositional and Eclipse solvent model also gives very similar cumulative production results and rates. It can be said that all simulators fairly agree for this problem.

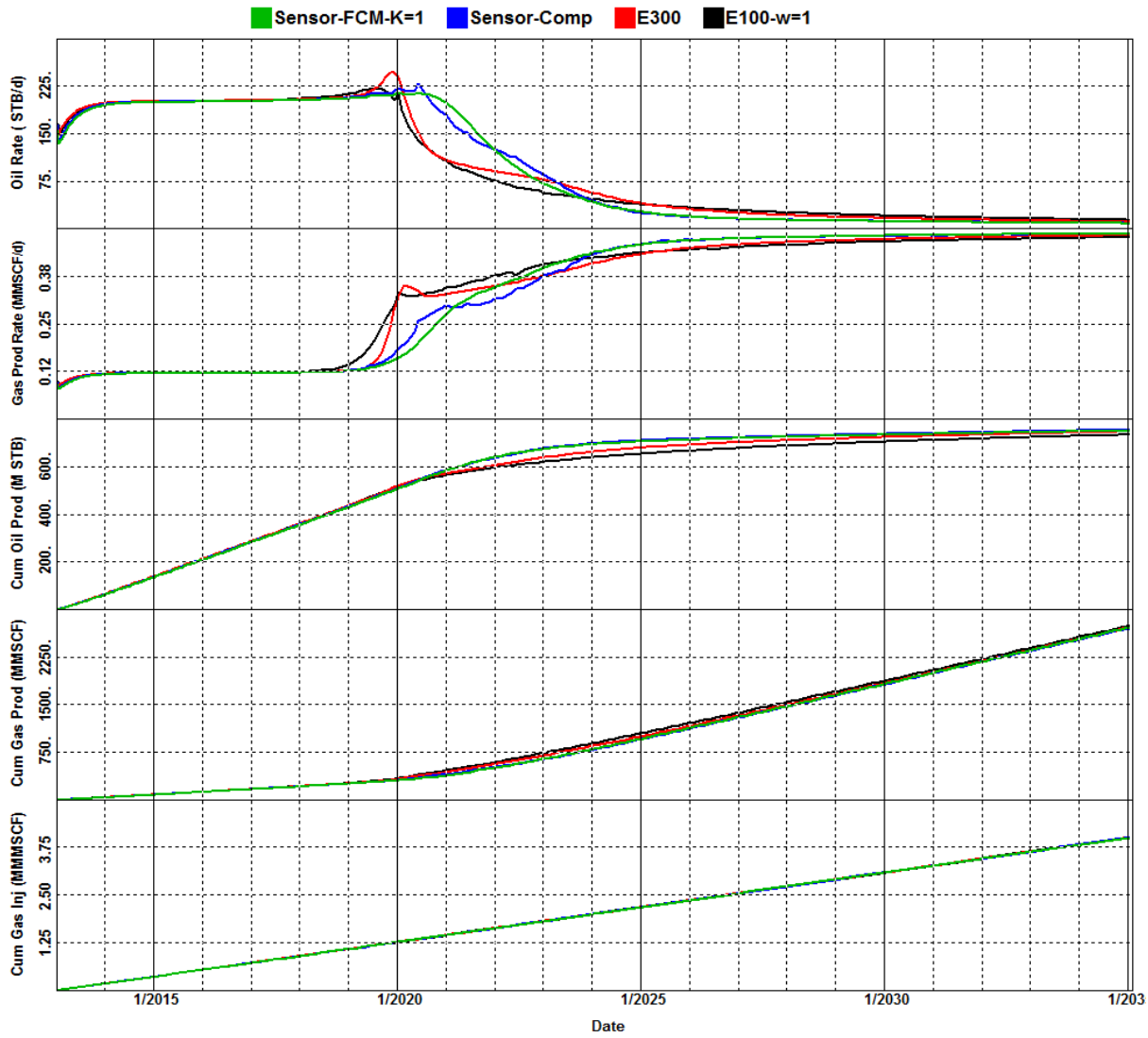

Figure 8.2 Recovery performance results of first-contact miscibility planar model for Sensor First Contact Miscibility Option, Sensor Compositional, Eclipse Compositional (E300) and Eclipse Solvent Model (E100).

Figure 8.3 compares the Eclipse solvent model with different Todd-Longstaff mixing parameters (w). Also cases with residual oil saturation to miscible flooding are included. Lower mixing parameter causes:

- Early gas breakthrough. The dominant factor is mixing parameter for breakthrough times. Breakthrough time range varies between about 1 year and 6 years.

- Lower oil production. If it is combined with residual oil saturation, oil recovery at the end of the simulation (~2.1 PVI) varies between 450 MSTB and 650 MSTB corresponding recovery factors of 0.56 and 0.81, respectively.
- Higher gas production. The variation of cumulative gas production is within 1-15% of the mean value. The main difference is the start time of gas production.

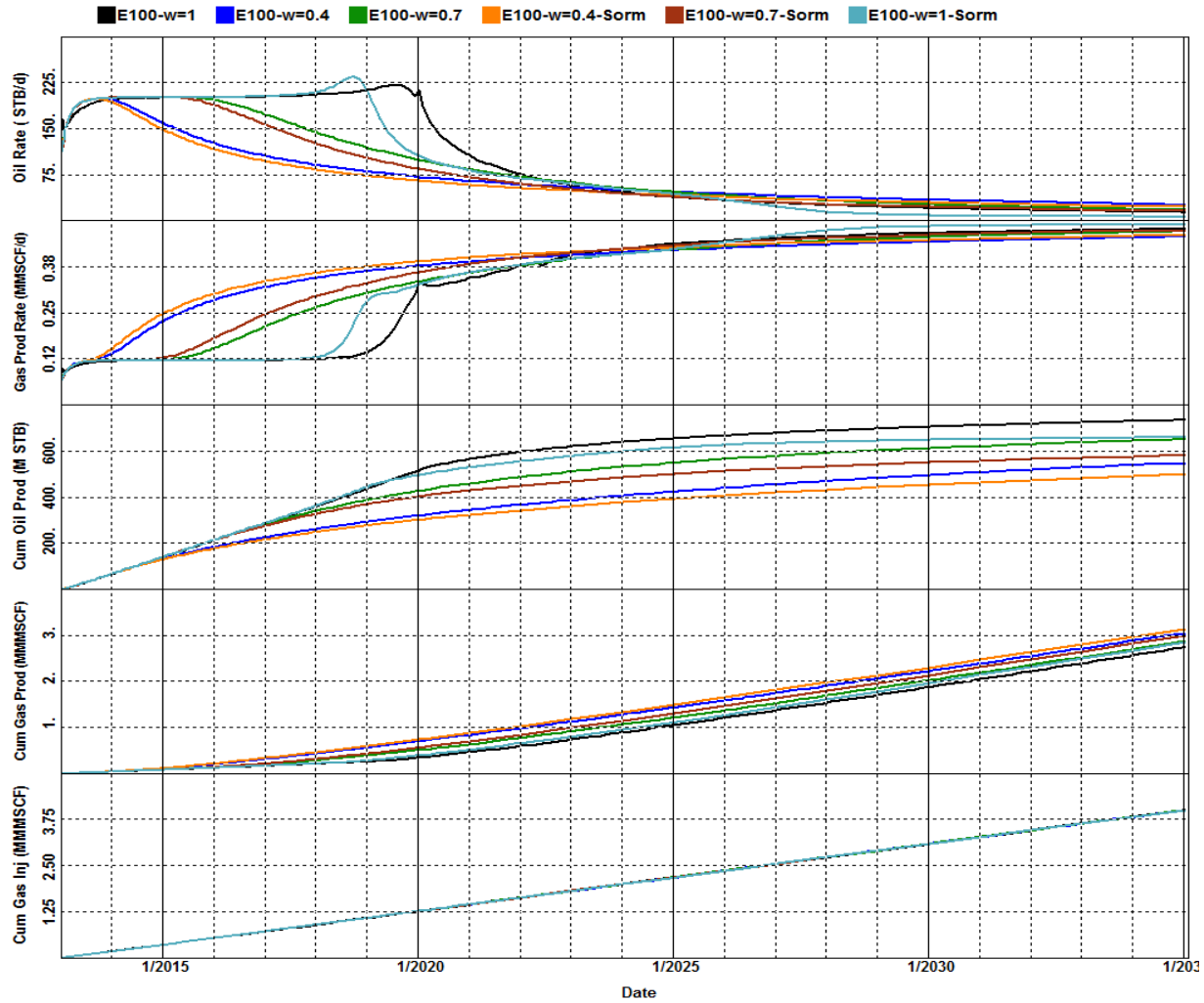

Figure 8.3 Recovery performance results of first-contact miscibility planar model for Eclipse Solvent Model (E100) with different Todd-Longstaff mixing parameter (w) and residual oil saturation (Sorm=0.1).

Including residual oil saturation decreases the cumulative oil production, increases the cumulative gas production, and causes early gas breakthrough. Because the model initialized at

80% oil saturation, the effect of residual oil saturation is not dominant but an important factor. Residual oil saturation after miscible flooding will be very important factor if the system is initialized with lower oil saturation, see chapter 9.

Exclusion of residual oil saturation to miscible flooding (Sorm=0.0) creates convergence problems for Eclipse Solvent model. Special time step tuning (very small initial time steps, small maximum time step size) may be required to be able to run Eclipse Solvent Model without any convergence problems.

Figure 8.4 compares the cases for Sensor first contact miscibility option with different dispersion control coefficient (K) and residual oil saturation to miscible displacement. Similar to Eclipse solvent model, Sensor gives a wide range of oil production data and breakthrough time. Higher dispersion control coefficient (K) causes:

- Early gas breakthrough. Breakthrough time range varies between about 2 years and 6 years.
- Lower oil production. If it is combined with residual oil saturation, oil recovery at the end of the simulation (~2.1 PVI) varies between 450 MSTB and 660 MSTB corresponding recovery factors 0.56 and 0.83, respectively.
- Higher gas production. The variation of cumulative gas production is within 1-10% of the mean value. The main difference is the start time of gas production.

Residual oil saturation to miscible flooding has a greater impact on results for Sensor FCM option compared with Eclipse solvent model. Because imposing residual oil saturation to the system creates an artificial viscous fingering effect as seen in Figure 8.5. This artificial viscous fingering effect overcomes the possible numerical dispersion/grid orientation effects that

can be experienced in compositional-type runs (Sorm=0.0) and creates physical dispersion (fingering). This mechanism causes early gas breakthrough.

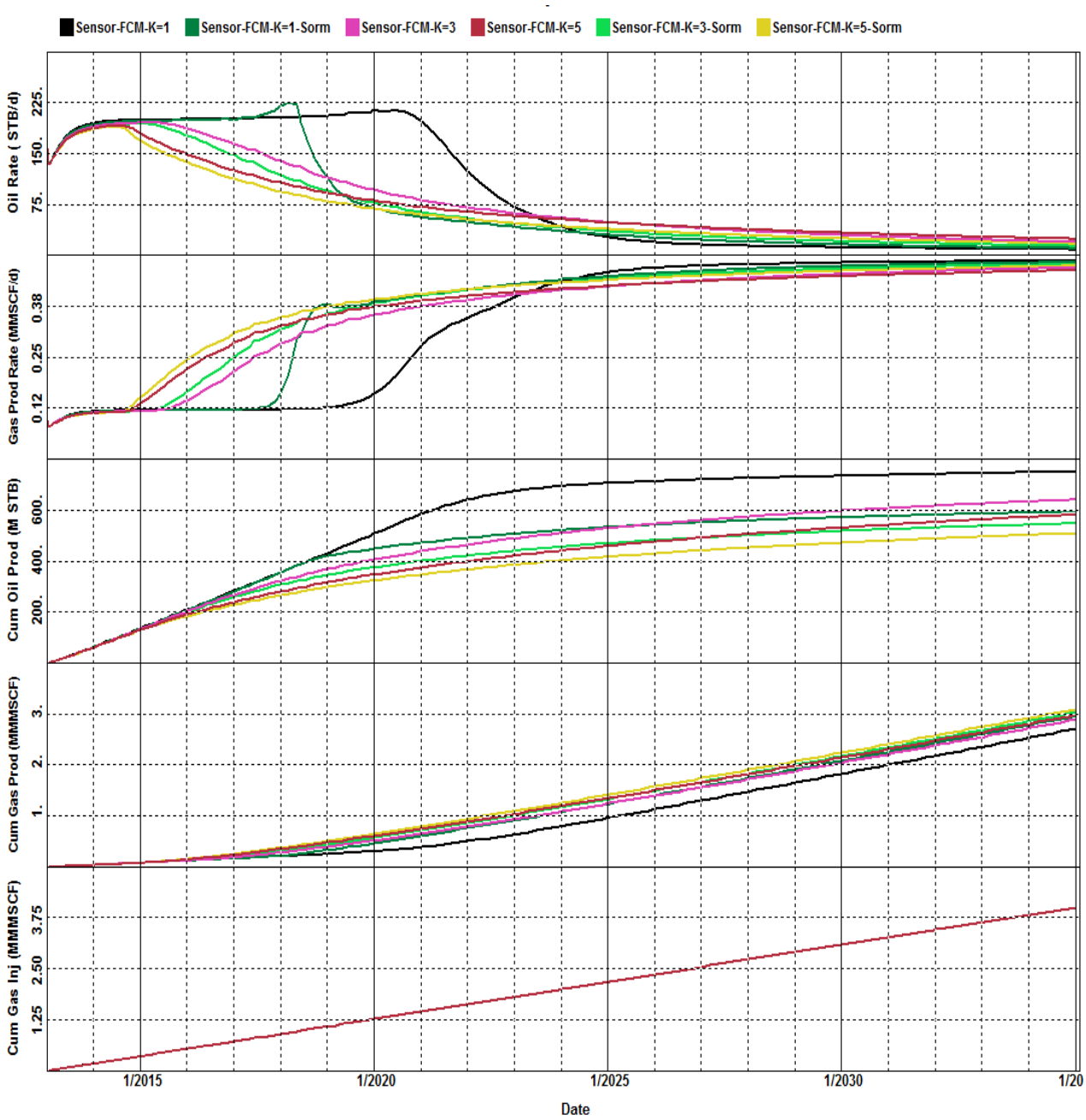

Figure 8.4 Recovery performance results of first-contact miscibility planar model for Sensor First Contact Miscibility Option with different dispersion control coefficients (K) and residual oil saturation (Sorm=0.1).

Figure 8.5 shows CO_2 mole fraction profiles in oleic phase at date 2017-1-1 after 4 years of continuous CO_2 injection (0.4 PVI) for Sensor and Eclipse compositional simulators, Sensor first contact miscibility option with different dispersion control coefficients (K) and residual oil saturations. Sensor compositional, Sensor FCM option (K=1) and Eclipse compositional gives almost the same profiles for CO_2 mole fraction. All these three cases suffer from grid orientation effects for 30x30 grid. Even higher resolution grid (40x40, 60x60 and 80x80) is not able to overcome this numerical artifact. Including residual oil saturation and dispersion control coefficients greater than 1 creates viscous fingers and mask this numerical dispersion. Also, compositional simulators and Sensor FCM with K=1 shows high sweep efficiencies resulting zero oil saturation especially in near well region. Figure 8.7 shows oil saturation for these simulators. CO_2 displace the oil and leaving no original reservoir oil behind the front.

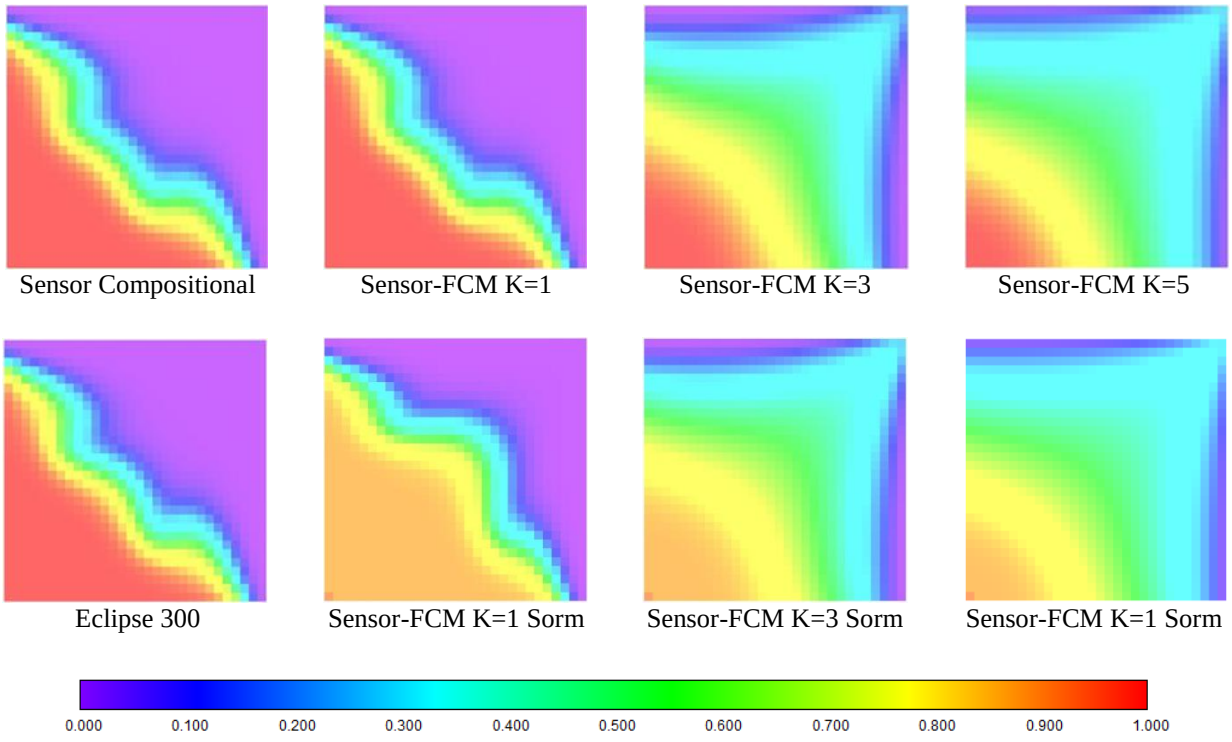

Figure 8.5 CO_2 mole fraction in oleic phase at 1/1/2017 (0.4 PVI) for first contact miscible planar model.

Figure 8.6 compares solvent/oil mixture saturation profile for Eclipse solvent model with different mixing parameters (w). Similar to Sensor FCM option, lower mixing parameter creates viscous fingering and early breakthrough.

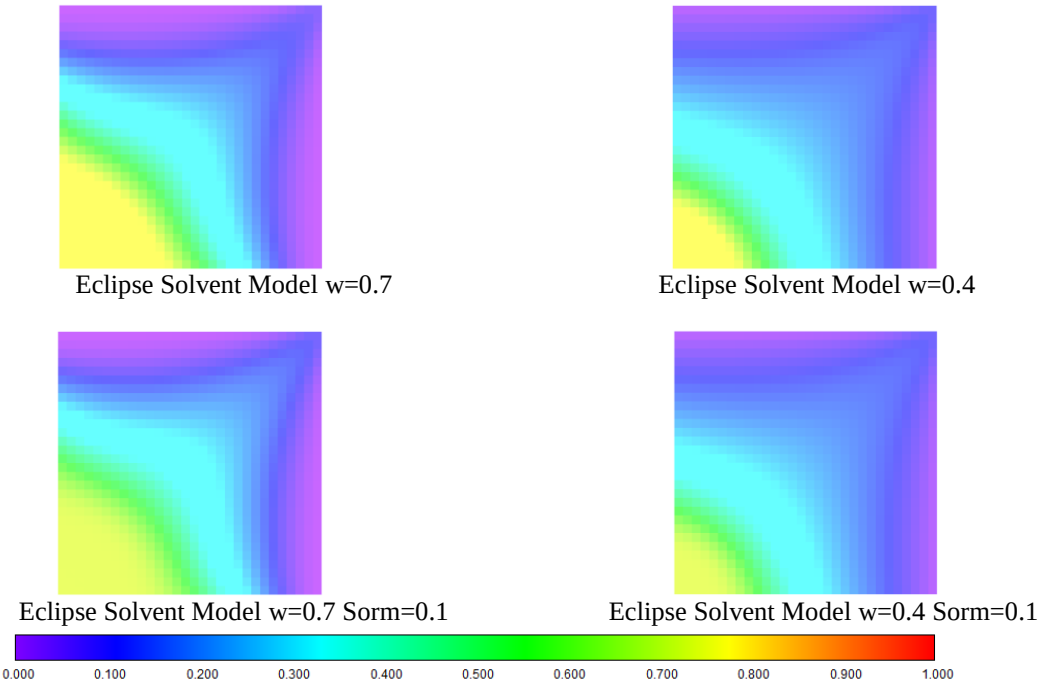

Figure 8.6 Solvent/oil mixture saturation 1/1/2017 (0.4 PVI) for first contact miscible planar model.

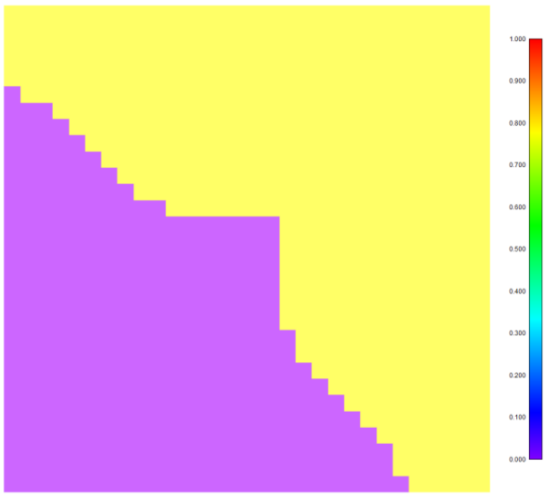

Figure 8.7 Original oil saturation profile of Sensor Compositional at 1/1/2017 (0.4 PVI) for first contact miscible planar model.

8.2.2 Cross-sectional Model

Table 8.4 gives specific parameters for cross-sectional model. Initialization results are given in Table 8.5. All simulators give the same initialization results. Model is initialized with 80% oil saturation and 20% water saturation. No free hydrocarbon gas is present in the system.

Table 8.4 Parameters for first-contact miscibility cross-sectional model

Parameter	Value
Grid	50x1x20
Grid Block Size, ft	20x200x3
CO_2 Injection Rate, MSCF/day	170
CO_2-Reservoir Pore Volume at 5100 psi, MMMSCF	0.59

Table 8.5 Fluid in-place results for first-contact miscibility cross-sectional model

Property	Value
Oil In-Place, MSTB	244
Water In-Place, MSTB	76
Gas In-Place, MMSCF	145

Recovery performance predicted by simulators is shown in Figure 8.8, Figure 8.9 and Figure 8.10. Figure 8.8 shows oil and gas rates and cumulative production and injection results for Sensor and Eclipse compositional simulators, Sensor first contact miscibility option and Eclipse solvent model. All simulators give similar production profiles for this case. Eclipse solvent model oil production is slightly lower compared to other simulators. Cumulative gas production values agree quite well. Sensor FCM option and Sensor compositional simulators

gives almost the same production profile and breakthrough time. Eclipse compositional and Eclipse solvent models gives slightly early breakthrough time compared with Sensor.

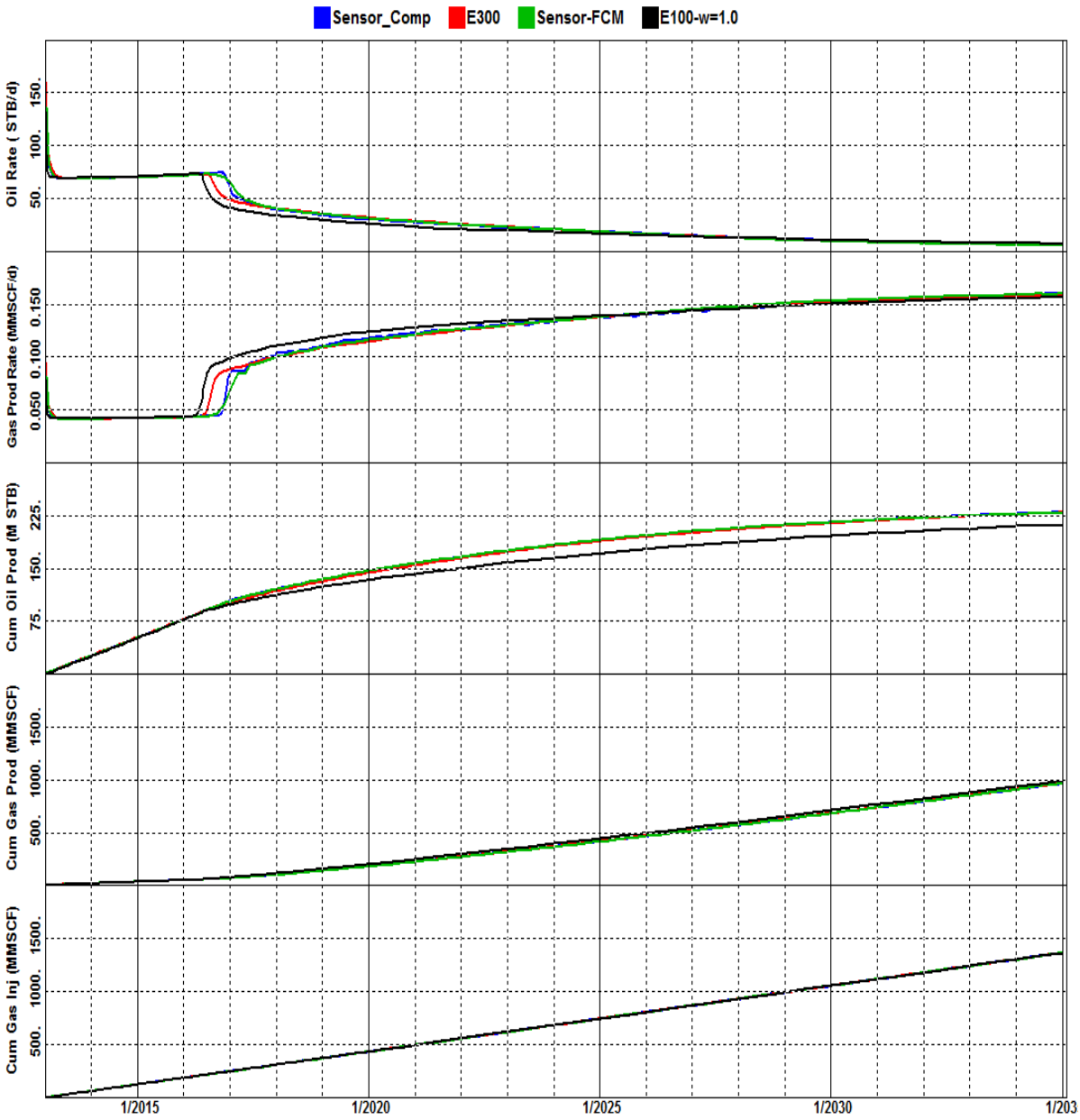

Figure 8.8 Recovery performance results of first-contact miscibility cross-sectional model for Sensor First Contact Miscibility Option, Sensor Compositional, Eclipse Compositional (E300) and Eclipse Solvent Model (E100).

Figure 8.9 compares the cases for Sensor first contact miscibility option with different dispersion control coefficient (K) and residual oil saturation to miscible displacement. Figure

8.10 compares the Eclipse solvent model with different Todd-Longstaff mixing parameters (w). Similar to planar case, Sensor FCM and Eclipse Solvent model with viscous fingering imposition shows a wide range of oil production data and breakthrough time. Higher dispersion control coefficient (K) or lower mixing parameter causes early gas breakthrough, lower oil production recovery factors and similar cumulative gas production.

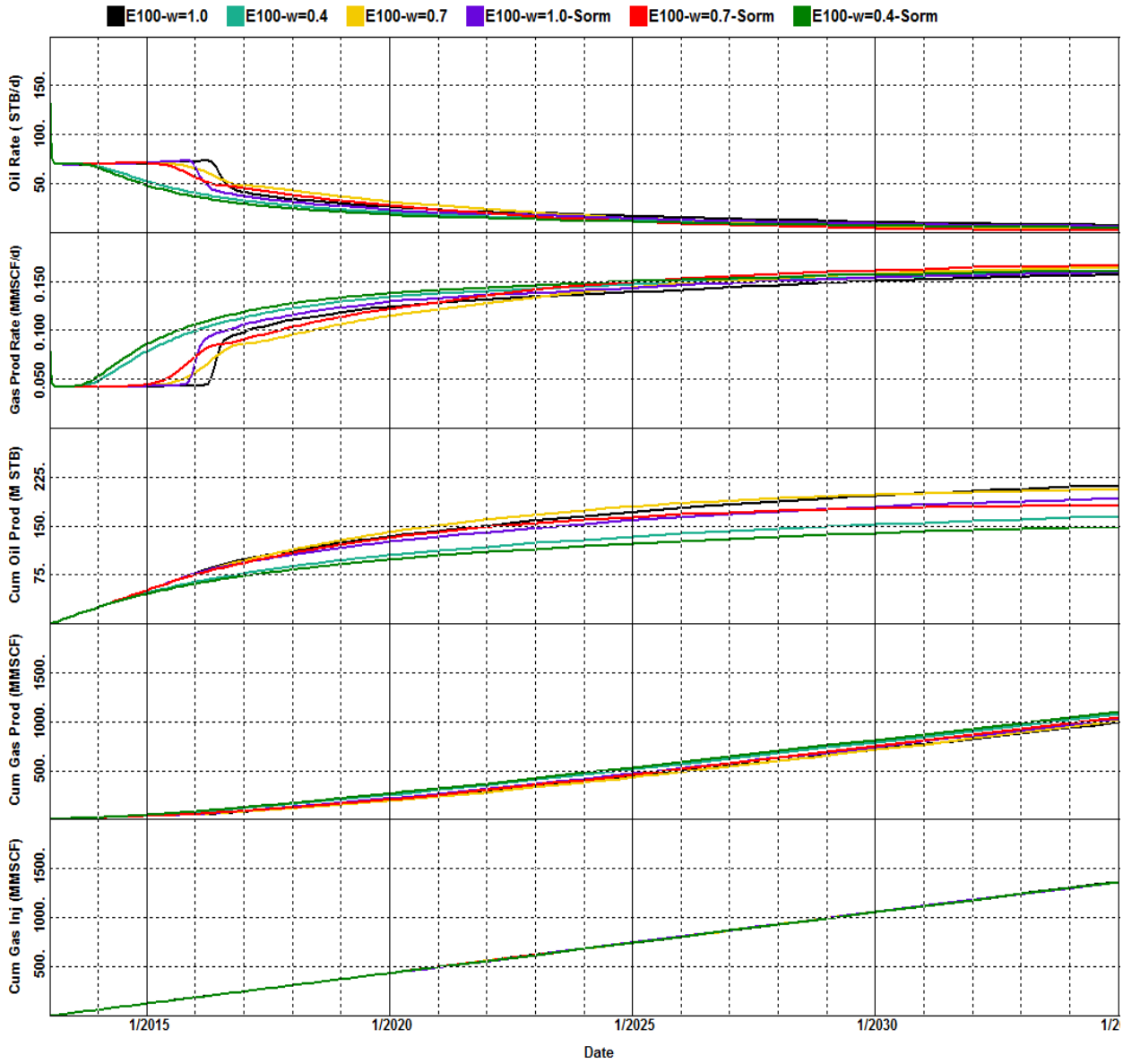

Figure 8.9 Recovery performance results of first-contact miscibility cross-sectional model for Eclipse Solvent Model (E100) with different Todd-Longstaff mixing parameter (w) and residual oil saturation (Sorm=0.1).

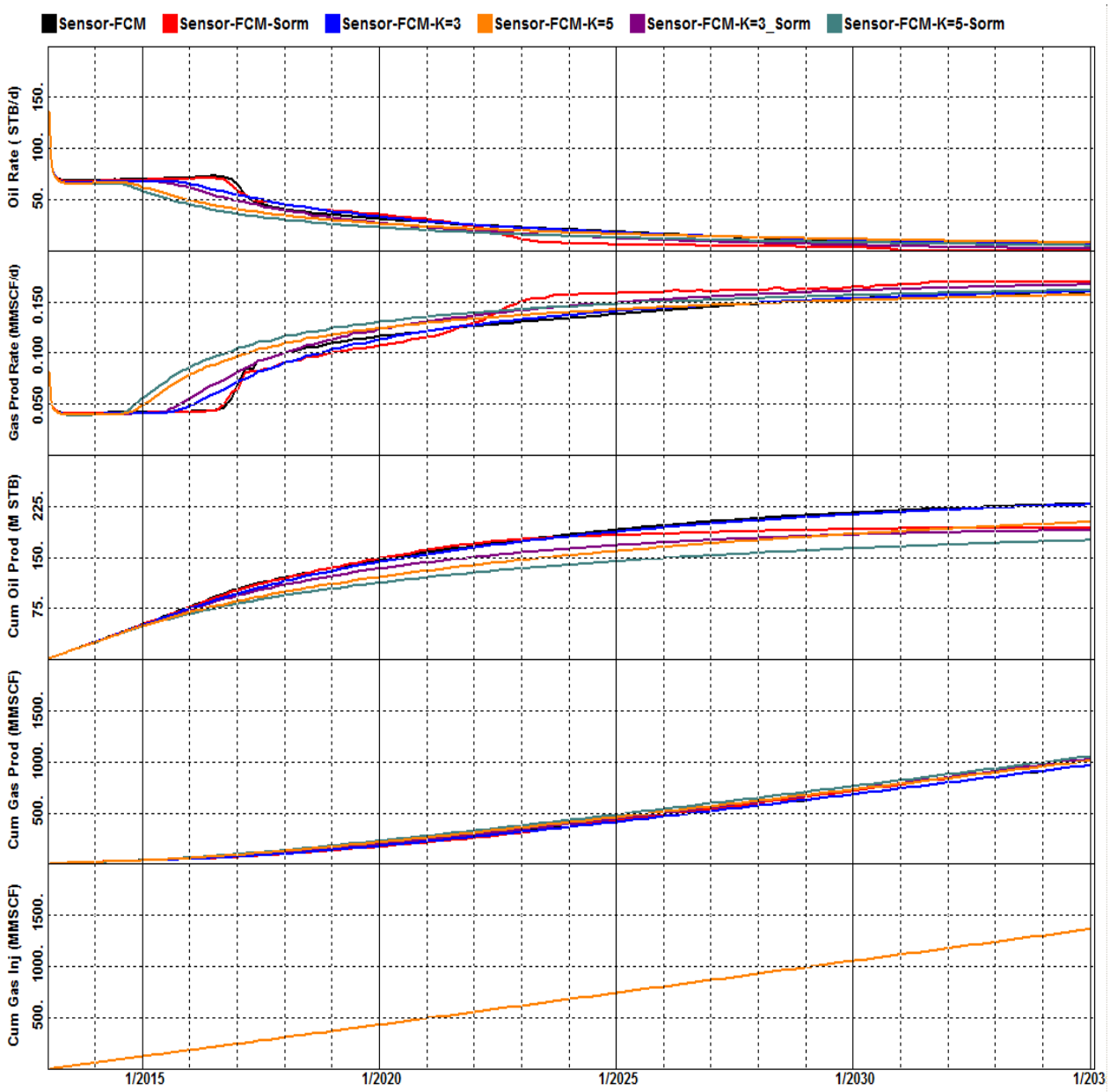

Figure 8.10 Recovery performance results of first-contact miscibility cross-sectional model for Sensor First Contact Miscibility Option with different dispersion control coefficient (K) and residual oil saturation (Sorm=0.1).

Figure 8.11 compares CO_2 mole fraction profiles in oleic phase at the date 2016-1-1 after 3 years of continuous CO_2 injection (0.5 PVI) for Sensor and Eclipse compositional simulators, Sensor first contact miscibility option with different dispersion control coefficients (K) and residual oil saturations. Sensor compositional, Sensor FCM option (K=1) and Eclipse

compositional gives almost the same result for CO_2 mole fraction. Figure 8.12 shows solvent/oil mixture saturation profile for Eclipse solvent model with different mixing parameters (w). Viscous fingering imposition overcomes the gravity-overriding as seen in Figure 8.11 and 8.12. Cases with viscous fingering dominate the gravity effects (density difference) and create a single-layer-like displacement.

Also, similar to the planar model, compositional simulators and Sensor FCM with K=1 shows high sweep efficiencies resulting zero oil saturation especially in near well region. Figure 8.13 shows oil saturation for these simulators. CO_2 displace the oil and leaving no original reservoir oil behind the front.

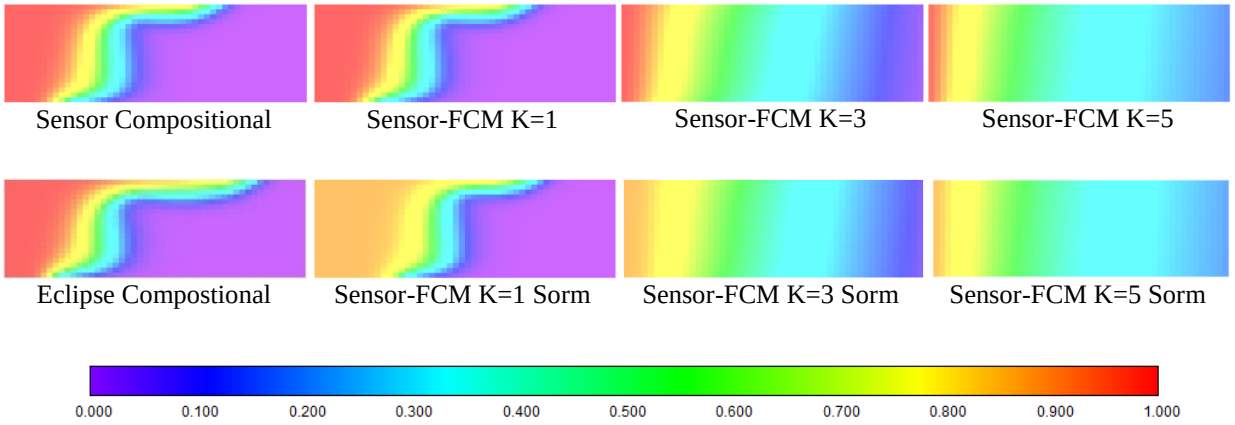

Figure 8.11 CO_2 mole fraction in oleic phase at 1/6/2015 (0.5 PVI) for first-contact miscible cross-sectional model.

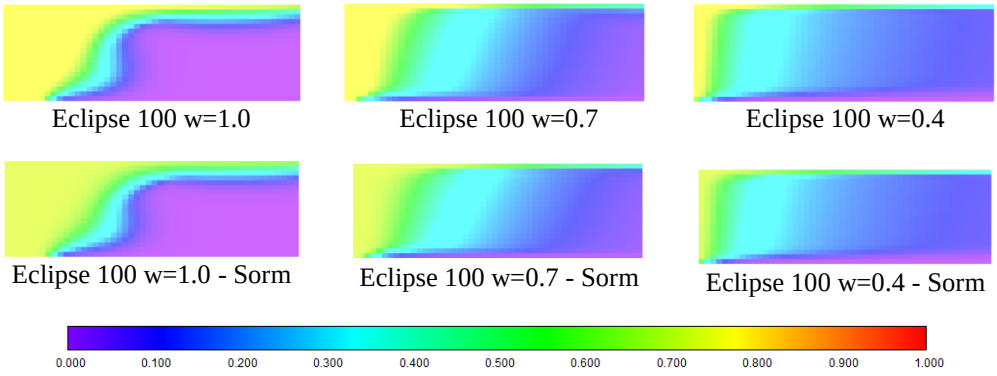

Figure 8.12 Solvent/oil mixture saturation at 1/6/2015 for first-contact miscible cross-sectional model.

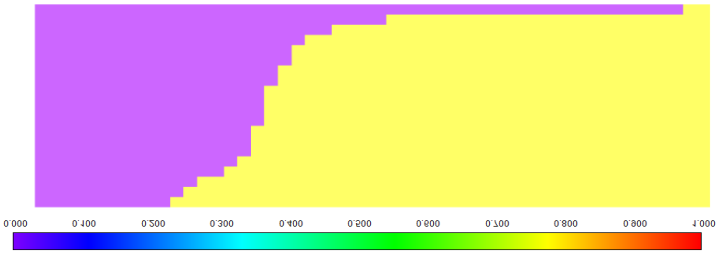

Figure 8.13 Original oil saturation profile of Sensor Compositional 1/6/2015 for first-contact miscible cross-sectional model.

8.2.3 3D Model

Table 8.6 gives specifications for 3D model. Note that 3D model configuration is identical to planar model except the number of layers. Therefore initialization results for 3D model are given in Table 8.3

Table 8.6 Parameters for first-contact miscibility 3D model

Parameter	Value
Grid	30x30x20 and 20x20x20 for E100
Grid Block Size, ft	27x27x3
CO_2 Injection Rate, MSCF/day	500
CO_2-Reservoir Pore Volume at 5100 psi, MMMSCF	1.93

Eclipse solvent model suffers from convergence problems for this problem. Time step tuning was unsuccessful to overcome convergence problems. Therefore 20x20x20 grid is used instead of 30x30x20 to get rid of convergence issues for Eclipse solvent model.

Recovery performance predicted by simulators is shown in Figure 8.14, Figure 8.15 and Figure 8.16. Case names indicate the simulation results. Figure 8.14 shows oil and gas rates and cumulative production and injection profiles for Sensor and Eclipse compositional simulators,

Sensor first contact miscibility option and Eclipse solvent model. Simulator results agree quite well.

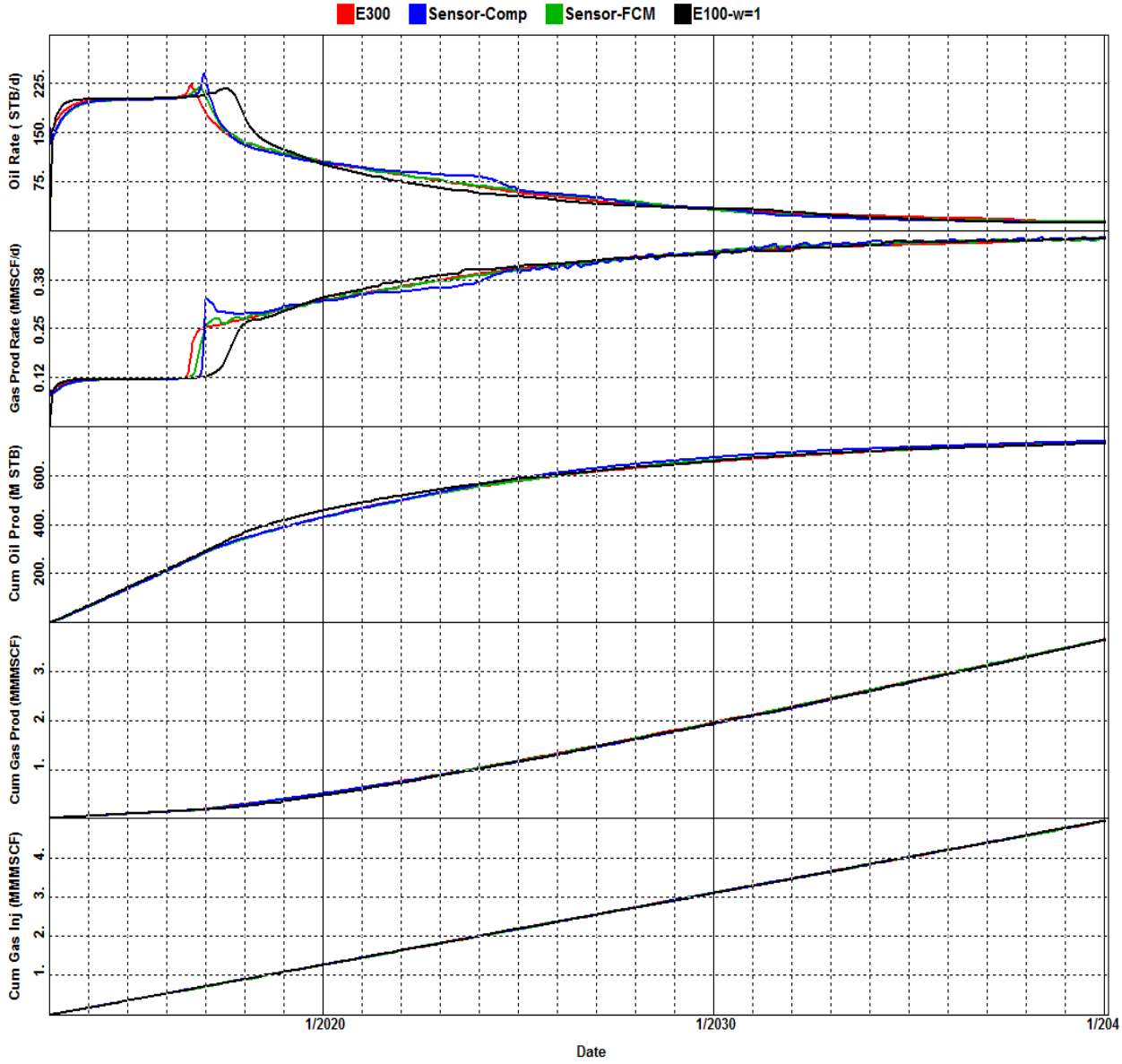

Figure 8.14 Recovery performance results of first-contact miscibility 3D model for Sensor First Contact Miscibility Option, Sensor Compositional, Eclipse Compositional (E300) and Eclipse Solvent Model (E100).

Figure 8.15 compares the Eclipse solvent model with different Todd-Longstaff mixing parameters (w). Figure 8.16 compares the cases for Sensor first contact miscibility option with different dispersion control coefficient (K) and residual oil saturation to miscible displacement.

Similar to planar case, Sensor FCM and Eclipse Solvent model with viscous fingering imposition shows a wide range of oil production data and breakthrough. Higher dispersion control coefficient (K) or lower mixing parameter causes early gas breakthrough, lower oil production recovery factors and similar cumulative gas production.

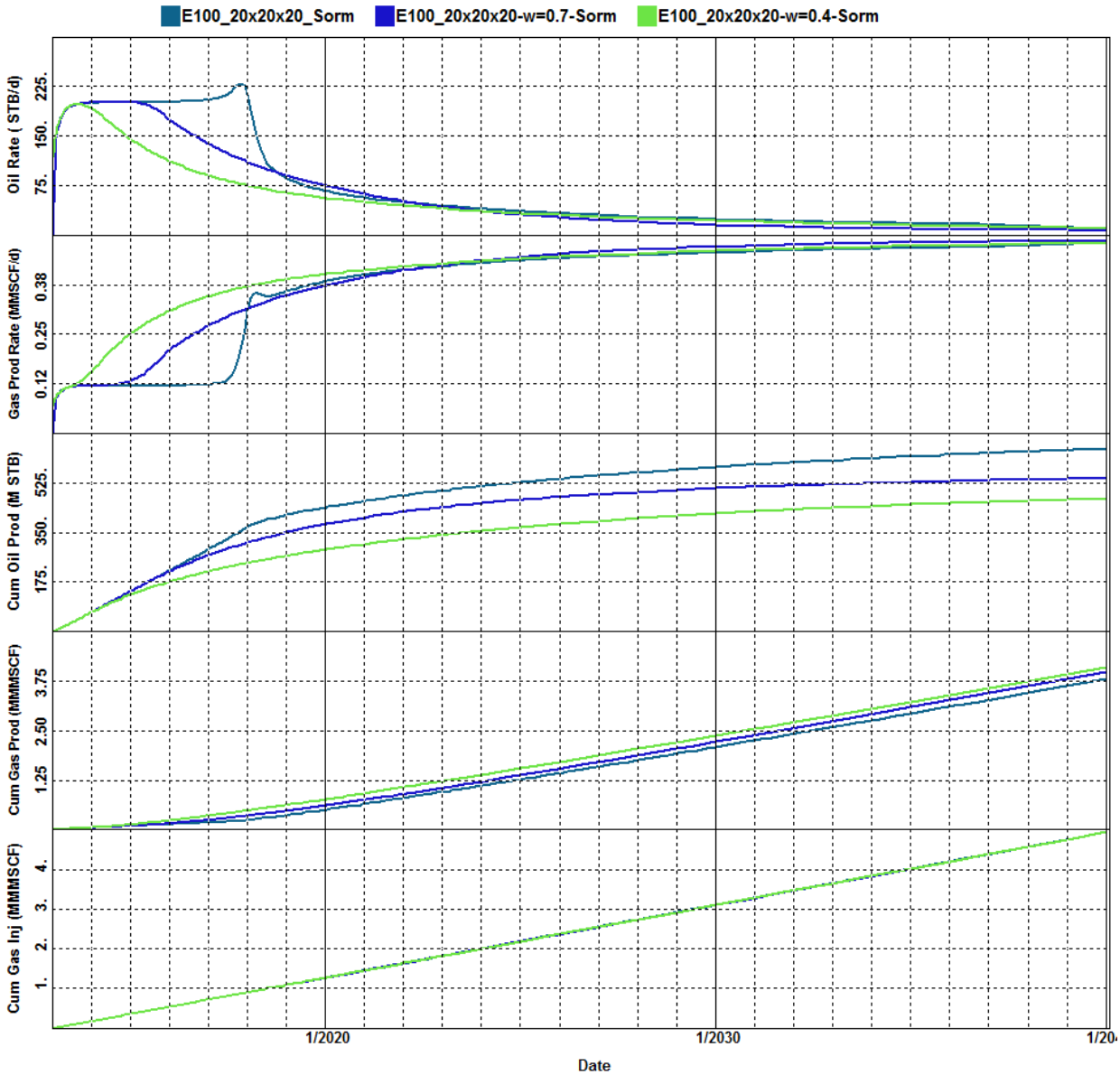

Figure 8.15 Recovery performance results of first-contact miscibility 3D model for Eclipse Solvent Model (E100) with different Todd-Longstaff mixing parameter (w) and residual oil saturation (Sorm=0.1).

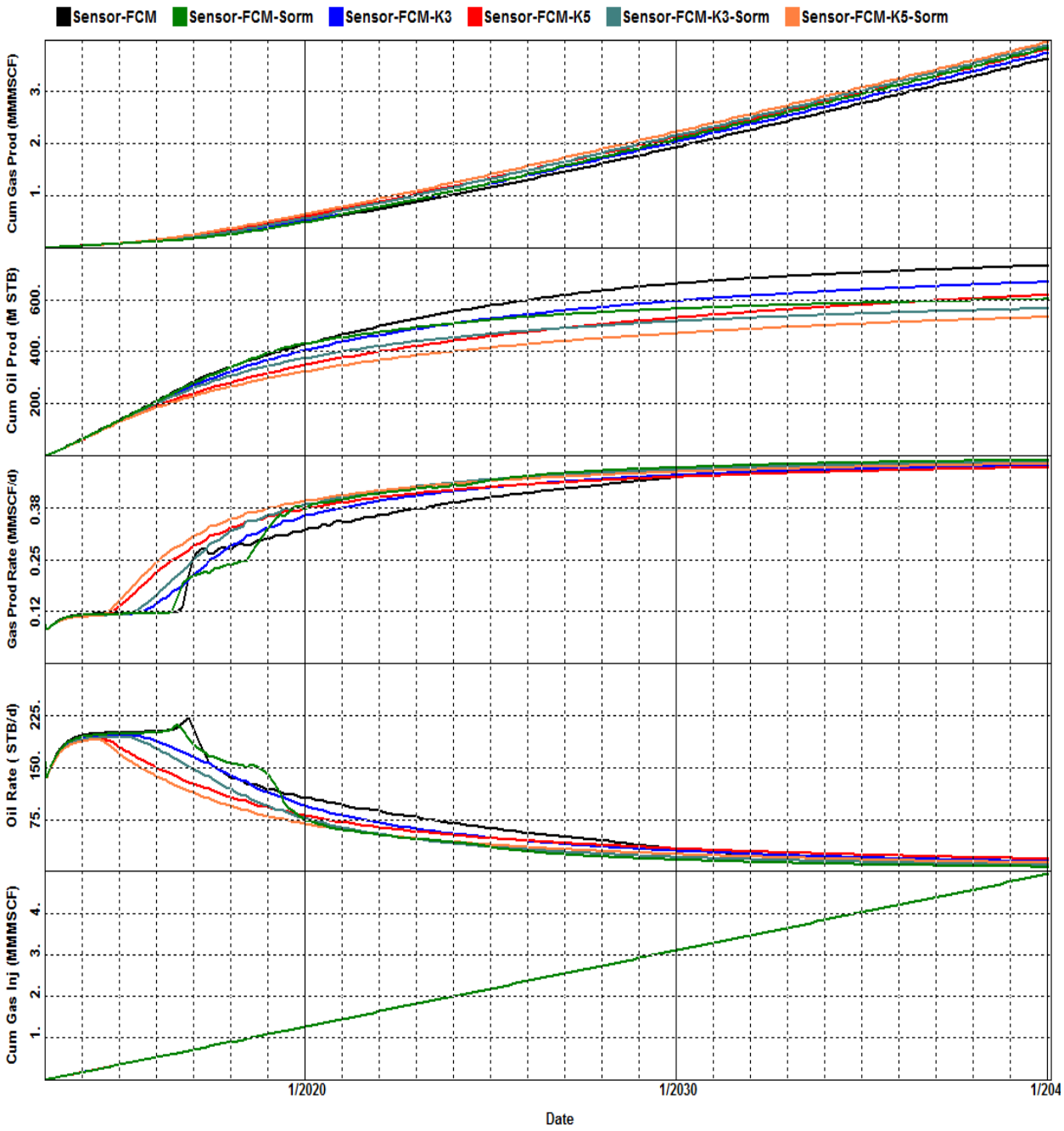

Figure 8.16 Recovery performance results of first-contact miscibility planar model for Sensor First Contact Miscibility Option with different dispersion control coefficient (K) and residual oil saturation (Sorm=0.1).

Figure 8.17 compares 3D and planar runs for first-contact miscibility study. When no viscous fingering imposition is used, different production profiles are observed. 3D planar model has early gas breakthrough (2 years), less oil production (maximum 25% difference) compared

with the planar model. All for these cases, gravity overriding is a dominant factor; therefore multiple layer models should be used. When viscous fingering imposition is used, 3D and planar models gives the exact same results. Thus, using single layer model is enough in case of viscous fingering dominance.

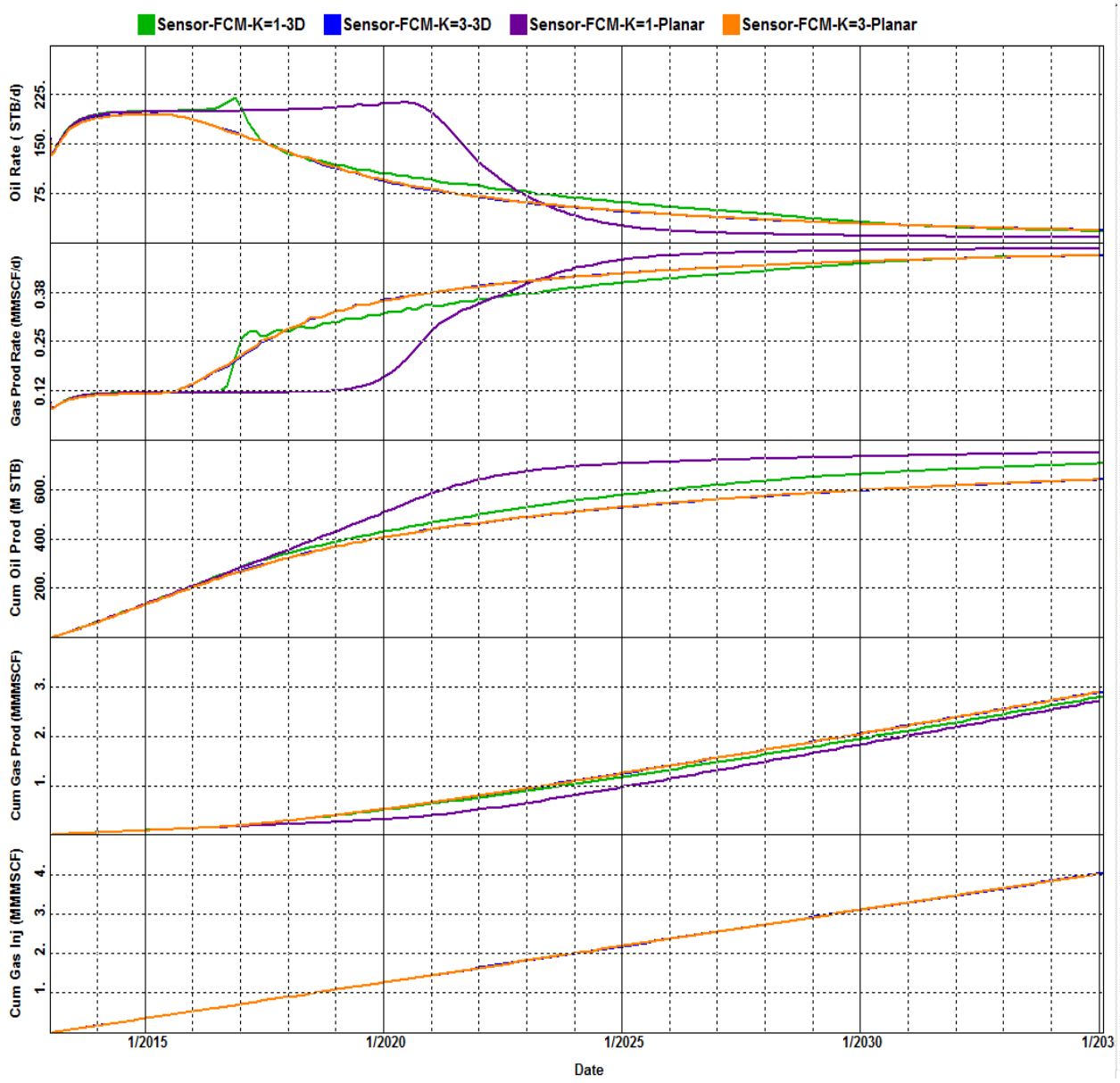

Figure 8.17 Comparison of 3D and planar model runs for first contact miscibility.

Figure 8.18 compares Sensor FCM option with different numerical dispersion control coefficient (K) and residual oil saturation. Sensor FCM option with K=1 and Sorm=0.0, leaving

zero oil saturation behind the front, displace original oil like a piston. When residual oil introduced the system an artificial viscous fingering mechanism is created and oil saturation (0.1) is left behind the front.

Figure 8.19 shows CO_2 mole fraction in oleic phase for Eclipse compositional and Sensor FCM option with different dispersion control coefficient (K) and residual oil saturation to miscible displacement. Mole fraction profiles are changing from top of the reservoir to bottom for cases without viscous fingering imposition. CO_2 breakthrough occurs earlier from top layers to bottom layers. On the other hand, cases with viscous fingering imposition shows a uniform CO_2 mole fraction and similar breakthrough times for each layer.

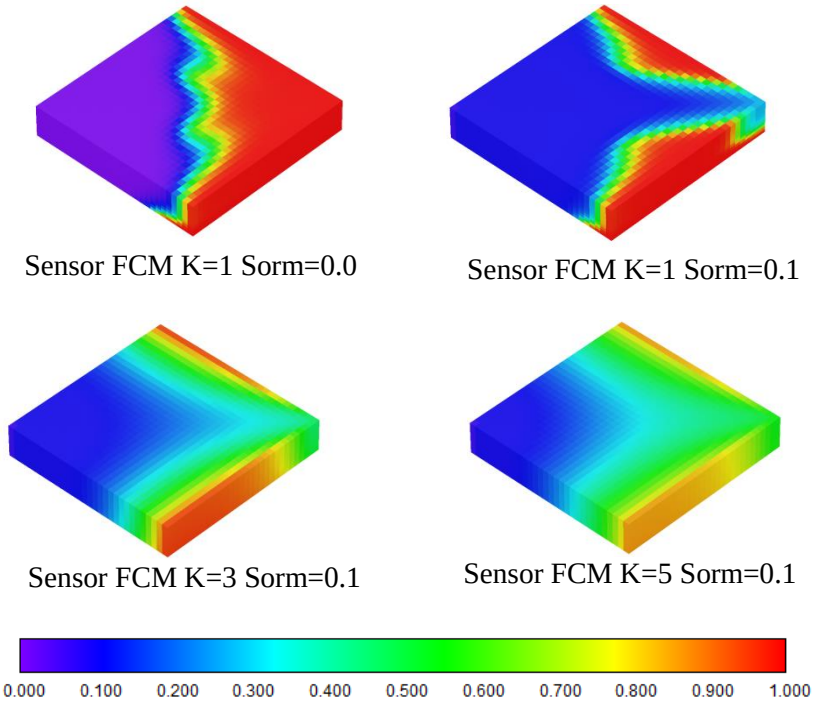

Figure 8.18 Oil component mole fraction of Sensor First Contact Miscibility Option with different dispersion control coefficient (K) at date 1-1-2020, Layer from 10 to 20 for first-contact miscible cross-sectional model.

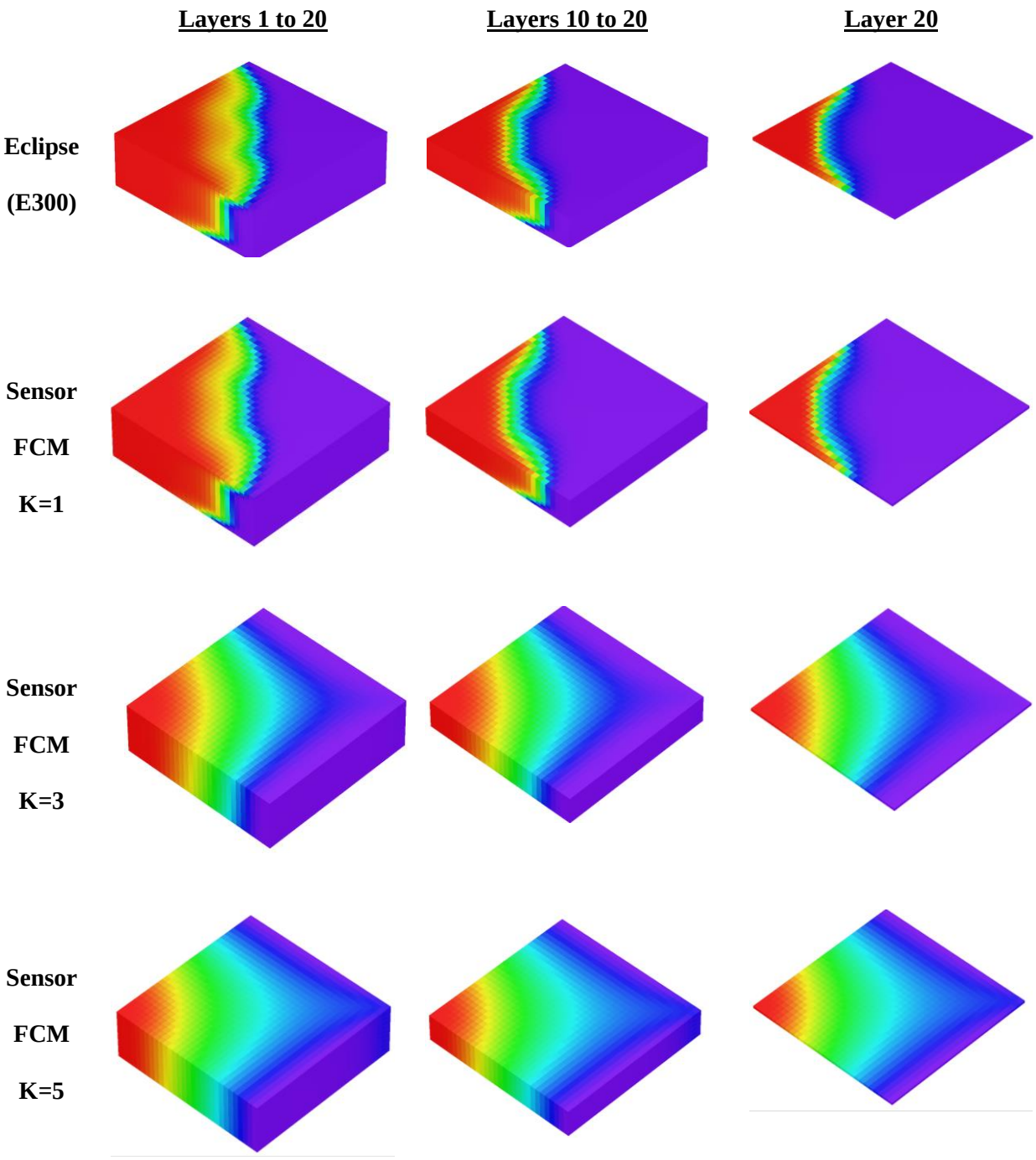

Figure 8.19 CO_2 mole fraction in oleic phase 1/6/2015 (0.4 PVI) for first-contact miscible cross-sectional model for Eclipse Compositional (E300) and Sensor First Contact Miscibility Option with different dispersion control coefficient (K).

CHAPTER 9

RESIDUAL OIL ZONE SIMULATION STUDY

Residual oil zones are defined as the reservoir interval with immobile oil and mobile water (Melzer et al, 2006). In the case of residual oil zone, a part of the reservoir has essentially been waterflooded by aquifer and requires enhanced oil recovery (EOR) technologies, such as CO_2 flooding, to produce the immobile residual oil. These residual zones approximately account for 16.3 billion barrels of technically recoverable oil in Permian, Big Horn and Williston basins (NETL, 2011). "Today, with advent of CO_2 EOR and several demonstration projects, this residual oil zone (often quite comparable in residual oil saturation with the waterflood swept interval in the main pay zone) has been shown to be a technically viable target for additional oil recovery"(Melzer, 2006). Honarpour et al. (2010) studied rock and fluid characteristics of residual oil zone in the Seminole San Andres Unit which is found below its producing oil-water contact. This residual oil zone contains significant amount of immobile oil ranging from 20% to 40% immobile oil saturation. Honarpour et al. (2010) showed that most probable average value of residual oil saturation is 30% and this value is used in this study as residual oil saturation value to be used at initialization of reservoir.

Unlike CO_2 floods in main oil pay zones, there is a limited understanding of CO_2 flood modeling in residual oil zones. Extended black oil formulations that are capable to model this kind of problems provides an alternative approach to compositional simulation. However, there is a limited understanding publication associated with the CO_2-EOR modeling of residual oil zones with extended black oil approaches.

This chapter includes comparing compositional and extended black oil simulators for miscible displacement in residual oil zone. Also, impact of CO_2 solubility in the water phase on the oil recovery in residual oil zones is investigated. 2-D planar models will be used to simulate CO_2 flooding in residual oil zone with COZSim, Eclipse Solvent Model, Eclipse 300 and Sensor-Compositional Simulators.

9.1 Description of Residual Oil Zone Simulation Study

The same fluid system described in Chapter 5 is used. Honarpour Reservoir initialized with uniform 70% water saturation and 30% oil saturation to create a residual oil zone. No free hydrocarbon gas is present in the system. Continuous CO_2 injection starts at 01/01/2013 and multi-contact miscibility operational parameters given in Table 9.1 is used. Planar model is used with dimensions 600x600x60 feet as static model. In-place values are given in Table 9.2. All simulators use STONE 2 as three phase relative permeability correlation. No CO_2 is dissolved in water phase.

Table 9.1 Parameters for ROZ multi-contact planar model

Parameter	Value
Grid	20x20x1
Grid Block Size, ft	30x30x60
CO_2 Injection Rate, MSCF/day	250
Initial Pressure, psi	3500
Production Well Bottom Hole Pressure, psi	3200
Injection Well Maximum Bottom Hole Pressure, psi	3900

Table 9.2 Fluid in-place results for ROZ planar model

Property	Value
Oil In-Place, MSTB	159
Water In-Place, MSTB	481
Gas In-Place, MMSCF	95

9.2 Results

This section presents the simulation results for multi-contact miscible CO_2 displacement study in residual oil zone with a planar static model for Eclipse and Sensor compositional simulators, Eclipse solvent model and COZSim. COZSim and Eclipse compositional simulators are also capable of modeling CO_2 solubility in water phase and residual oil saturation to miscible flooding. Those capabilities will be included in the study.

Figure 9.1 and Figure 9.2 shows oil, gas and water rate and cumulative production results for and Eclipse Solvent Model with mixing parameter w=1, Sensor Compositional, Eclipse Compositional simulators. CO_2 solubility in water and residual oil saturation to miscible flooding is not included in this case. Eclipse solvent model (w=1 and Sorm=0.0) Eclipse and Sensor compositional simulators predict the same production profiles. COZSim predicts lower oil production (20% less cumulative oil at the end of the simulation) because it uses a built-in mixing parameter calculation based on the interfacial tension. Breakthrough times are similar for each simulator around 3 years.

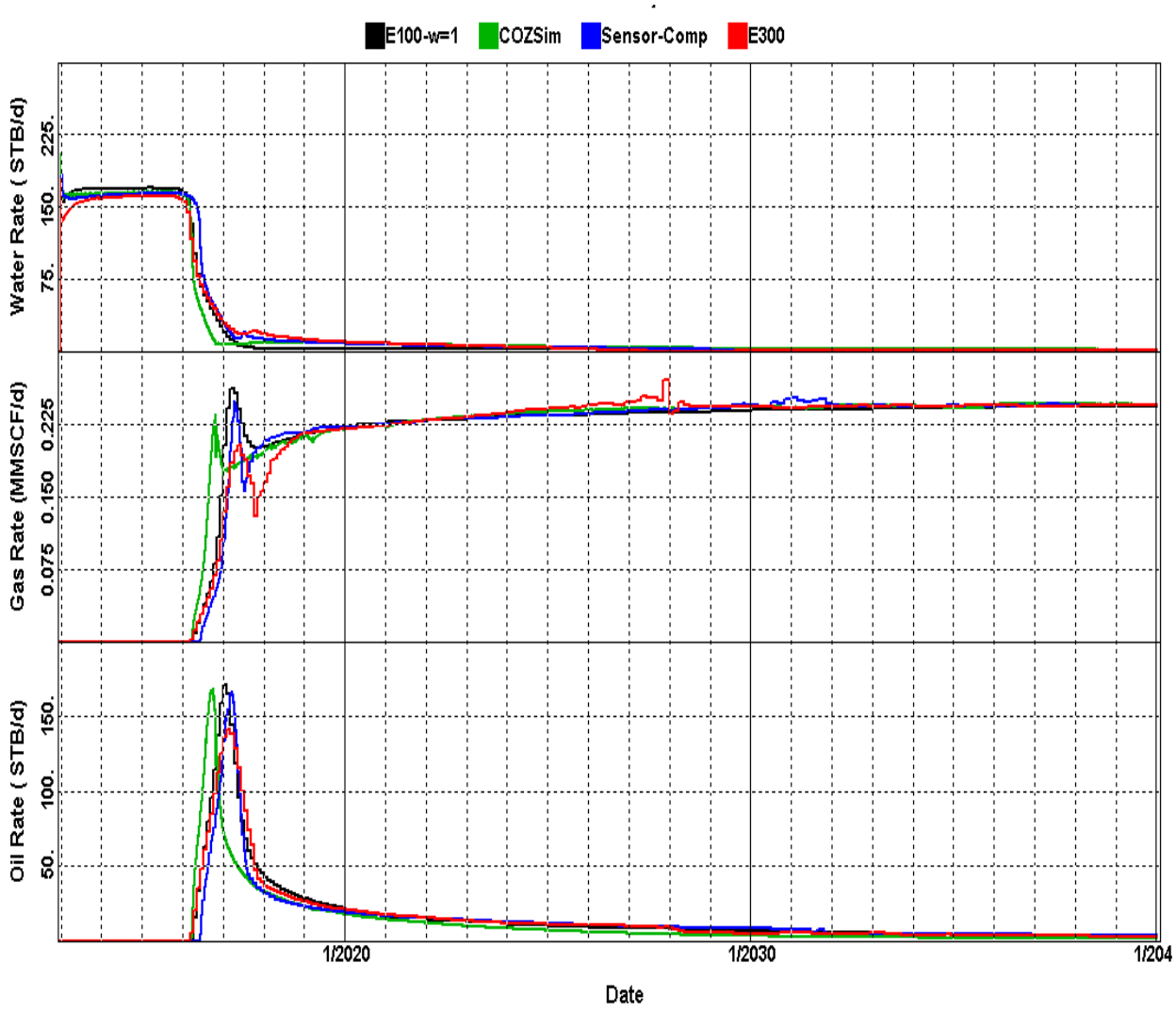

Figure 9.1 Oil, gas, water rate results of ROZ miscibility planar model for COZSim and Eclipse Solvent Model (E100) - w=1, Sensor Compositional, Eclipse Compositional (E300) simulators – No CO_2 solubility in water and Sorm=0.0.

Figure 9.3 compares the Eclipse solvent model with different Todd-Longstaff mixing parameters (w) and COZSim. Similar to the main oil zone cases, Eclipse Solvent model with viscous fingering imposition shows a wide range of oil production data (recovery factors ranging from 0.86 and 0.52) and breakthrough time (2.5 years to 4 years). Lower mixing parameter causes early gas breakthrough, lower oil production recovery factors and similar cumulative gas production. Mixing parameter values for COZSim varies between 0.5and 0.9 as shown in Figure 9.5.

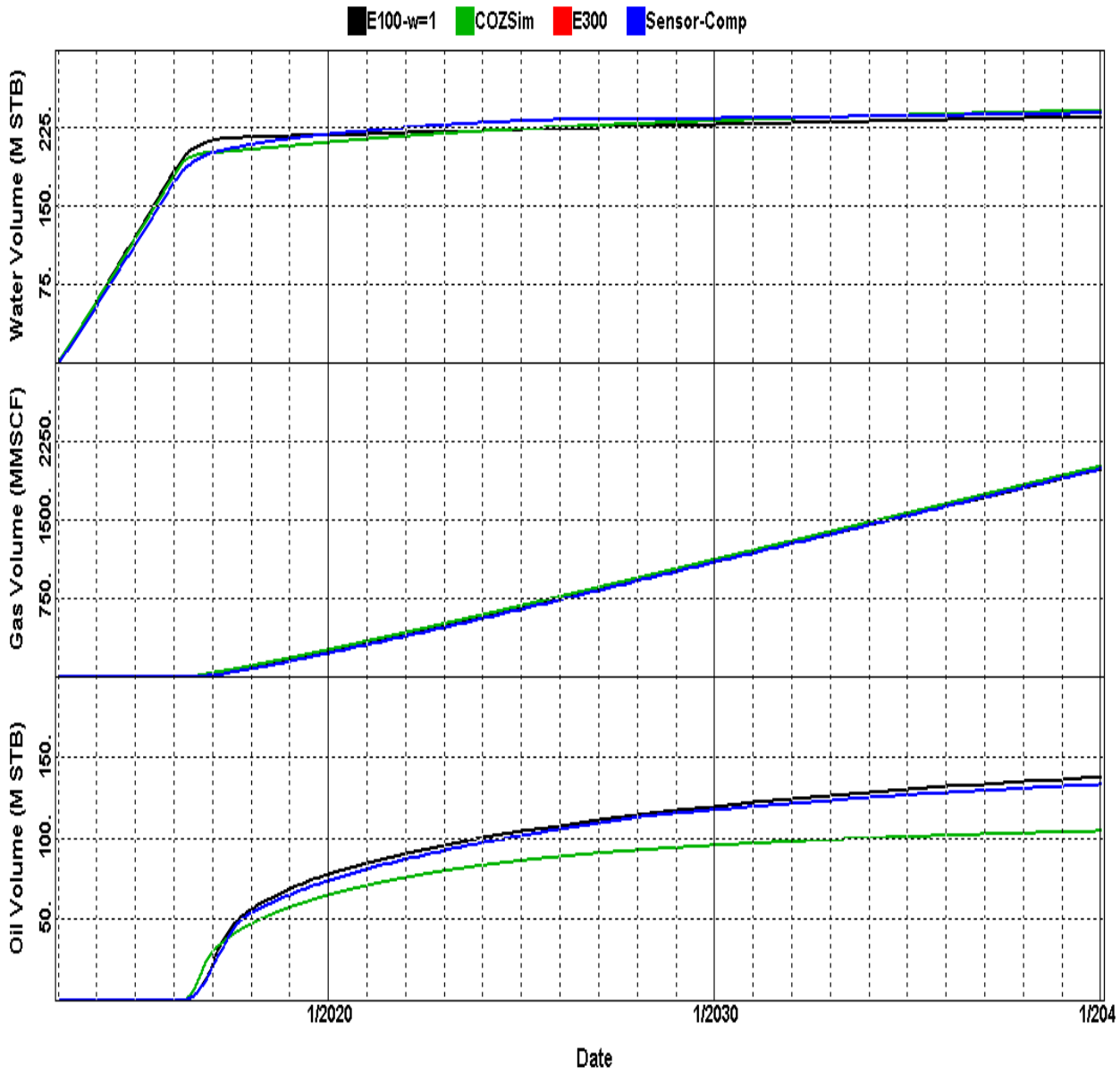

Figure 9.2 Oil, gas, water cumulative production results of ROZ miscibility planar model for COZSim and Eclipse Solvent Model (E100), Sensor Compositional, Eclipse Compositional (E300) simulators.

Figure 9.4 compares cumulative oil production results of COZSim and Eclipse compositional simulator with different cases including residual oil saturation to miscible flooding and solubility of CO_2 in water phase. Base cases Eclipse compositional (E300) and COZSim shows a significant differences in recovery values. Eclipse compositional simulator predicts 133 MSTB oil recoveries whereas COZSim predicts 105 MSTB. The difference caused

by mixing parameter calculation of COZSim. CO_2 solubility in oil does not affect cumulative oil production for Eclipse compositional simulator and COZSim for the particular cases. Introducing residual oil saturation along with CO_2 solubility in water significantly reduces cumulative oil production. These mechanisms reduce recovery factors from 0.84 to 0.75 for Eclipse compositional simulator and 0.66 to 0.58 for COZSim.

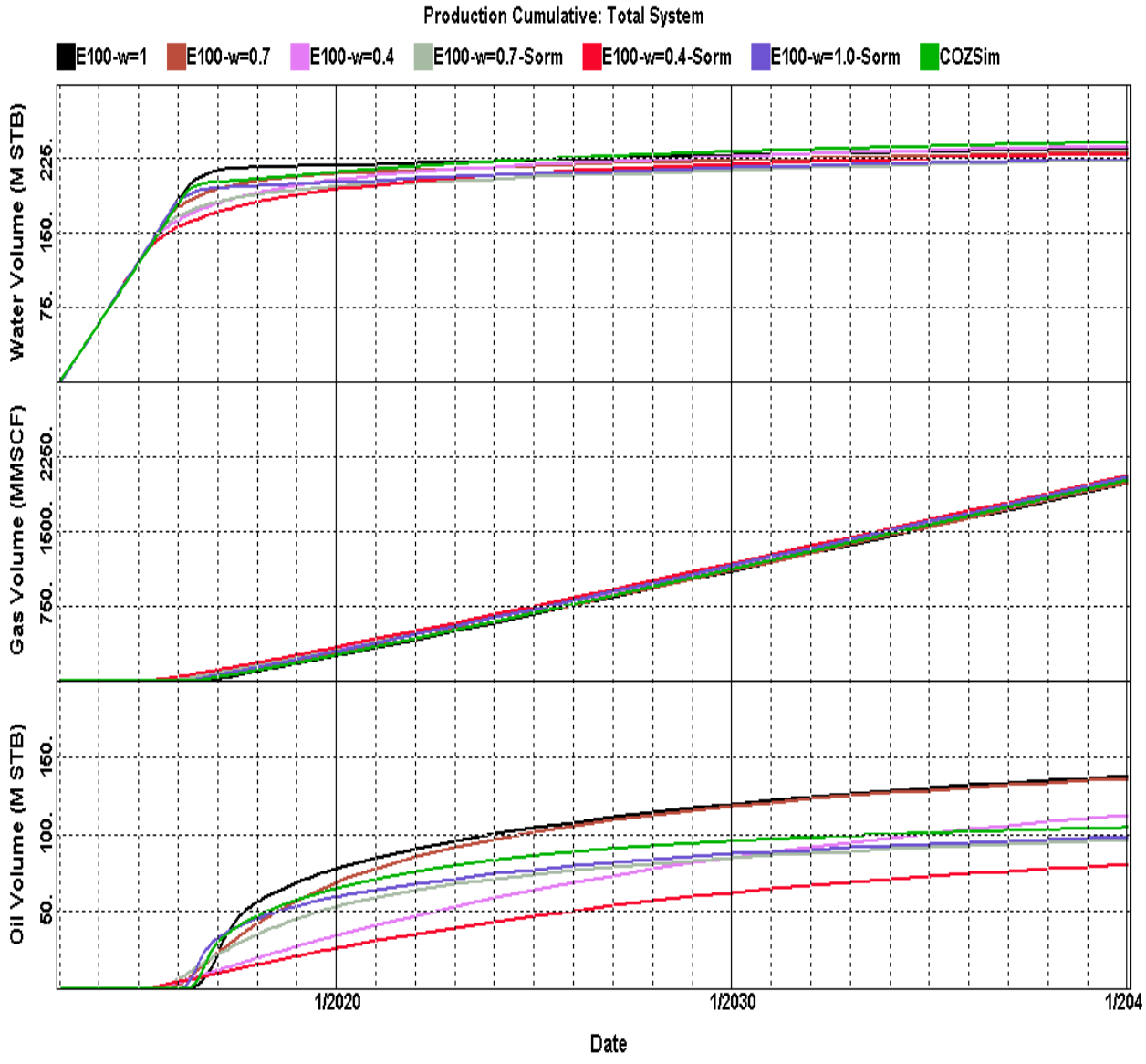

Figure 9.3 Recovery performance results of multi-contact miscibility cross-sectional model for Eclipse 100 (solvent model) with different Todd-Longstaff mixing parameter (w) and residual oil saturation (Sorm) and COZSim.

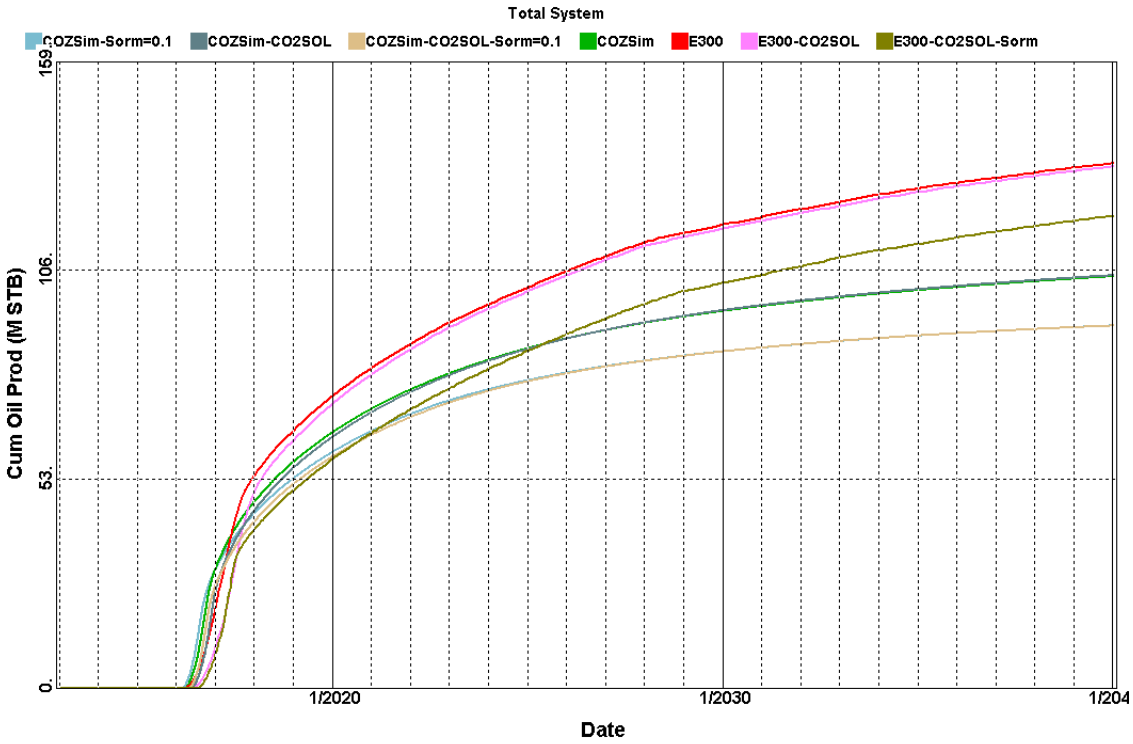

Figure 9.4 Oil, gas, water cumulative production results of ROZ miscibility planar model for COZSim and Eclipse Solvent Model (E100), Sensor Compositional, Eclipse Compositional (E300) simulators.

Figure 9.5 shows gas saturation profiles for various cases saturation profiles for Eclipse solvent model (w=1), COZSim, Eclipse and Sensor compositional simulators for various cases. Figure 9.6 shows oil saturation profiles Compositional simulators predict zero oil saturation around the injection wells. Figure 9.7 shows mixing parameter profiles for given dates.

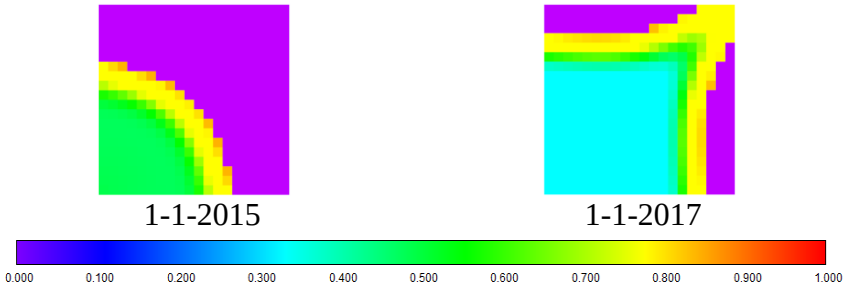

Figure 9.5 COZSim mixing parameter at the given date for ROZ study.

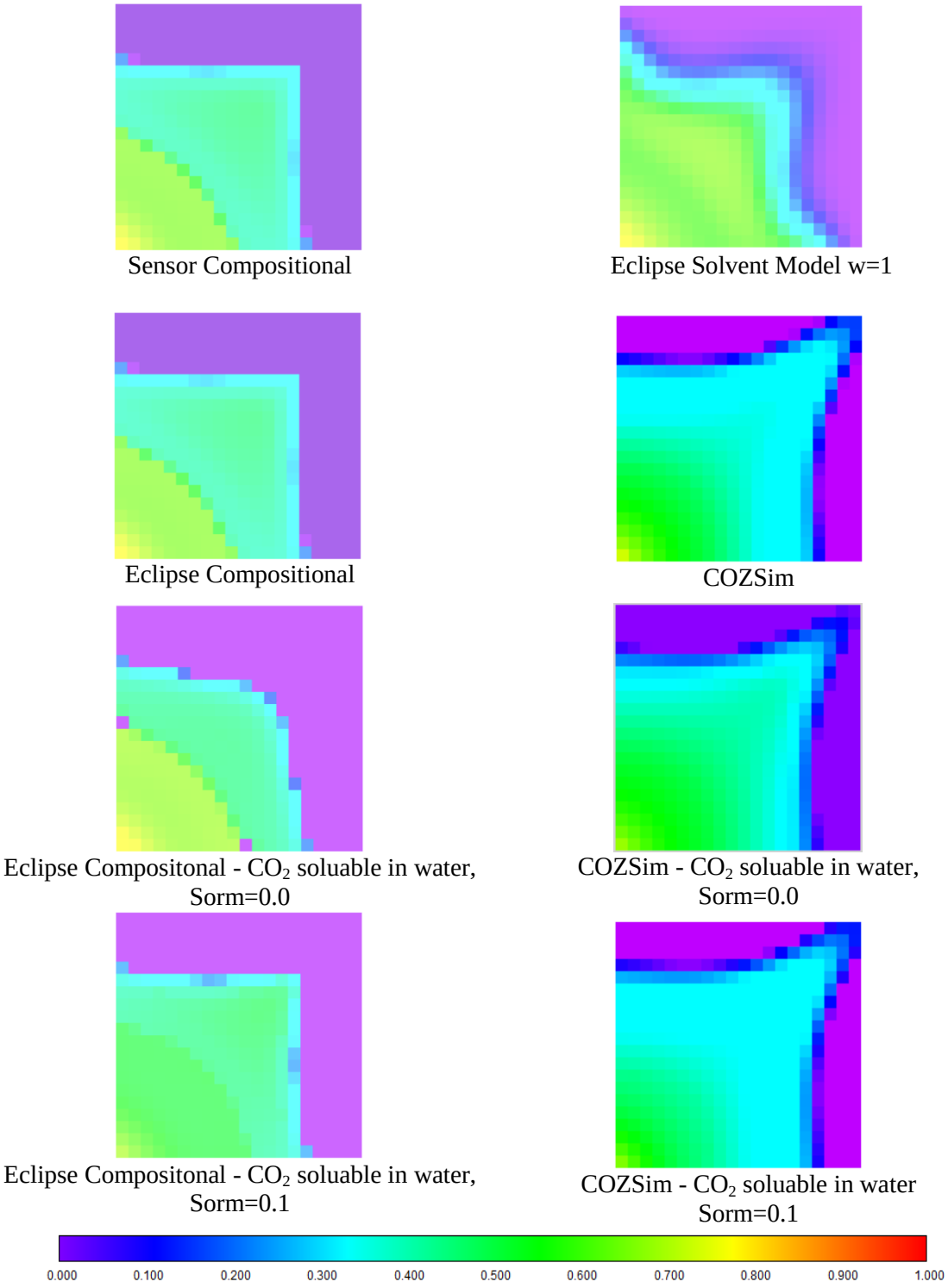

Figure 9.6 Gas saturation profiles at 2017-1-1 (0.57 PVI) for COZSim and Eclipse Solvent Model (E100) - w=1, Sensor Compositional, Eclipse Compositional (E300) simulators for various cases.

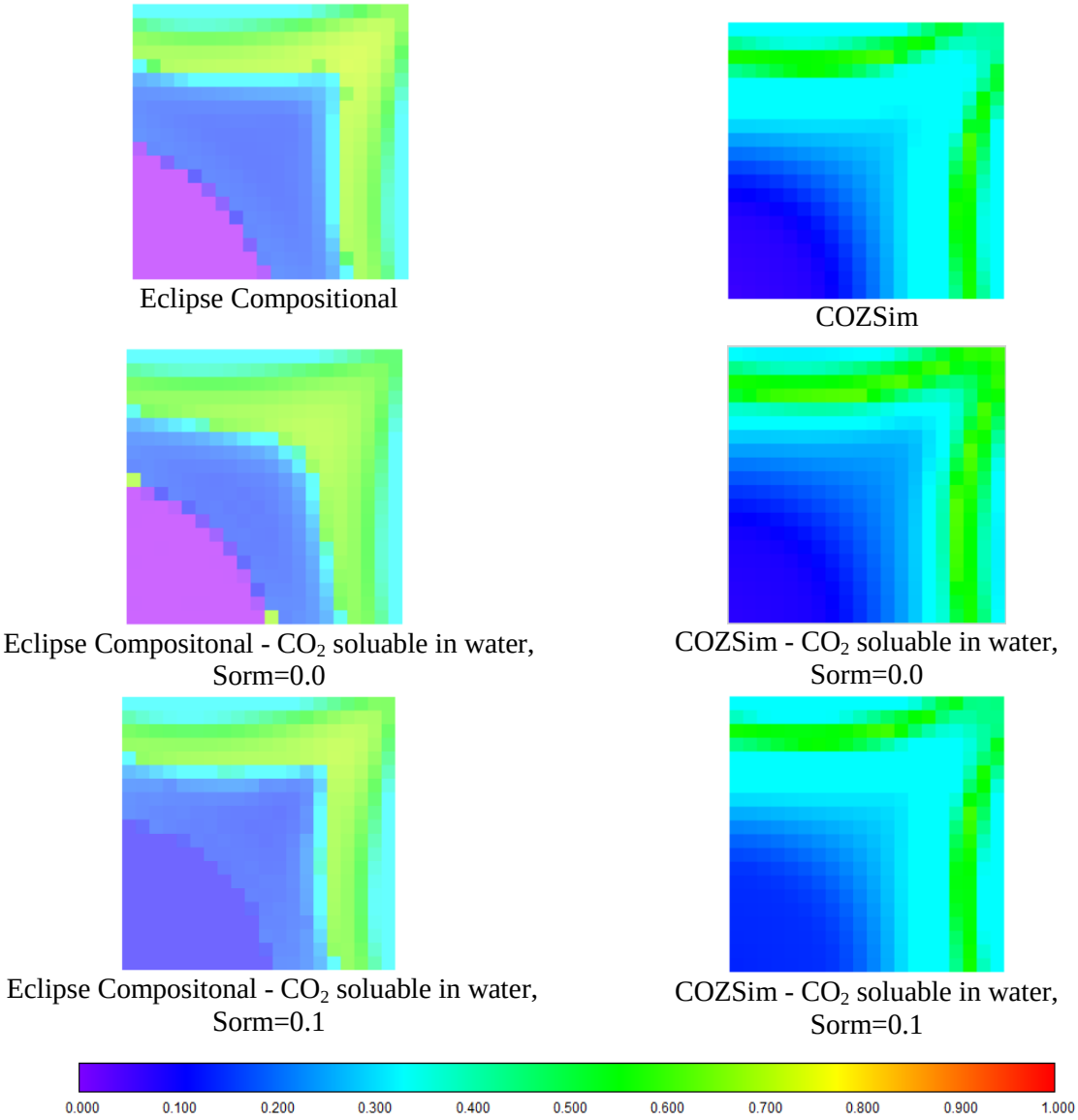

Figure 9.7 Oil saturation profiles at 2017-1-1 (0.57 PVI) for COZSim and Eclipse Compositional (E300) simulators for various cases.

CHAPTER 10

DISCUSSION AND CONCLUSIONS

This chapter provides a discussion and conclusion of the study and summarizes the comparison results explained throughout the study.

10.1 Discussion of the Results

Compositional and extended black-oil simulators were investigated for modeling different CO_2 flooding mechanisms, immiscible (near miscible), multi-contact and first-contact miscible flooding. This study shows that extended black-oil simulators are capable to simulate CO_2 flooding problems. This section will provide a discussion of capabilities, advantages, disadvantages and limitations of simulators that are investigated for each of these CO_2 displacement mechanisms.

Compositional simulators are capable of modeling wide range reservoir fluid types including near-critical fluid systems because they are able to handle mass transfer between phases. Extended black-oil simulators can only simulate black-oil type fluids with no mass transfer between phases. On the other hand, compositional simulators require more fluid and phase behavior data based on the complex fluid analysis (tuned EOS) whereas extended black-oil simulators use classical black-oil type fluid data.

Compositional simulators predict high oil recoveries for miscible CO_2 displacement processes due to the assumption of total displacement of the oil in the swept regions disregarding the unstable flow and by-passed oil which is caused by adverse mobility ratio of CO_2 and in-place oil. Multi-contact and first-contact miscible studies reveal that a wide range of oil recovery

performance can be predicted depending on the simulator and mixing parameters used. It is shown that compositional and extended black oil simulations (with full mixing and zero residual oil saturation) give very similar recovery profiles regardless of the displacement mechanism. On the other hand, the mixing parameter is a dominant factor for both multi-contact and first-contact miscibility in main oil zone studies. 3D studies show that including a mixing parameter in the system may reduce the oil recovery up to 35%, depending on the value of the mixing parameter. Also breakthrough times significantly change depending on the value of mixing parameter.

The dominant displacement mechanism is determined by viscous forces that drive viscous fingering and gravitational forces that attempt to create gravity tongue. Both Eclipse Solvent Model and Sensor First Contact Miscibility option use constant mixing parameter values and this approach ignores the dependency of mixing to the phase saturations, interfacial tension between the oil and gas phases and the gravitational forces. It is shown that when a constant mixing parameter is used, viscous fingering forces become the dominant displacement mechanism and these mask the gravitational fingering resulting from density differences of CO_2 and in-place oil.

Calculation of a constant mixing parameter is not straight forward. Todd and Longstaff (1972) suggest setting the mixing parameter to 0.3 - 0.4 for field-scale simulations. However, the mixing parameter is generally regarded as a history matching parameter. Koval (1963) suggests a formulation to calculate mixing parameter (dispersion control coefficient-K) using a constant viscosity ratio of in-place oil and CO_2. This calculation assumes constant viscosities of in-place oil and CO_2. Therefore a constant mixing parameter assumption would have a limited use unless the mixing parameter itself is modeled over a wide range of values. COZSim calculates mixing

parameters depending on the interfacial tension of oil and gas phases. It is shown that this calculation yields mixing parameters ranging from 0.4 to 0.9 and corresponding overall recovery performance is generally between the cases with Todd-Longstaff mixing parameter of w=1.0 and w=0.7. It is also found that variable mixing parameter calculation does not mask the gravitational fingering when compared with the constant mixing parameter approach.

One of the main limitations of compositional simulation is that zero oil saturation created especially in near the injection well due to complete vaporization of oil rather than the residual oil to gas flooding (Sorg) for immiscible, and residual oil to miscible flooding (Sorm) for miscible cases. This causes high oil recovery predictions; especially it will become a very important factor if the distance between injection and production wells decreases. Eclipse compositional simulator has an option to set a residual oil saturation to avoid vaporization of oil due to the continuous gas injection. This option excludes a specified fraction of oil from the flash calculations. However, it is found that this option has a couple of disadvantages. First, if a specified fraction of oil is excluded from flash calculations, this excluded volume of oil will not release its solution hydrocarbon gas. Therefore, if system pressures fall below the bubble point pressure, less hydrocarbon gas will come out from the solution, see Chapter 6. Second, excluding a specified fraction of oil from flash calculations creates an artificial mixing modification (viscous fingering). This artificial viscous fingering effect leads to very low oil recovery up to 40% in 3D immiscible flooding cases. Besides, it is observed that excluding a part of the oil from the system leads unavoidable convergence problems. Miscible flooding, higher fluxes within the system and lower pore volume of grid blocks make this option more unstable. Therefore, this option should not be used for miscible case studies.

Since the models in main oil zone studies are initialized at 80% oil saturation, the effect of residual oil saturation is not dominant yet an important factor. Residual oil saturation after miscible flooding will be a very important factor if the system is initialized with lower oil saturation. Residual oil zone simulation studies show that residual oil saturation to miscible flooding has a very significant impact in residual oil zone. That is because about 30% of oil in the system will be by-passed and cannot be produced. Results from the Eclipse solvent model shows that the dominant factor for residual oil zone studies is the residual oil saturation value rather than the mixing parameter which still has an important effect on oil recovery results. On the other hand, COZSim with a variable mixing parameter shows that the system does not reach the residual oil saturation. Including residual oil saturation imposition in the Eclipse compositional model reduces oil recovery about 10%. That number does not match with the Eclipse solvent model, therefore it can be said that residual oil saturation imposition in compositional run may overestimate the oil recovery in residual oil zones.

CO_2 solubility in water phase is also investigated for residual oil zone studies. COZSim predicts 12% less oil recovery when CO_2 solubility in water phase is included to the system, whereas the Eclipse compositional simulator predicts 1% less oil recovery. The difference is caused by the treatment of CO_2 mixing in compositional runs because CO_2 is contacted with all of the oil and water in the grid block and partitioned to whole volume of oil presented in the grid block. However, COZSim considers that a part of CO_2 does not contact with oil and this volume of CO_2 dissolves in the water phase and result in less oil recovery. Therefore the difference in results for the Eclipse compositional simulator and COZSim is caused by the partitioning coefficient of CO_2 into the water phase.

It is observed that extended black oil simulators (Eclipse solvent model and COZSim) have difficulties to solving fine-grid problems. Convergence problems arise when grid block volumes are small or CO_2 injection rates are high. Compositional simulators Eclipse and Sensor, and extended black-oil formulation Sensor First Contact Miscibility Option provide very stable solutions in terms of convergence and time step sizes. On the other hand, it is observed that compositional simulators suffer from grid orientation effects independent from the number of grid blocks, especially, for first-contact miscible cases.

10.1 Conclusions

- Multi-contact and first-contact miscible studies reveal that a wide range of oil recovery performance can be predicted by Eclipse Solvent Model and Sensor First Contact Miscibility Option depending on the mixing parameters that are used.
- It is shown that when a constant mixing parameter is used (e.g. Eclipse Solvent Model and Sensor First Contact Miscibility Option), viscous fingering forces become the dominant displacement mechanism and it can mask the gravitational fingering. It is also found that the variable mixing parameter calculation (e.g. COZSim) does not mask the gravitational fingering. Therefore, simulators that use ca onstant mixing parameter may overestimate the oil recovery due to more efficient sweep of oil for multi-layer simulation models.
- Eclipse Solvent Model shows that the dominant factor for the residual oil zone studies is the value of residual oil saturation rather than the mixing parameter. On the other hand, COZSim results (with a variable mixing parameter) show that the system does not reach the residual oil saturation during the simulation period due to partial mixing.

- Compositional simulators may underestimate the impact of CO_2 solubility in water on oil recovery due to the different CO_2 partitioning coefficient used in Eclipse compositional simulator and COZSim.
- Compositional simulators are more stable than the extended black-oil simulators for the fine-grid models.
- It is shown that extended black-oil simulators are capable of simulating CO_2 flooding cases for every CO_2 displacement mechanism. The compositional and extended black-oil simulators (with full mixing and zero residual oil saturation assumption) predict very similar recovery profiles regardless of the displacement mechanism. Compositional simulation models are capable of modeling a wide range reservoir fluid types including the near-critical fluid systems because they are able to handle mass transfer between phases. On the other hand, extended black oil simulators can only simulate black-oil type fluids with no mass transfer between phases.

NOMENCLATURE

B = Formation volume factor

K = Dispersion control coefficient

k_r = Relative permeability, component specified with additional subscript

k_{rn} = Imbibition relative permeability of the non-wetting phase

R_s = Solution gas-oil ration

S_g = Gas saturation, fraction

S_o = Oil Saturation, fraction

S_n = Non-wetting phase saturation, fraction

S_{org} = Residual oil saturation to immiscible gas flooding, fraction

S_{orm} = Residual oil saturation to miscible flooding, fraction

S_{twb} = Water-blocking function

S_{orw} = Residual oil to water

P = Pressure, psi

z = Overall composition

Greek Symbols

μ = Viscosity, cp

ω = Mixing parameter

ρ = Density

β = Parameter to weaken the water blocking function

α = Parameter providing transition from immiscible conditions to miscible conditions

Subscripts

a = Aqueous

o = Oil

w = Water

g = Hydrocarbon gas

s = Solvent

i = Components

e = Effective

m = Mixture

n = Non-wetting

os = Oil-solvent mixture

gs = Hydrocarbon gas-solvent mixture

Superscript

sc = Standard conditions

REFERENCES CITED

Ammer, J. R., Sams, W. N., and Brummert, A. C. 1988. An Extended Black Oil Miscible Simulator That Rigorously Treats Variable Bubble Point Problems. Paper SPE 18533-MS presented at the SPE Eastern Regional Meeting, Charleston, West Virginia, 1-4 November. http://dx.doi.org/10.2118/18533-MS.

Aziz, K., and Settari, A. 1979. Petroleum Reservoir Simulation, Vol. 476. London: Applied Science Publishers.

Barker, J. W., Prévost, M., & Pitrat, E. 2005. Simulating Residual Oil Saturation in Miscible Gas Flooding Using Alpha-Factors. Paper SPE 93333-MS. presented at the SPE Reservoir Simulation Symposium, Houston, Texas, 31 January – 2 February. http://dx.doi.org/10.2118/93333-MS.

Bilhartz, H. L., Charlson, G. S., Stalkup, F. I., and Miller, C. C. 1978. A Method for Projecting Full-Scale Performance of CO2 Flooding in the Willard Unit. Paper SPE 7051-MS presented at the SPE Symposium on Improved Methods of Oil Recovery, Tulsa, Oklahoma, 16 - 17 April. http://dx.doi.org/10.2118/7051-MS.

Bolling, J. D. 1987. Development and Application of a Limited-Compositional, Miscible Flood Reservoir Simulator. Paper SPE 15998-MS presented at the SPE Symposium on Reservoir Simulation, San Antonio, Texas, 1-4 February. http://dx.doi.org/10.2118/15998-MS.

Chase Jr, C., and Todd, M. 1984. Numerical Simulation of CO_2 Flood Performance (includes associated papers 13950 and 13964). SPE Journal, 24(6), 597-605. SPE-10514-PA. http://dx.doi.org/10.2118/10514-PA.

Chang, Y. B., Coats, B., and Nolen, J. 1998. A compositional model for CO2 floods including CO2 solubility in water. SPE Reservoir Evaluation and Engineering, 1(2), 155-160.

Coats, K. 1980. An Equation of State Compositional Model. SPE Journal, 20(5), 363-376. SPE 8284-PA. http://dx.doi.org/10.2118/8284-PA.

Coats, K. 1982. Reservoir Simulation: State of the Art (includes associated papers 11927 and 12290). Journal of Petroleum Technology, 34(8), 1633-1642. SPE 10020-PA. http://dx.doi.org/10.2118/10020-PA.

Coats, K.H. 1987. Reservoir Simulation. In Petroleum Engineering Handbook, ed. Howard B. Bradley, Chap. 48, Richardson, Texas: Society of Petroleum Engineers.

Eclipse, Version 2012.2 Technical Description.

Enick, R. M., and Klara, S. M. 1992. Effects of CO_2 Solubility in Brine on the Compositional Simulation of CO_2 Floods. SPE Reservoir Engineering, 7(2), 253-258. SPE 20278-PA. http://dx.doi.org/10.2118/20278-PA.

Fussell, L. T., and Fussell, D. D. 1979. An Iterative Technique for Compositional Reservoir Models. SPE Journal, 19(4), 211-220. SPE 6891-PA. http://dx.doi.org/10.2118/6891-PA.

Garder Jr., A.O., Peaceman, D.W. and Pozzi Jr., A.L. 1964. "Numerical Calculation of Multidimensional Miscible Displacement By The Method Of Characteristics." SPE Journal 4.1 (1964): 26-36. SPE 683-PA. http://dx.doi.org/10.2118/ 683-PA

Haajizadeh, M., Fayers, F. J., Cockin, A. P., Roffey, M., and Bond, D. J. 1999. On the Importance of Dispersion and Heterogeneity in The Compositional Simulation of Miscible Gas Processes. In SPE Asia Pacific Improved Oil Recovery Conference. Kuala Lumpur, Malaysia 25-26 October. http://dx.doi.org/10.2118/57264-MS

Heris, A.E. 2011. Integrated Flow Simulation and Time-Lapse Seismic Reservoir Characterization in Conjunction with an Enhanced Oil Recovery Project, Postle Field, Texas County, Oklahoma, PhD Dissertation. Colorado School of Mines. Golden, Colorado.

Honarpour, M. M., Nagarajan, N., Grijalba Cuenca, A., Valle, M., and Adesoye, K. 2010. Rock-Fluid Characterization for Miscible CO2 Injection: Residual Oil Zone, Seminole Field, Permian Basin. Paper SPE 102964-MS presented at the SPE Annual Technical Conference and Exhibition, Florence, Italy, 19-22 September. http://dx.doi.org/10.2118/133089-MS.

Huan, G. R. 1985. A Flash Black Oil Model. Paper SPE 13521-MS presented at the SPE Reservoir Simulation Symposium, Dallas, Texas, 10-13 February. http://dx.doi.org/10.2118/ 13521-MS.

NETL. 2011 Improving Domestic Energy Security and Lowering CO2Emissions with "Next Generation" CO2-Enahanced Oil Recovery (CO2-EOR), National Energy Technology Laboratory, Advanced Resources International

Jarrell, P. M., Fox, C. E., Stein, M. H., and Webb, S. L. 2002. *Practical Aspects of CO_2 Flooding*, Vol. 22, Richardson, Texas: Monograph Series, SPE.

Killough, J. 1995. Ninth SPE Comparative Solution Project: A Reexamination of Black-Oil Simulation. Paper SPE 29110-MS presented at the SPE Symposium on Reservoir Simulation, San Antonio, Texas, 12-15 February. http://dx.doi.org/10.2118/29110-MS.

Kazemi, H., Vestal, C. R., and Shank, D. 1978. An Efficient Multicomponent Numerical Simulator. SPE Journal, 18(5), 355-368. SPE 6890-PA. http://dx.doi.org/10.2118/6890-PA

Koval, E. J. 1963. A Method for Predicting the Performance of Unstable Miscible Displacement in Heterogeneous Media. SPE Journal, 3(2), 145-154. SPE 450-PA. http://dx.doi.org/10.2118/450-PA.

Lantz, R. B. 1970. Rigorous Calculation of Miscible Displacement Using Immiscible Reservoir Simulators. SPE Journal, 10(2), 192-202. SPE 2594-PA. http://dx.doi.org/10.2118/ 2594-PA

Lasater, J. A. 1958. Bubble point pressure correlation. Journal of Petroleum Technology, 10(5), 65-67

Melzer, L., Kuuskraa, V., and Koperna, G. 2006. The Origin and Resource Potential of Residual Oil Zones. Paper SPE 102964-MS presented at the SPE Annual Technical Conference

and Exhibition, San Antonio, Texas, 24-27 September. http://dx.doi.org/10.2118/102964-MS.

Montel, F. O., and Quettier, L. 2004. Getting the Best from the Black-oil Approach for Complex Reservoir Fluids. Paper SPE 90926-MS presented at the SPE Annual Technical Conference and Exhibition, Houston, Texas, 26-29 September. http://dx.doi.org/10.2118/90926-MS.

NETL. 2011 Carbon Dioxide Enhanced Oil Recovery: Untapped Domestic Energy Supply and Long Term Carbon Storage Solution. http://www.netl.doe.gov/technologies/oil-gas/publications/EP/CO2_EOR_Primer.pdf (downloaded February 2013)

Nolen, J. S. 1973. Numerical Simulation of Compositional Phenomena in Petroleum Reservoirs. Paper SPE 4274-MS presented at the SPE Symposium on Numerical Simulation of Reservoir Performance, Houston, Texas, 11-12 January. http://dx.doi.org/102112/4274-MS

Nghiem, L. X., Fong, D. K., and Aziz, K. 1981. Compositional Modeling with an Equation of State (includes associated papers 10894 and 10903). SPE Journal, 21(6), 687-698. SPE 9306-PA. http://dx.doi.org/10.2118/9306-PA

Peaceman, D. W., and Rachford Jr., H.H., 1962. Numerical Calculation of Multidimensional Miscible Displacement. SPE Journal, 2(4), 327-339. SPE 471-PA. http://dx.doi.org/10.2118/471-PA

Raimondi, P., and Torcaso, M. 1964. Distribution of The Oil Phase Obtained Upon Imbibition Of Water. SPE Journal, 4(1), 49-55. SPE 570-PA. http://dx.doi.org/10.2118/ 570-PA.

Sensor Manual. Compositional and Black Oil Reservoir Simulation Software, Version 2011

Stalkup, F. I. 1983. *Miscible displacement,* Vol. 8, 71-80, Dallas: Monograph Series, SPE.

Tang, D. E., and Zick, A. A. 1993. A New Limited Compositional Reservoir Simulator. Paper SPE 25255-MS presented at the SPE Symposium on Reservoir Simulation, New Orleans, Louisiana, 28 February-3 March. http://dx.doi.org/10.2118/25255-MS.

Thele, K. J., Lake, L. W., and Sepehrnoori, K. 1983. A Comparison of Three Equation-of-State Compositional Simulators. Paper SPE 12245 presented at the SPE Reservoir Simulation Symposium, San Francisco, California, 15-18 November. http://dx.doi.org/10.2118/ 12245-MS.

Todd, M.R. and Longstaff, W.J. 1972. The Development Testing and Application of a Numerical Simulator for Predicting Miscible Flood Performance. Journal of Petroleum Technology 24(7): 874-882. SPE 3484-PA. http://dx.doi.org/10.2118/3484-PA.

User Guide IMEX. 2012. CMG Compositional Reservoir Simulator.

Watkins, R. 1982. The Development and Testing of a Sequential Semi-Implicit Four Component Reservoir Simulator. Paper SPE 10513-MS presented at the SPE Reservoir Simulation Symposium., New Orleans, Louisiana, 31 January-3 February. http://dx.doi.org/10.2118/10513-MS.

Wattenbarger, R.A. 1970. Practical Aspects of Compositional Simulation. Paper SPE 2800 presented at the SPE of AIME Symposium on Numerical Simulation Reservoir performance, Dallas, Texas, 5-6 February. http://dx.doi.org/102112/2800-MS.

Whitson, C., and Torp, S. 1981. Evaluating Constant Volume Depletion Data. SPE Annual Technical Conference and Exhibition., San Antonio, Texas, 4-7 October. http://dx.doi.org/ 10.2118/10067-MS.

Young, L., and Stephenson, R. 1983. A Generalized Compositional Approach for Reservoir Simulation. Old SPE Journal, 23(5), 727-742. SPE-10516-PA http://dx.doi.org/10.2118/10516-PA